Vanadium complexes and clusters for (potential) industrial and medicinal application

Dissertation

for the acquirement of the Dr. rer. nat. degree
by the Fachbereich Chemie der
Universität Hamburg
Germany

submitted by
Dongren Wang
from Jilin, P. R. China

Hamburg 2002

The first referee: Prof. Dr. D. Rehder

The second referee: Prof. Dr. R. Kramolowsky

Date of the final oral examination: September 23, 2002

For my wife and my daughter

Statement

To the best of my knowledge, this thesis contains no material which has been presented for any other degree or diploma at any University and contains no material previously published, personally communicated or written by another person except where due reference is given.

I pledge myself to announce that all work for this thesis has independently been realized by the author.

Hiermit versichere ich, daß die vorliegende Arbeit selbständig angefertigt und ich keine andern als die angegebenen Hilfsmittel benutzt habe. Nach meiner besten Kenntnis sind alle in meiner Dissertation vorgestellten Ergebnisse zuvor nicht bekannt gewesen, ausgenommen die Resultate, zu denen entsprechende Literaturezitate angegeben sind.

Hamburg, July 2002

All work with relevance for this Thesis has been carried out from May 1999 to March 2002 in the Institut für Anorganische und Angewandte Chemie der Universität Hamburg under the supervision of Prof. Dr. D. Rehder

To Prof. Dr. D. Rehder, who has been the supervisor of my promotion to the Dr. rer. nat. degree, I express my deep thanks both for his advices and numerous meaningful suggestions during this work as well as for the financial support through the DFG during the time when I and my family were in Germany. His serious scientific attitude has always inspired me and will inspire me.

I would like to thank our research group for the friendly admission and the good co-operative atmosphere. To Mahin, Henning, Cerstin, Gabriella, Martin, Marian, Axel, and Jessica I express my sincere thanks for their kind help both in my work as well as in activities outside the lab.

To Carola, Cerstin and Wenjian I express my best thanks for their help in the calculation and refinement of crystal structures. I would like to give my best gratitude to Prof. Dr. U. Behrens for his helpful advice in the crystal structure analyses.

I moreover thank all Technical assistants of the analytical and NMR department for analyses of the samples.

I thank Professor Beate Meier, Entrischenbrunn, for performing the in vitro tests.

Last, not least, I would like to express my deep gratitude to the Chinese Service Centre for Scholarly Exchange, to the Deutsche Forschungsgemeischaft and Interdisciplinary Graduate School (Design and Characterisation of Functional Materials) for their financial support during the time when my family and I were in Germany.

Abbreviation

acac	acetylacetonate
AMP	adenosine-monophosphate
Ar. ar.	aromatic
C22	4,13-Diaza-18-Crowne-6, 1,7,10,16-Tetraoxa-4,13-diazacyclooctadecan
C23	1,7,10,13,19-Pentaoxa-4,16-diazacycloheneicosan
C221	4,7,13,16,21-Pentaoxa-1,10-diazabicyclo[8.8.5]-tricosane
C211	4,7,13,18-Tetraoxa-1,10-diazabicyclo[8.5.5]-eicosane
DMF	N, N-Dimethylformamide
DMSO	Dimethylsulfoxide
h	hour
HPA	heteropoly acid
L	ligand
Maltol	3-hydroxy-2-methyl-4-pyrone
Me	methyl
Me_2CO	acetone
Nap	2-Hydroxynaphthalene-1-carbaldehyde
o-vanillin	3- Methoxy-salicylaldehyde
PBMC	peripheral blood mononuclear cells
Ph	phenyl
POMs	polyoxometalates
STZ	streptozotocin
THF	tetrahydrofuran for solvent
thf	tetrahydrofuran for ligand
TMS	tetramethylsilane
TSC	Thiosemicarbazone

The used ligand

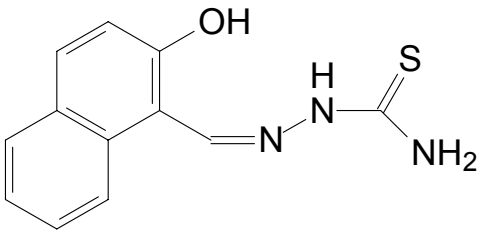

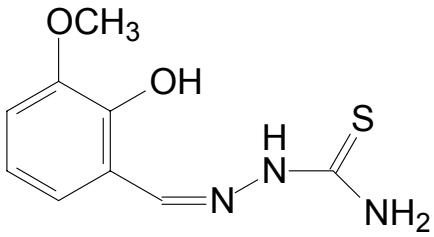

3- Methoxy-salicylaldehyde Thiosemicarbazone(L2)

2-Hydroxynaphthalene-1-carbaldehyde Thiosemicarbazone (L1)

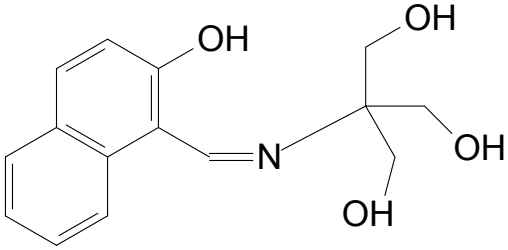

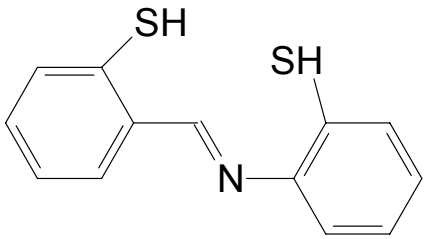

N-(2-mercaptophenyl)thiosalicylideneaminate

2-Hydroxynaphthalene-1-carbaldehyde-tris(hydroxymethyl)aminomethane (L3)

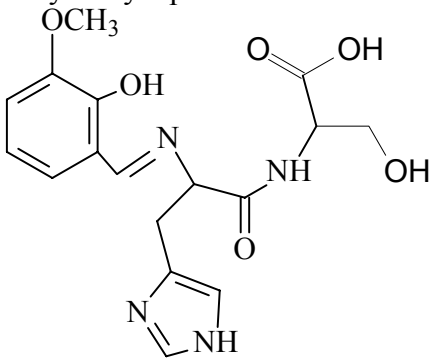

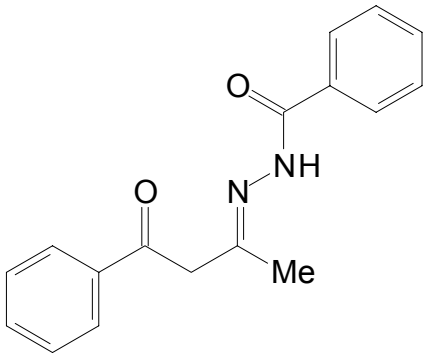

N-(2-oxido-3-methoxysalicylidene)-histidyl-serine

Phenylacetylacetonato-benzoylhydrazone

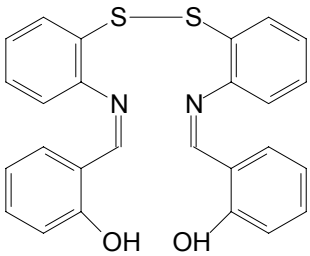

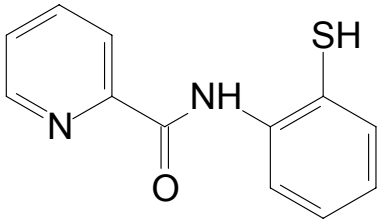

N,N'-[dithiobis(phenylene)]bis(salicylideniminate)

N-2-mercaptophenyl-2’-pyridinecarboxamide

The used cryptands

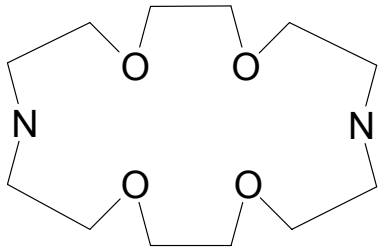

C22

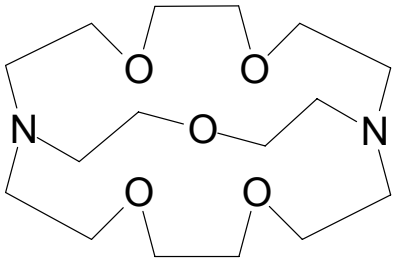

C221

4,13-Diaza-18-Crowne-6, 1,7,10,16-Tetraoxa-4,13-diazacyclooctadecan

4,7,13,16,21-Pentaoxa-1,10-diazabicyclo[8.8.5]-tricosane

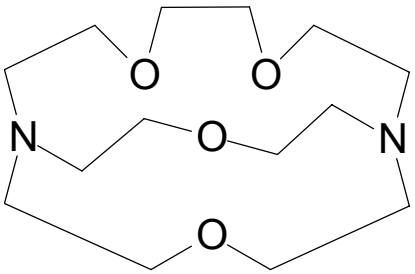

C211

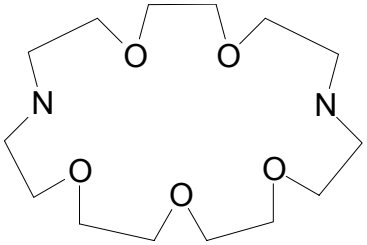

C23

4,7,13,18-Tetraoxa-1,10-diazabicyclo[8.5.5]-eicosane

1,7,10,13,19-Pentaoxa-4,16-diazacycloheneicosan

Contents

1. Introduction

The abundance of vanadium - 0.015% of the Earth's crust - compares to that of zinc, and, again comparable to zinc, vanadium is omnipresent, an important precondition for the potential use of a metal during evolution of life. Even more important, since it is thought that life evolved in the aqua sphere, is the comparably high abundance of vanadium in sea water. Next to molybdenum, vanadium is in fact the most abundant transition metal available in sea water, and this is due to its ability to form easily soluble vanadate under aerobic conditions, where it is present in the form of dihydrogenvanadate, ion-paired with sodium ions from the salt contents of sea water. The average concentration of $Na^{+}H_2VO_4^{-}$ amounts to 30 nM; compare 100 nM for molybdate, and 0.02-1 nM for iron.

Availability is one important factor for the biological use of an element. Another essential factor arises from the necessity for an organism to employ an element in some kind of processes essential to maintain its metabolism. This condition is again fulfilled for vanadium, since it easily switches between the oxidation states +V (in the form of vanadate, VO^{3+} or VO_2^{+}) and +IV (commonly in the vanadyl form, VO^{2+}). The +V state is the stable one under aerobic conditions, the +IV state under anaerobic conditions, i.e. in the cytoplasm. At pH 7 and a vanadate:vanadyl ratio of 10^3, the redox potential is -0.17 V, hence in a range where redox chemistry under physiological conditions occurs. The +III state (V^{3+}) is also feasible. Consequently, vanadium thus takes over the role of a cofactor in redox enzymes and in oxo-transfer enzymes and thus resembles molybdenum, to which there exists a diagonal relationship.

Two vanadium-dependent enzymes are known to date: One of these enzymes is vanadium-nitrogenase from nitrogen fixing bacteria of the genus Azotobacter. Vanadium, in medium oxidation states, is a constituent of an iron-vanadium cofactor, bonded to three bridging sulfides, a histidine and the vicinal carboxylate and alkoxide of homocitrate. The second group of enzymes are vanadate-dependent haloperoxidases from marine sea weeds, terrestrial lichens and moulds. Here, vanadate(V) is coordinated covalently to a histidine of the protein matrix. Haloperoxidases catalyze the two-electron oxidation, by peroxide, of halide to hypohalous acid, which halogenate organic substrates. Haloperoxidases also exhibit a sulfide-peroxidase activity and, in their apo-form, phosphatase activity.

The latter aspect is of interest in the context of a general antagonism between vanadate und the structurally related phosphate. Vanadate inhibits many phosphate-metabolizing enzymes, such as phophatases, kinases and ribonucleases, and it stimulates a few other enzymes, e.g. certain phosphamutases. The inhibition of phosphatases is of particular interest, since the insulin-mimetic behavior (stimulation of glucose uptake by glucose-metabolizing cells) of vanadium compounds has been traced back to the inhibition of an intracellular protein-tyrosine-phosphatase, which otherwise deactivates the signal transduction path-way in the absence of insulin (diabetes mellitus type 1) or in case of insulin tolerance (diabetes mellitus type 2). This has led to extensive investigations into a potential medicinal application of vanadium coordination compounds for the oral treatment of diabetes, an aspect which is also included in the present thesis.

A vanadium compound, once administered and absorbed, will encounter thiolate (cysteinate), disulfide (cystine) and thioethers (methionine) in biofluids, particularly glutathione and its oxidised form in the intracellular medium. It is therefore of interest, and has thus been included in the present studies, to model the coordination behavior of thiofunctional ligands on the one hand, and their redox interaction with vanadium on the other hand. Again, these investigations are also related to the direct vanadate-phosphatase interaction, since several phosphatases contain cysteine at their active center; and inhibition by vanadate can thus be achieved either by coordination to or redox-inactivation of active center cysteinate.

An additional medicinal aspect with respect to vanadium chemistry is the inhibitory action towards phosphatases not only by simple vanadates, but also by the highly condensed form of vanadate, viz. decavanadate, which forms as the pH drops below 6.3. Decavanadates, like other polyoxometallates, have also been shown to be potent anti-viral and -retroviral agents - leaving apart their importance as redox catalysts in oxo transfer reactions. At the low overall vanadium concentrations in biofluids and a pH commonly higher than 6.3, condensed forms of vanadate can only exist if they are stabilized. A putative assumption is that stabilzation is carried out by ionophores. Ionophore models such as cryptands and related macrocyclic ligands have thus been used in the present investigations to check their stabilizing effects towards iso- and heteropolyvanadates.

2. background and present stand of research

2.1 Vanadium complexes with thio-containing Schiff bases and related ligands, and their insulin-mimetic activities

Vanadium coordination chemistry and biochemistry have attracted increasing interest during the last few years [1]. This is mainly due to the discovery that vanadium is an essential element in biological systems. Vanadium, participates in enzymatic reactions such as the halogenation of a variety of organic substrates by haloperoxidases [2], and nitrogen fixation by vanadium nitrogenases [3] The use of (oxo)vanadium complexes in oxidation and oxo transfer catalysis [4] has been noted. The potential medicinal application such as the treatment of diabetes type I (insulin deficiency) and II (insulin resistance) [5] has further stimulated research into vanadium coordination compounds; the recent human clinical trials of oral treatment of diabetes with oxomaltolatovanadium(IV) species appears to be promising. In addition, vanadate has shown great utility as a tool in molecular biology for recognizing and understanding the structure of phosphate binding proteins, and as a mediator of catalytic photo-cleavage of the peptide backbone [6]. In order to understand and elucidate the biological role of vanadium, many low molecular weight model complexes with the biologically important oxidation states +II to +V have been synthesized and characterized in recent years [7,8]. In particular, vanadium complexes with ligands containg thiol functions have been paid great attention to, due to the fact that vanadium complexes with thiofunctional ligands model vanadium nitrogenase, and contribute to a better understanding of the redox behaviour of vanadate compounds in the intracellular medium, also in the context of insulin-mimetic effects, which may be traced back to the redox-inhibition of a tyrosine kinase or tyrosine phosphatase [9,10] containing a cysteine residue at the active site.

2.1.1 Vanadium complexes with thiol-containing Schiff-base ligands

Although there are still many difficulties in the synthesis of vanadium complexes with thiol-containing Schiff-base ligands (on the one hand, if a Schiff-base ligand contains a thiolate group, it is usually unstable, isomerises to thiazoline and finally is oxidized to thiazol [11,12]; on the other hand, the reaction of vanadium (V) or (IV) with thiol-containing molecules usually results in the reduction of vanadium and in the concomitant oxidation of

the thiol-containing molecules to disulfide [13]), many vanadium complexes have been successfully synthesized until now.

J. C. Dutton et al. have prepared a thiol-contaning vanadium (IV) complex by using a one-pot method [14]. The presence of vanadium cannot only catalyze the formation of the Schiff base, but also stabilize the ligand against isomerisation. In this compound (Fig. 1), the vanadium ion is in a distorted tetragonal pyramidal environment consisting of two imine nitrogens and two thiophenolates in the basal plane, from which it is displaced by 0.668Å.

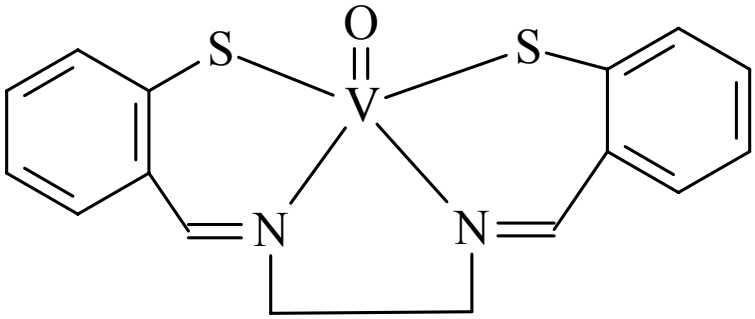

Fig. 1 Scheme of $V^{IV}O$(tsalen) [14]

M. Farahbakhsh has successfully synthesized a $V(ONS)_2$ vanadium complex (Fig. 2) by using an indirect method [15]: $[VOCl_2(thf)_2]$ was first reacted with o-mercapto-aniline and possibly forms a V^{IV} intermediate. After addition of *o*-hydroxy-naphthaldehyde, $V(ONS)_2$ was formed. The coordination of this trifunctional Schiff base ligand apparently prevents it from isomerising to a thiazoline, a conversion which is observed in the absence of a stabilising coordination centre. Here, vanadium is in a highly distorted trigonal prismatic

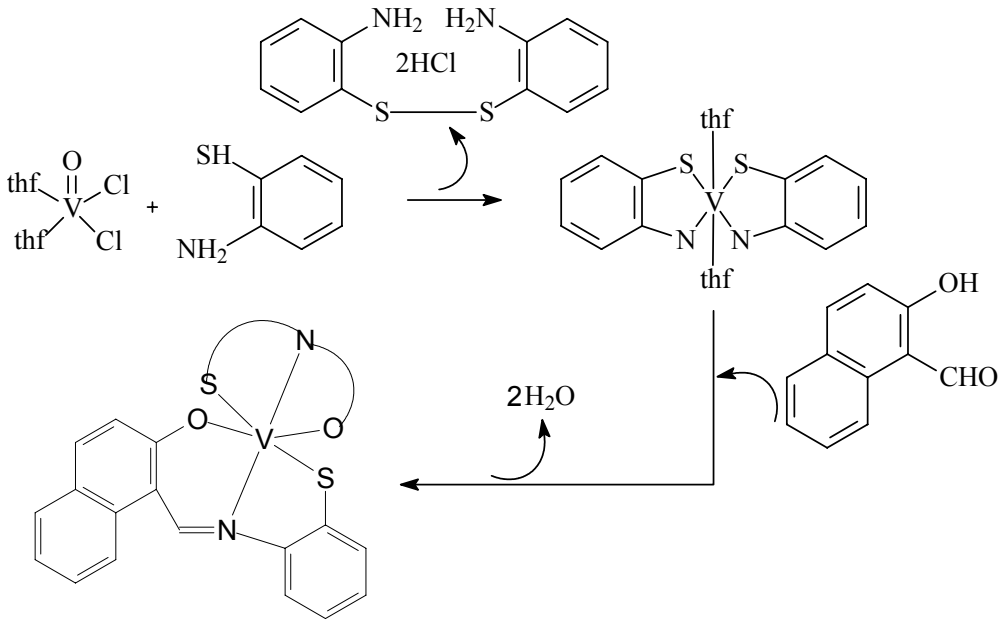

Fig. 2 Synthesis of compound $V^{IV}(ONS)_2$

environment; the twist angle between the two trigonal planes spanned by S, N, and O amounts to 69°, the two planes are inclined towards each other by 28.6°.

M. Ebel has synthesized a series of vanadium(V) complexes, containing thiolate in the Schiffbase related ligand, by using dithiocarbonylhydrazone [16]. Using hydrazone ligands with a "masked" thiolate function could be the major reasons to resist the common oxidation of thiolates to disulfides by vanadium and the isomerization of the ligand. Here, vanadium(V) is in a tetragonal pyramidal environment (Fig. 3) consisting of one imine nitrogen, one thiophenolate, one alcoholate and one phenolate in the basal plane Vanadium is 0.49Å above the mean plane defined by the basal atoms. The bicyclic system formed between the vanadium centre and the tridentate ligand is slightly folded along the V-N1 axis: The angle between the planes V-O3-C6-C11-C3-N1 and V-N1-N2-C2-S2 amouts to 16.92.

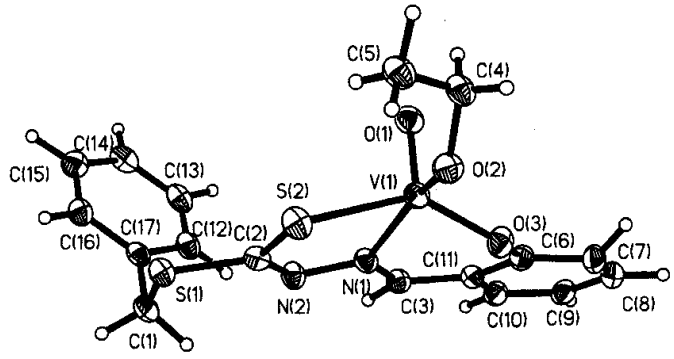

Fig.3 Scheme of $[V^{V}(OEt)(ONS)]$ [16]

2.1.2 Vanadium complexes with related ligands

In order to understand vanadate haloperoxidase, which contain vanadate covalently linked to a histidine nitrogen, many complexes containing ligands with O_xN_y functions including Schiff bases have been synthesized in recent years. These compounds have in common that their coordination sphere is dominated by oxygen functions, one to two of which are oxo groups, and the others are coming from an alkoxide, alcoholate, phenolate or carboxylate donor. The nitrogen functions are provided either by imines or amines. The coordination geometries of the complexes vary between trigonal-bipyramidal and tetragonal-pyramidal.

D. C. Crans has synthesized oxovanadium(V)triethanolamine in 1993 [17] (Fig. 4). The structure shows that the amine nitrogen and the oxo group occupy the axial positions in a trigonal-bipyramidal coordination array. The vanadium atom is pulled out of the plane formed

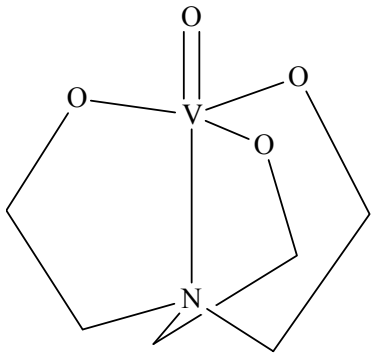

Fig.4 Structure of $[V^{V}O\{(OCH_2CH_2)_3N\}]$ [17]

by the triethanolaminate oxygen atoms in the direction of the doubly-bonded oxygen by 0.342Å; the distortion of the trigonal bipyramidal vanadium geometry is thus toward a tetrahedral geometry rather than a square planar geometry. The N-V bond length of 2.276(7)Å *trans* to the oxo group appears long when compared to V-N bond lengths in other penta-coordinate vanadium complexes, which can be traced back to the *trans* influence of the oxo group.

M. Bashirpoor has synthesized {VO(acetylacetonato)[(*R*)(*S*)-N,N-bis-(2-oxiethyl)]-1-phenylaminoethane} in 1996 (Fig. 5). The complex has been found to catalyse the oxidation of organic sulfides to sulfoxides by peroxide [18,19]. Here, vanadium(V) is in a tetragonal bipyramidal environment, with an oxo group and the amine nitrogen in the axis, and three alcoholate and one carbonyl functions in the basal plane. Vanadium is 0.28Å above the basal plane. The distance V-N = 2.526Å is obviously longer than in other complexes, a possible reason for the activity in the catalysis of the oxidation of organic sulfides to sulfoxides by peroxide: the weak bond may break under turn-over conditions, making available a site for substrate binding.

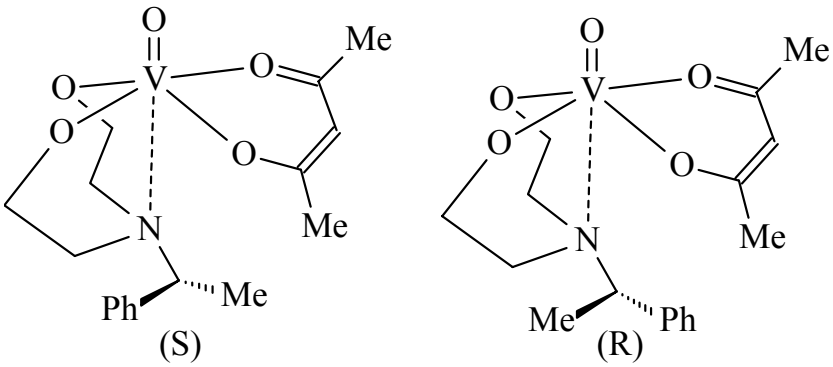

Fig. 5 Structural model of the active site of vanadate-dependent haloperoxidase

2.1.3 Disulfide-Schiffbase complexes

Although many disulfides RS-SR are easily reduced by metal ions, this is not always the case. Several complexes of copper, cobalt, nickel, iron etc. [20-22] have been synthesized and their structures have been determined by X-ray diffraction analysis. Therefore, the existence of the disulphide bond in metal complexes has been clearly demonstrated.

J. A. Bertrand et al. have synthesized an iron complex, which contains a disulfide Schifbase ligand, chloro[bis(salicylideneiminophenyl)disulphide]iron(III), [Fe(salps)Cl] (Fig. 6). The structure reveals a monomeric Fe^{III} complex in a distorted octahedral coordination environment [23]. The dianion functions as a pentadentate ligand, coordinating to the iron atom through the two phenolic oxygens, the two imine nitrogens and one of the sulfur atoms of the disulfide group. The ligand forms three six-membered chelate rings and one five-membered chelate ring; one of the phenolic oxygens is *trans* to the coordinating sulfur atom, the second sulphur atom is at a distance of 3.79Å from the iron atom and is not considered coordinated (Fe-S1 = 2.53Å).

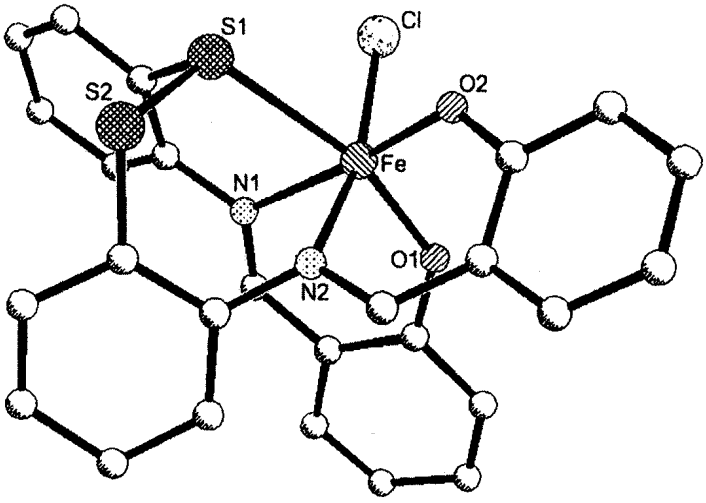

Fig. 6 Structure of [Fe(salps)Cl] [23]

2.2. Insulin-mimetic activities of vanadium complexes

Diabetes is a mammalian disease in which the amount of glucose in the blood plasma is abnormally high [24]. The condition can be acutely life-threatening, since patients with diabetes suffer from a number of secondary complications, such as atherosclerosis, microangiopathy, renal disease, cardiac disease and diabetic retinopathy and other vision disorders including blindness. Millions of sufferers control diabetes by daily insulin

administration and/or a special diet. Insulin supplementation is the easiest method to control chronic diabetes; however, insulin is not orally active and must be taken by injection. In addition, insulin is essentially inactive in type II diabetes, which is by far the more freqent type of this disease. The development of insulin-mimetic compounds for oral administration would thus be very useful [25]. In fact, vanadium compounds have a long history as insulin mimetic agents. Sodium vanadate was reported to have an oral insulin-like effect in human diabetes in 1899 [26]. However, it is only in the last decade or so that the pharmacological potential of vanadium has been systematically explored, starting with Heyliger et al. in 1985 [27]. Possible actions of vanadium are illustrated in Fig. 7.

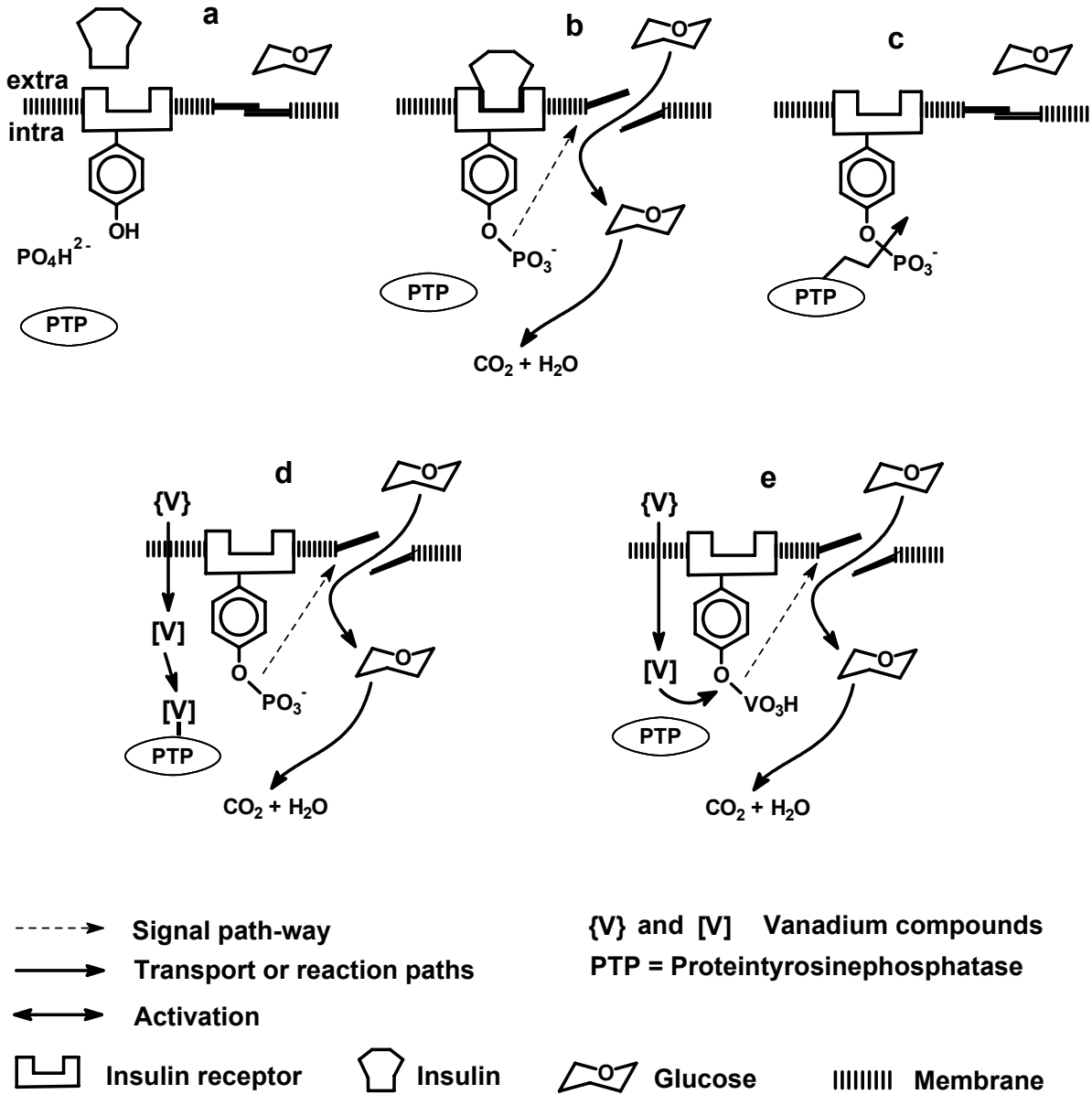

Fig. 7 Possible insulin-mimetic action of vanadium compounds:

(**a**) Starting situation; (**b**) Insulin docks to the membrane receptor and induces tyrosine phosphorylation, which in turn triggers glucose intake; (**c**) Protein-tyrosine-phosphatase hydrolyses the phosphate-tyrosine bond and thus interrupts signal transduction in the absence of (or resistence against) insulin; (**d**) Vanadate inhibits PTP; signal transduction remains intact through autophosphorylation of tyrosine; (**e**) Alternatively, tyrosine is vanadylated.

Aside of vanadium complexes, many other metal compounds, such as derived from molybdenum, tungsten [28] and zinc [29] have been tried, both *in vivo* and *in vitro*, but none have rivaled vanadium salts as effective insulin substitutes. A possible reasons could lie in the structural resemblance between vanadate and phosphate, which leads vanadium complexes to have the ability either to inhibit the protein tyrosine phosphatase or to activate the insulin receptor kinase and/or glucose carrier, thus triggering glucose intake into cells (Fig. 7).

Since 1980, considerable evidence has been provided that vanadium salts, specifically tetravalent vanadyl, usually found as the divalent cation VO^{2+}, and pentavalent vanadate, $H_2VO_4^-$, have the ability to mimic insulin action in a number of isolated cell systems and to produce dramatic glucose lowering effects when given orally to animal models of both types I and II diabetes mellitus [30,31]. Sodium orthovanadate has been found to stimulate glucose uptake and glucose oxidation in rat adipocytes, stimulate glycogen synthesis in rat diaphragm and liver and inhibit hepatic gluconeogenesis [32]. A very exciting finding was that vanadate could be administered orally, with a long-term insulin mimetic effect, *in vivo*. Oral vanadium(V) treatment of diabetic animals partially or completely restored liver and muscle enzyme activities involved in glycolysis [33-35], without stimulating increased insulin synthesis [36,37]. In addition, McNeill et al. have shown that oral administration of vanadyl sulfate also lowers blood glucose and blood lipids in STZ (streptozotocin) induced diabetic rats, and prevents secondary complications of diabetes such as cataracts and cardiac dysfunction [38-40]. As far as toxicity is concerned, the vanadyl ion (VO^{2+}) is superior to vanadate in that it is less toxic. At pH values > 4.5, however, i.e. as soon as the vanadyl sulfate leaves the stomach, sparingly soluble oxovanadium hydroxides are formed. The absorption thus depends on the formation of secondary compounds with ligands provided by the intestinal medium, a process which reduces the absorption rate to about 2% [41]. In consideration of the low intestinal absorption of vanadyl and the high toxicity of vanadate (vanadate is an effective inhibitor of many phosphate-metabilzing enzymes), a search for alternative vanadium compounds containing organic ligands has been initiated. The recent successes achieved with organic transition metal complexes suggest that modifications of the

metal ion chemistries by the organic ligands not only increased efficacy but also decreased toxicity.

Most of the compounds reported contain bidentate ligands and have a 1:2 metal-to-ligand stoichiometry. An example is [VO(maltolate)$_2$] (BMOV) [42], which is prepared nearly quantitatively in water (>90% yield) by combining vanadyl sulfate trihydrate and maltol (3-hydroxy-2-methyl-4-pyrone) (1:2), and which dissolves (mM scale) in a number of organic solvents and water. BMOV has one unpaired electron, characteristic of the vanadyl unit, and a fairly high V=O stretching frequency in the IR (995 cm^{-1}), suggesting that there is no ligand (or just a weakly bound solvent) in the sixth position. The crystal structure of this compound shows that the two ligands are oriented *trans* to each other in the base of a square pyramid [43] (Fig. 8). BMOV has been shown to have a strong glucose-lowering effect; in *in vivo* studies; it is roughly three times more effective than uncomplexed vanadyl (in the form of vanadyl sulfate) [44], with no evidence of toxicity. Clinical tests are in progress [42].

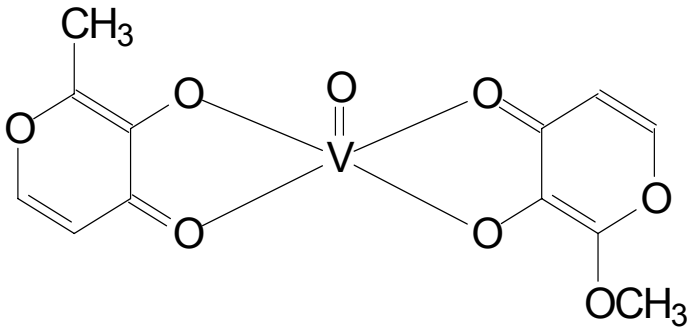

Fig. 8 BMOV [42]

H. Sakurai et al. have prepared a series of complexes with the $V^{IV}O(N_2O_2)$ coordination mode, in order to study the structure-activity relationship of antidiabetic vanadyl complexes (Fig. 9). Among these, Vo(picolinate)$_2$ (VOPA) has been found to be very effective in normalizing the serum glucose levels of STZ-induced diabetic rats when given intraperitoneally or orally [46]. In *in vivo* testing, M. Melchior et al. have also found that VOPA has modest glucose lowering activity, without accompanying plasma insulin elevation or food intake suppression [47].

In addition, organic vanadium complexes containing polydentate ligands and having a 1:1 stoichiometry have also been paid great attention to [50-52]. Dipicolinic acid has been successfully tested in this respect recently [51,52]. The respective vanadium complex is desirable because of its low toxicity and its amphophilic nature. The synthesis and structure of [VO$_2$dipic]$^-$ were reported previously [52,53]; vanadium is five-coordinate (Fig. 10).

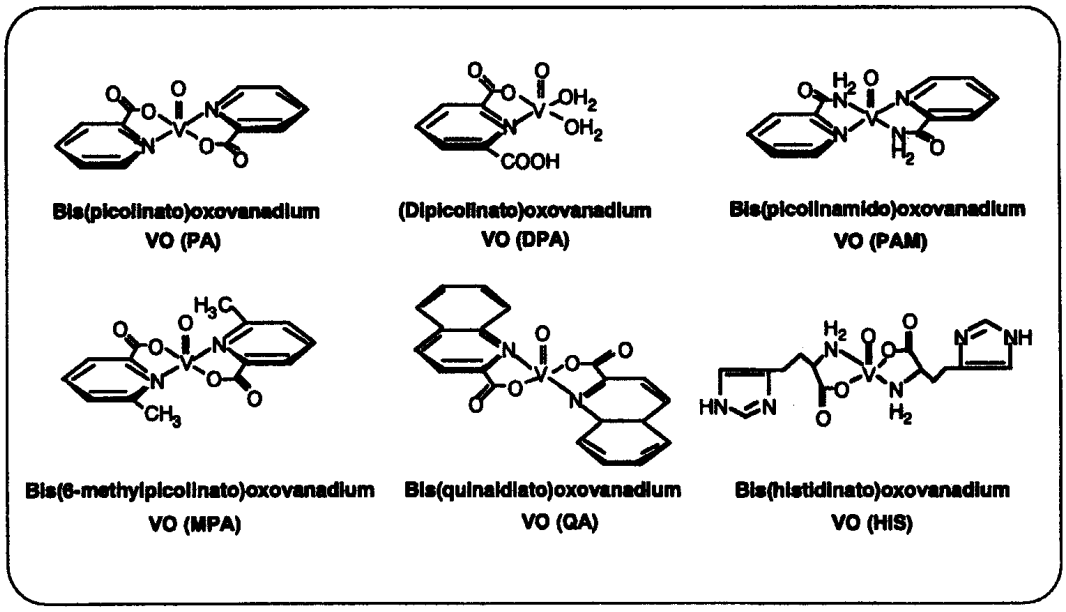

Fig. 9 Structures of vanadyl complexes synthesized by H. Sakurai et al. [45]

Differing from all known effective insulin-mimetic organic vanadium compounds, which have a neutral charge, $[VO_2dipic]^-$ is anionic. After finding that the vanadium(V)-dipicolinate is a more potent inhibitor for phosphatases than the corresponding vanadium(IV) complex [54], D.C. Crans et al. have continued to study the activity of $[VO_2dipic]^-$ *in vivo*, and found that it is effective as an oral agent [51-53]. The compound has also been successfully applied orally to diabetic cats [55].

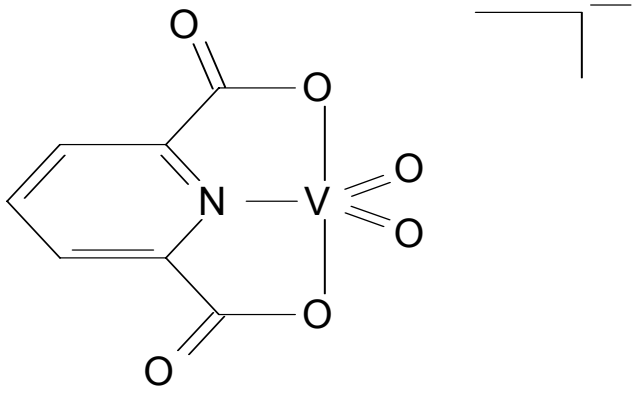

Fig. 10 Structure of $[VO_2dipic]^-$

2.3 Polyoxovanadate-ionophore systems

Early transition metals in their highest oxidation states are able to form metal-oxygen cluster anions, commonly referred to as polyoxoanions [56] or polyoxometalates (POMs) [57]. According to the components, they can be divided into two generic families: the isopoly compounds (also called isopolyanions or isopolyoxometalates) that contain only the d^0 metal cation and oxide anions (e.g. $V_{10}O_{28}^{6-}$), and the heteropoly compounds (also called heteropolyanions or heteropolyoxometalates) that contain one or more p-, d- or f- block heteroatoms in addition to the other ions [57,58] (e.g. $XM_{12}O_{40}^{3-}$ or $X_2M_{18}O_{62}^{6-}$). The heteroatom in the heteropoly compounds can reside in either a buried (not solvent accessible) or a surface (solvent accessible) position in the POM structures.

Few, if any, other classes of compounds can be so extensively modified. Virtually all molecular properties that impact the utility of this class of compounds in catalysis, medicine, and material science can be altered in POMs, e.g. the molecular composition, size, shape, charge density, redox potential (ground and excited state), acidity and solubility. The extreme variability of the accessible POMs derives in good measure from the point that most of the elements in the periodic table can be incorporated into the structural framework of these compounds. On the basis of these properties, they have been extensively investigated in the last century, especially in the catalytic field. Systematic research into heterogeneous catalysis that started in the mid-1970s has disclosed the presence of quantitative relationships between the acid or redox properties and catalytic performance of heteropoly catalysts as well as their unique behaviour in heterogeneous catalysis [59-72]. Several new industrial processes that utilize heteropoly catalysts, such as oxidation of methacrolein, hydration of olefins (propene and butenes), polymerisation of tetrahydrofurane etc. have recently been developed and commercialized [73,74] Especially the direct oxidation of ethylene to acetic acid, which is catalysed by palladium plus heteropolyacids (HPAs), has been developed at the end of 1997 in Japan (100,000 tons/year) [75]. Other processes or technologies based on derivatives of POMs are in rapid development.

As for the study of POMs in medicine, it can be traced back to the seventies of the 20^{th} century, when the first POM compound, HPA-23 (Fig. 11) [76-80], was found to have antiviral activity. As has been said above, nearly every molecular property that impacts the recognition and reactivity of POMs with target biological macromolecules can be altered. Since then many different kinds of POMs have been tested *in vivo* and *in vitro* and found to be biologically active. For example, the vanadate dimer $H_2V_2O_7^{2-}$ has been found to be both an inhibitor and an activator for dehydrogenases, isomerases, and phosphatases [81]. The

vanadate tetramer $V_4O_{12}^{4-}$ inhibits dehydrogenases and aldolases [81,82]. The vanadate tetramer also appears to be the active species in the photolytically-induced cleavage

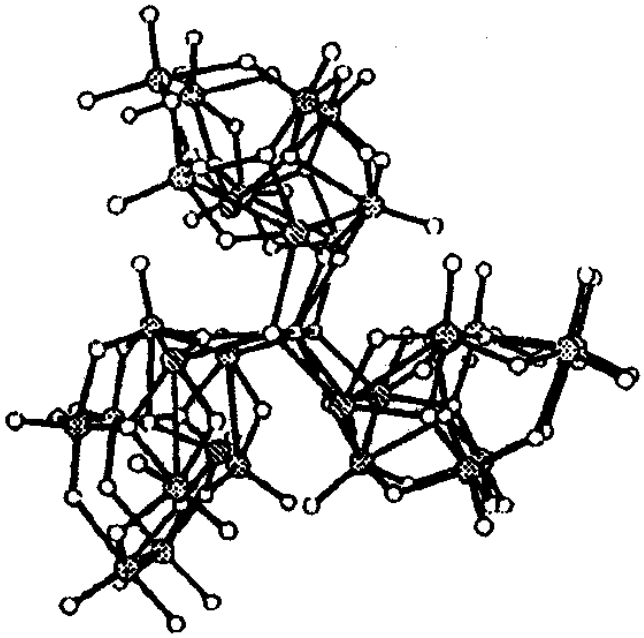

Fig. 11 Structure of HPA-23, $[NaSb_9W_{21}O_{86}]^{18-}$, [76-80]

of myosin at the phosphate binding sites, despite of the fact that the tetramer only has a modest affinity for this protein [83]. Vanadate decamers $H_xV_{10}O_{28}^{(6-x)-}$ show high affinity for selected kinases, phosphorylases and reverse transcriptases, as illustrated by the potent inhibition of phosphofructokinase [84]. Decavanadate has previously been used to facilitate crystallization of proteins, and the Ca^{2+} transport by ATPase and adenylate kinase [85].

A key point in all biological/physiological studies of POMs is the issue of whether the POMs stay intact during treatment. Many POMs are thermodynamically and kinetically unstable in water at physiological pH and degrade into a mixture of inorganic products. At pH around 7 and nanomolar vanadium concentrations, decavanadate hydrolyses to monovanadate [86], which is further reduced in the intracellular medium to VO^{2+}. Once administered, however, or formed at special cell sites, polyoxometalates become inaccessible to degradation. Several lines of evidence using different techniques and types of experiments indicate that POMs remain intact inside the cell. Cholewa et al. used a scanning proton microprobe to confirm the presence of $[Co_4(H_2O)_2(PW_9O_{34})_2]^{10-}$, a sandwich-type heteropolytungstate, inside the cellular membrane of human peripheral blood mononuclear cells (PBMC) [87]. They have made two observations consistent with the POM remaining

intact inside the cells: first, the W/Co ratio remained the same as that in the intact POMs, and second, both elements were located in the same area of the cell.

The stability of POMs under physiological condition is possibly a result of the association with suitable biogenic molecules, such as proteins (kinase, phosphorylase, oligopeptides like kemptide) or macrocyclic ligands (ionophores). In order to testify this possibility, POMs with organic ligands can be taken as model system. For example, J. M. Arrieta has synthesized many different kinds of pyridinium-decavanadate complexes in 1992 [88]:

Tetrakis(pyridinium)dihydrogendecavanadate $[(C_5H_5NH)_4(V_{10}O_{28}H_2)]$,

Tetrakis(2-ethylpyridinium)dihydrogendecavanadate $[(C_7H_9NH)_4(V_{10}O_{28}H_2)]$,

Tetrakis(3-ethylpyridinium)dihydrogendecavanadate $[(C_7H_9NH)_4(V_{10}O_{28}H_2)]$,

Hexakis(pyridinium)decavanadate $[(C_5H_5NH)_6(V_{10}O_{28})]$,

Hexakis(3-methylpyridinium)decavanadate $[(C_6H_7NH)_6(V_{10}O_{28})]$,

Hexakis(4-methylpyridinium)decavanadate $[(C_6H_7NH)_6(V_{10}O_{28})]$.

The presence of the corresponding organic cation is suggested by the existence of two weak bands in the IR around 2300-2100 cm^{-1}, appertaining to the vibration of the $C=NH^+$ bond. The distances between the nitrogen atoms of pyridinium and oxygen atoms of the decavanadate anion are 2.63-2.90 Å, suggesting that there are hydrogen-bonding interaction among the

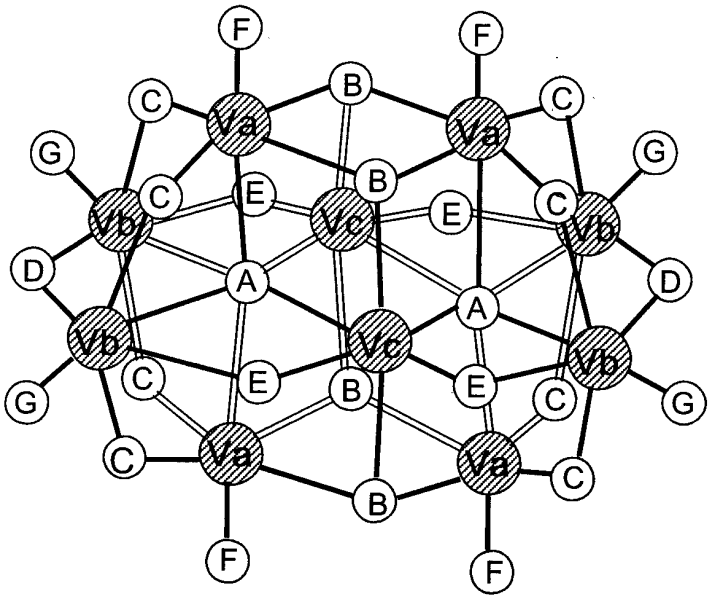

Fig. 12 Schematic drawing of the decavanadate anion, showing the 3 different vanadium and 7 different oxygen sites

components. This phenomenon can also be testified by IR spectrometry, i.e. the νCH (1028-1015 cm^{-1} for the free bases) vibrations are split and/or displaced by 3-21 cm^{-1} for all of the above compounds, which indicates the existence of an intermolecular hydrogen bond via the pyridinium nitrogen. The oxo ligands of the decavanadate taking part in hydrogen bonding are either trebly (**B**) or doubly (**C**) bridging oxygens (Fig.12). In order to detect the protonation sites, the valence bond orders $\sum_s = \left(d / R_o \right)^{-N}$, introduced by Brown, can be employed. While d is the experimental V-O bond length; R_o and N are listed constants, which have values of 1.79 and -5.1[89], respectively, for oxygen bound to vanadium. The calculations indicate that the protonation sites are **B** or **C** type bridging oxygens of the decavanadate anion, showing that these oxygens are more basic than the terminal ones (**F** and **G**) and other bridging oxygens (**D**, **E**, **A**). Kempf et al. have also confirmed this result by means of ab initio and electrostatic potential calculation [90].

In order to model the interactions of POMs with proteins, D. C. Crans et al. have structurally characterized a decavanadate-dipeptide compound, viz. $(NH_4)_6$(Gly-Gly)$_2V_{10}O_{28}\cdot 4H_2O$ in 1994 [91]. In this compound (Fig. 13), the C-O distances observed for

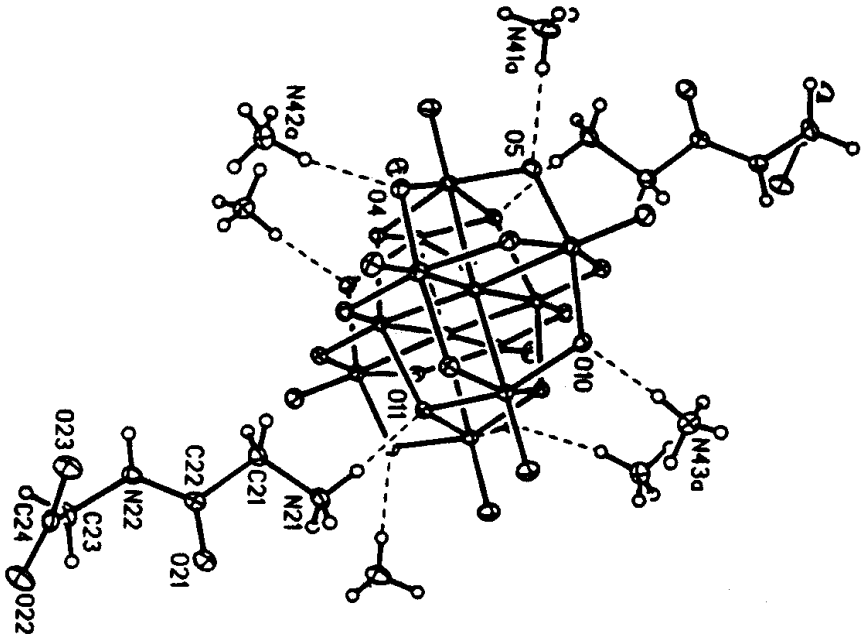

Fig. 13 Crystal structure of $(NH_4)_6$(Gly-Gly)$_2V_{10}O_{28}\cdot 4H_2O$ [91]

the gly-gly carboxylate groups are in the range for deprotonated carboxylate, suggesting that the dipeptide is present as a zwitterion. In addition, the water molecules and ammonium ions interact with the decavanadate anion via hydrogen bonding. Each of the ammonium ions

forms a hydrogen bond with a doubly bridging oxygen atom of the decavanate anion (N41---O5 = 2.731 Å; N42----O4 = 2.812 Å; N43----O10 = 2.799 Å). Simultaneously, the protonated amino terminus of the dipeptide(Gly-Gly) forms a hydrogen bond to a trebly bridging oxygen atom (N21----O11 = 2.707 Å).

Whether POMs can also be protected against hydrolysis in this way is still our researching goal. By studying the vanadate/adenosine-monophosphate (5'-AMP) system, M. Farahbakhsh has seripenditiously synthesized a cryptand-decavanate system, viz $[C222(H^+)_2]_2[H_2V_{10}O_{28}]\cdot 2H_2O$ [92]. It crystallizes in the centro-symmetric space group P-1. In this compound, the oxygen atoms of the cryptand cation are oriented inwards towards the cryptand cativity in a symmetrical manner, and the protons form an inter-cavity hydrogen-bonding network. The cryptand cations interact with the decavanadate anion by using only

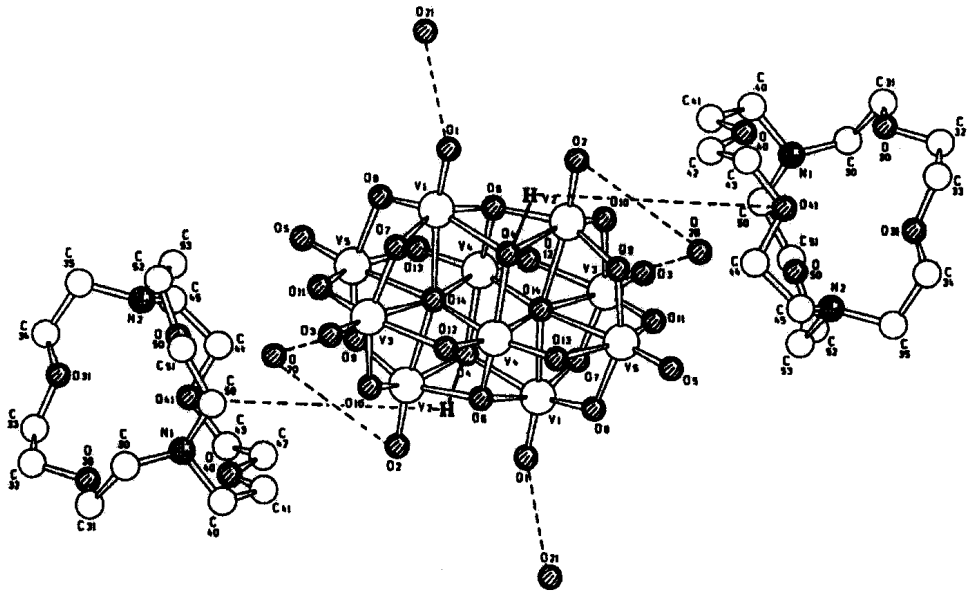

Fig. 14 Crystal structure of $[C221(H^+)_2]_2[H_2V_{10}O_{28}]\cdot 4H_2O$ [93]

part of the heteroatoms. A sandwiched structure is formed, i.e. the decavanadate anion is inlayed between the two diprotonated cryptand cations. In order to further testify the possibility of stabilising decavanadate by cryptands, a second system was synthesized, namely $[C221(H^+)_2]_2[H_2V_{10}O_{28}]\cdot 4H_2O$ (Fig. 14), by the slow diffusion method [93]. Like the first one, it forms a centro-symmetric sandwiched structure. In addition, there is a (relatively weak: *d*(O4----O41) = 3.006 Å) hydrogen-bonding interaction between the **B** type μ_3-O4 and one of the ether oxygens of the diprotonated cryptand cations, leading to an orientation of the decavanadate with respect to the sandwiching cryptand cations different from the compound $[C222(H^+)_2]_2[H_2V_{10}O_{28}]$.

3. Results and Discussion

1. Vanadium complexes and their insulin-mimetic activity

As previously stated, vanadium compounds are of particular interest due to their biological properties. Certainly, one of the most promising aspects in this context is their potential as a substitute for insulin. Many vanadium compounds have been synthesized, structurally characterized and tested for insulin-mimetic activity, some of them have been found to enhance insulin action when administered orally, such as BMOV[42]. In order to be effective as biomimetic drugs, vanadium complexes should fulfil a number of precondition:

1. Hydrophilicity and lipophilicity should be balanced by an appropriate design of the ligand systems in order to allow absorption and transport in the blood stream.
2. The complex should be stable, at least to the extent where it partially survives the acidic conditions in the stomach.
3. The ligand sphere should contain a site for bio-recognition in order to facilitate the transmembrane transport.
4. The complex should contain an empty or easily accessible (by ligand exchange) site for coordination to the target molecule.
5. At the end, the complexes should, of course, exhibit minimized toxicity.

In the light of these requirements, some vanadium compounds have been prepared by chosing different kinds of ligands in the following work, and tested for their insulin-mimetic efficacy and toxicity by using modified fibroblast cells from mice.

1.1 Preparation and characterization of complexes

The ligands, which were used in the following work, contain different donor atom sets, such as ONS, NS, and N_xO_y. The corresponding complexes are presented in Table 4 by structural formulae, based on structure determination or deduced on the basis of known structures of related complexes, elemental and spectroscopic analyses.

1.1.1 *[VOCl{(N-thiosemicarbazone)-5,6-benzosalicylidene-aminate}* (**1**)

Reaction of $VOCl_2(thf)_2$ and the thiosemicarbazone ligand in abs. THF in an inert gas atmosphere resulted in the formation of green complex **1** (yield: 50%). **1** is air stable in the

solid state, moderately soluble in acetone, but highly soluble in DMF and DMSO. The Schiff base ligand containing a thioamide function -NH-C(S)- may exhibit thione-thiol tautomerism (Fig.15). The IR spectra of the Schiff base, however, do not display any ν(S-H) band at ca. 2500cm^{-1}, but show the ν(NH) band at 3165cm^{-1}, indicating that, in the solid state, it remains as the thioketo tautomer. The peaks at 3276 and 3137 cm^{-1} are present also in the free ligand (3263 and 3165 cm^{-1}) ,

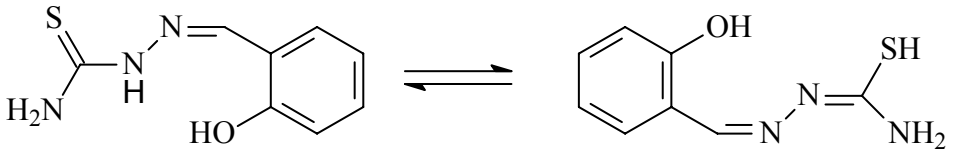

Fig. 15 Tautomeric forms of the thiosemicarbazone ligand

indicating that the ligand coordinates to the vanadium ion in its monoanionic tridentate keto form, a fact verified by the structure determination and the EPR spectrum (see below). The band at 1626 cm^{-1} associated with the ν(HC=N) stretching frequency of the free ligand is shifted to 1618 cm^{-1} in the corresponding complex **1**, indicating the coordination of the azomethine nitrogen. The ν(V=O) is at 995 cm^{-1}. An additional sharp and intense band observed for the crystal of **1**·Me_2CO at 1696 cm^{-1} is assigned to the ν(C=O) of acetone of crystallization. The bathochromic shift with respect to free acetone is due to the involvement of the carbonyl group in hydrogen bonding interaction with N-NH and C-NH_2 of the semicarbazone ligand, as identified by the X-ray structure analysis.

*Crystallographic studies of compound **1**·Me_2CO*

1·Me_2CO, obtained from the recrystallization of complex **1** in acetone, crystallizes in the monoclinic space group $P2_1/c$. Selected bond lengths and bond angles are listed in Table 1. Vanadium is in a tetragonal-pyramidal environment (Fig.16) with the doubly bonded oxo group O1 of the vanadyl moiety in the apical position, and the chloro ligand, O2, N1, and S3 of the tridentate thiosemicarbazone in the plane. Vanadium is 0.1378 Å above the the plane spanned by O2, N1, S3 and Cl. The bicyclic system formed between the vanadium centre and the tridentate ligand is slightly folded along the V1-N1 axis: The angle between the planes V1-S3-C12-N2-N1 and V1-N1-C11-C10-C1-O2 is 20.72°. There is some distortion towards a trigonal bipyramid, quantified by a τ value of 0.28, where τ is defined by τ = [(O2–V–S3) – (N1-V-Cl2)]/60; τ = 0 for an ideal tetragonal pyramid, and τ = 1 for an ideal trigonal bipyramid. Compared with the N1-C11 bond (1.303Å), the N2-C12 bond (1.334Å) is

significantly longer, and the S3-C12 bond (1.708Å) is shorter than in most structurally characterized Ni and Cu complexes with comparable ligands (ca.1.73-1.76 Å) [94-95],

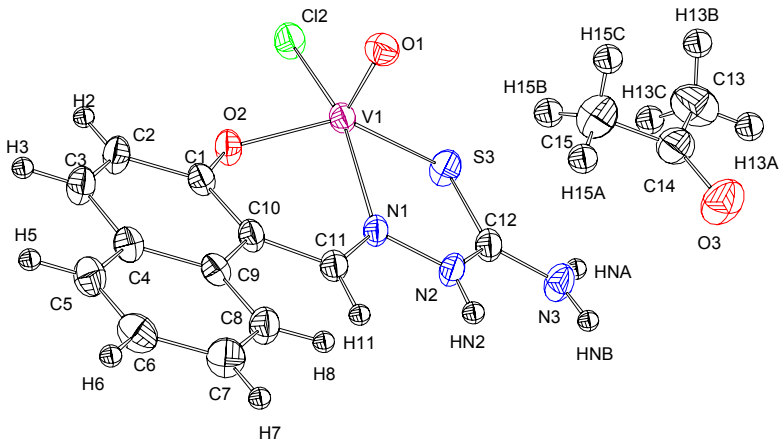

Fig. 16 Molecular structure of **1** (50% probability level)

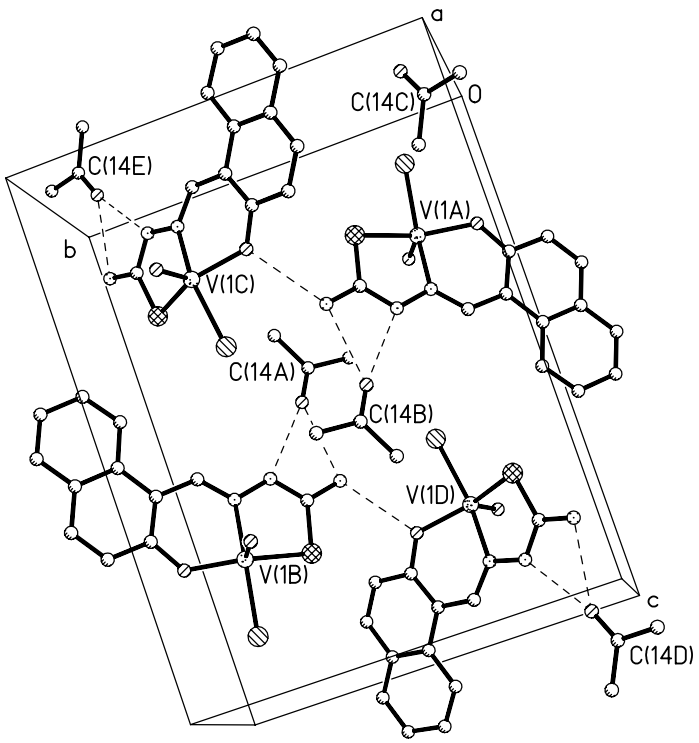

Fig. 17 Cell drawing of **1**

indicating coordination of the ligand through thiocarbonyl rather than through enthiolate. This is also verified by the localization of the hydrogen atom on the nonbonding N2, which is

Table 1. Bond Lengths (Å) and Angles (deg) for **1**·Me_2CO

V(1)-O(1)	1.590(2)	O(1)-V(1)-O(2)	111.03(11)
V(1)-O(2)	1.914(2)	O(1)-V(1)-N(1)	99.57(11)
V(1)-N(1)	2.087(3)	O(2)-V(1)-N(1)	84.36(9)
V(1)-Cl(2)	2.3408(10)	O(1)-V(1)-Cl(2)	105.78(9)
V(1)-S(3)	2.3579(10)	O(2)-V(1)-Cl(2)	89.71(7)
S(3)-C(12)	1.708(3)	N(1)-V(1)-Cl(2)	154.42(8)
O(2)-C(1)	1.334(4)	O(1)-V(1)-S(3)	110.58(9)
N(1)-C(11)	1.303(4)	O(2)-V(1)-S(3)	137.50(7)
N(1)-N(2)	1.391(3)	N(1)-V(1)-S(3)	80.69(7)
N(2)-C(12)	1.334(4)	Cl(2)-V(1)-S(3)	87.15(3)
		C(12)-S(3)-V(1)	98.63(11)
		C(1)-O(2)-V(1)	126.78(18)
		C(11)-N(1)-V(1)	125.4(2)
		C(11)-N(1)-N(2)	116.3(2)
		N(2)-N(1)-V(1)	118.07(18)

Table 2. Intermolecular interactions in **1**·Me_2CO and **2**·4DMF

1 ·$OCMe_2$				**2**·4DMF			
S3	→	H7	2.930	O1	→	H21B	2.792
		H8	3.091	O3	→	H21B	2.649
		H13A	3.115			H30	2.691
		H2	3.262			H22B	2.933
O3	→	HNB	2.028	O5	→	H31C	2.743
		HN2	2.154			O20	2.689
O2	→	HNA	2.019	O20	→	HO5	1.851
O1	→	H2	2.481			H21C	2.503
		H15B	2.846	O30	→	H21A	2.653
		H3	2.674			H20	2.666
		H6	2.608				
		H13B	2.656				

linked by an intermolecular hydrogen bond to the carbonyl oxygen atom O3 of acetone of crystallization; *d*(O3---H-N2) = 2,154 Å. Further, intermolecular hydrogen bonds exist between the hydrogen atoms on the primary amine group (N3) and O3 [*d*(O3---H-N3) = 2,02

Å], and there is intramolecular hydrogen bonding between the phenolate oxygen atom O2 and N3 [*d*(O2---H-N3) = 2,019 Å] (see Fig.16 and Table 2). The V-S bond and the V-N bonds (2.087, 2.358 Å) are obviously shorter than those in the [VO(H_2O)L], where H_2L is thiosemicarbazone-bis(acetate); [*d*(V-S) = 2.435, *d*(V-N) = 2.362 Å] [96]. The V-Cl bond (2.341 Å) is similar to that in other chloro-vanadium complexes [97] (see also Table 2).

EPR study of compound ***1***·*Me_2CO*

The EPR spectrum of crystals of **1**·Me_2CO dissolved in THF was recorded in solution at ambient temperature as well as in cryogenic glasses at 100 K. The eight line fluid solution spectra of the oxovanadium(IV) compounds are accounted for by a single $S = 1/2$ species in which the unpaired electron in a d_{xy} orbital is coupled to the nuclear spin of the vanadium nucleus ($I = 7/2$). Its cryogenic glass spectra are characterized by two overlapping sets of eight lines corresponding to the *g*-anisotropy of an axial system.

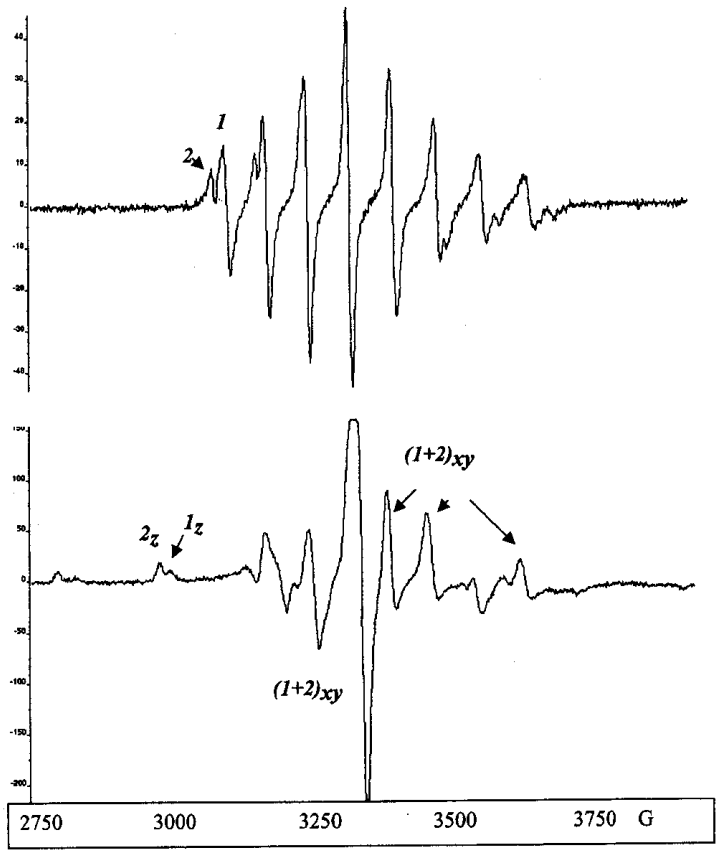

Fig. 18 EPR spectrum of **1** ·$OCMe_2$ in THF solution at room temperature (top) and at 100K

Along with the main species in this spectrum, characterized by a hyperfine coupling constant $A_0 = 98.7 \cdot 10^{-4}$ cm^{-1}, there is a second species with a rather high value (A_0 =

$101.0 \cdot 10^{-4}$ cm^{-1}). This situation is also revealed by the anisotropic spectrum in frozen THF solution (Fig.18), which is a superposition of the parallel (z) and perpendicular (xy) parts of the main(1) and the minor components(2). The A_z values are $A_z^{(1)} = 161 \cdot 10^{-4}$ and $A_z^{(2)} = 173 \cdot 10^{-4}$ cm^{-1}. Based on the additivity relationship $A_z = \sum n_i A_{zi}$ (n_i denotes the nature of the four equatorial ligand functions, and A_{zi} are the corresponding contributions to A_z) [98], a value of $161 \cdot 10^{-4}$ cm^{-1} is in agreement with an equatorial Cl,O,N,S donor set, while a value of $173 \cdot 10^{-4}$ cm^{-1} should indicate addition of an oxygen-functional ligand L in solution, such as THF, possibly accompanied by a rearrangement of the tridentate ligand so as to place the sulfur donor atom into an axial position.

Taking 45.7 and $33.9 \cdot 10^{-4}$ cm^{-1} as the contributions of a relatively weak O donor such as THF [94] and the thiocarbonyl function, respectively, a calculated value of $A_z^{(2)} = 172.8 \cdot 10^{-4}$ cm^{-1} is obtained, in very good agreement with the found coupling constant of $173 \cdot 10^{-4}$ cm^{-1}. We hence suggest an equilibrium as depicted in Fig.19, where species (1)

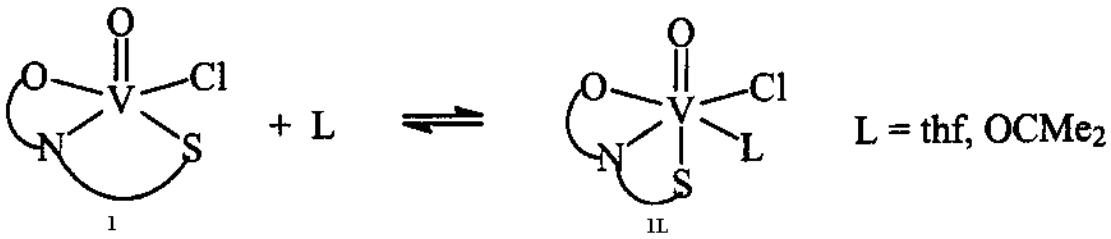

1 1L

Fig. 19 Equilibrium for (1) in the solution

is represented by compound **1** and species (2) by *trans*-**1**(L), where *trans* denotes axial position of S (*trans* to the doubly bonded oxo ligand). In THF solutions, L would presumably be THF.

1.1.2 *[V_2O_2{naphthalylidene[hydroxymethyl-bis(oxymethyl)]-aminomethane}$_2$]* (**2**)

Reaction of $VO(acac)_2$ and the ligand (H_4nap-tris) in abs. ethanol under an inert gas atmosphere results in the formation of green complex **2** (yield: 60%). **2** is air stable in the solid state, and soluble in DMF and DMSO. The IR bands at 1636 cm^{-1} associated with the ν(HC=N) stretching frequency of the free ligand is shifted to 1618 cm^{-1} in the corresponding complex **2**, indicating the coordination of the azomethine nitrogen. The bands at 3486, 1067 and 1034 cm^{-1} were assigned to the nonbonding $–CH_2OH$ group, which has also been testified by X-ray structural analysis. The ν(V=O) band is at 974 cm^{-1}. An additional sharp and intense band observed in the IR spectra of the crystals of **2**·4DMF at 1662 cm^{-1} is assigned to the

ν(C=O) of DMF. The bathochromic shift with respect to free DMF is due to the involvement of the aldehyde group in hydrogen bonding interaction with the uncoordinated oxygen atom, as identified by the X-ray structure analysis. The ^{51}V NMR spectrum of complex **2** exhibits a peak at 553 ppm, corresponding to a vanadium complex, the coordination sphere of which is dominated by alkoxide functions.

*Crystallographic studies of compound **2**·4DMF*

2·4DMF, obtained from the recrystallization of complex **2** in DMF, crystallizing in the monoclinic space group $P2_1/c$ (Fig.20, Fig. 21), exhibits a dinuclear monooxovanadium(V) structure having an inversion center. Selected bond lengths and bond angles are listed in Table 3. Both vanadium atoms are in a distorted octahedral environment of an NO_5 core. Out of the three CH_2OH groups, one is free and uncoordinated, while the other two are coordinated to the metal center upon deprotonation. Among these two, one is bound to vanadium through a

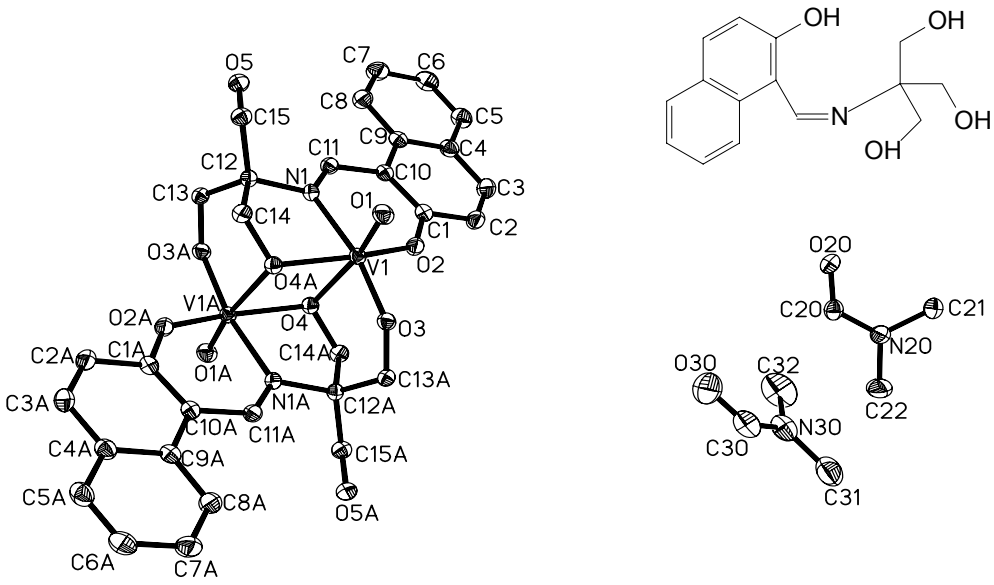

Fig. 20 Molecular structure of **2** and corresponding ligand

five-membered chelate and bridges the two vanadium centers, while the other binds to the vanadium that is generated by the inversion center. Each vanadium center also possesses terminal oxo (V=O), phenolate and alkoxo oxygens, and an imine N in its primary coordination sphere, with the doubly bonded oxo group O1 of the oxovanadium moiety and a bridging alkoxide (O4) being in the apical positions. The angle O1-V1-O4 is 171.47(4)°. Thus, the dinuclear complex **2** can be viewed as a dimer of a distorted square-pyramidal complex with O4 and O4A (*trans* to O1 and O1A) forming a weak bridge between the two

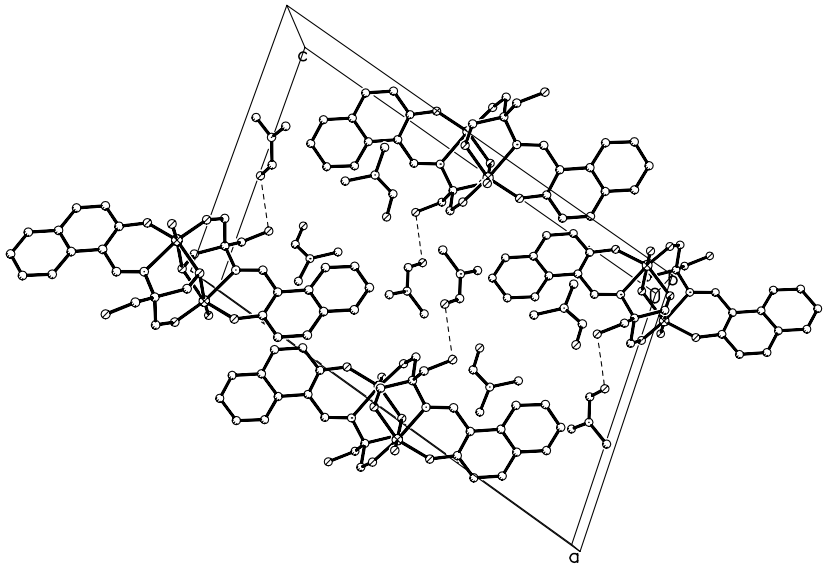

Fig. 21 Cell of **2**

Table 3. Bond Lengths (Å) and Angles (deg) for **2**·4DMF

V(1)-O(1)	1.6052(10)	O(1)-V(1)-O(3)	101.65(5)
V(1)-O(3)	1.7862(9)	O(1)-V(1)-O(2)	101.41(5)
V(1)-O(2)	1.8838(9)	O(3)-V(1)-O(2)	96.76(4)
V(1)-N(1)	2.1139(11)	O(1)-V(1)-N(1)	90.88(5)
V(1)-O(4)	2.3187(9)	O(3)-V(1)-N(1)	166.84(4)
V1A-O(4)	1.907(1)	O(2)-V(1)-N(1)	84.53(4)
O(5)-C(15)	1.4195(16)	O(1)-V(1)-O(4)	171.47(4)
N(1)-C(11)	1.2968(16)	O(3)-V(1)-O(4)	85.33(4)
N(1)-C(12)	1.4951(16)	O(2)-V(1)-O(4)	82.43(4)
C(1)-C(10)	1.3992(18)	N(1)-V(1)-O(4)	81.86(4)
O(2)-C(1)	1.3224(16)	C(1)-O(2)-V(1)	137.34(9)
		C(11)-N(1)-C(12)	117.75(11)
		C(11)-N(1)-V(1)	127.85(9)
		C(12)-N(1)-V(1)	114.40(8)

halves of the molecule. The vanadium ion is 0.7153 Å out of the the plane defined by O2, O3, O4A, and N1, and the distance of the two planes formed by N1, O2, O3, O4A and N1A, O2A, O3A, O4 is 2.102Å. The asymmetrically bridged oxygens O4 and O4A have distances of 1.907(1) and 2.3190 (11) Å to the two vanadium centers. The V---V non-bonding distance in

2 is 3.37 Å, marginally longer than in other octahedral dimeric complexes [99], but close to a dimeric complex with distorted trigonal bipyramidal arrangement around vanadium [100]. Alkoxides and aryloxides usually form dimeric complexes, except of $VO(OCH_3)_3$, which is polymeric [101]. The V(1)--O(4)--V(11a) angle for **2** (105.29°) is close to that observed for $[VO(cyclo\text{-}C_5H_9O)_3]_2$ [100] (108°), $[VO(OCH_2CH_2Cl)_3]_2$ [102] (109°), and $[VOCl\{OC(CH_3)_2\}_2]_2$ [103] (108.6°).

The bicyclic system formed between the vanadium center and the the tridentate ligand is slightly folded along the O3-V1-N1 axis: The angle between the planes O4-O3-V1-N1 and O2-O3-V1-N1 amounts to 14.02°.

In addition to the vanadium complex, there are also four molecules of DMF in the cell. They connect with each other through hydrogen bonds between the DMF molecules and the uncooedinated oxygen atoms [d(O5--O20) = 2.689 Å] (Table 2).

1.1.3 Other vanadium complexes

Table 4. Suggested structures for complexes **3**-**7**

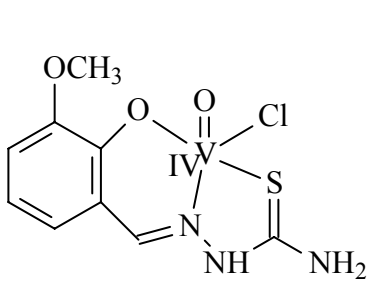

3 DMF

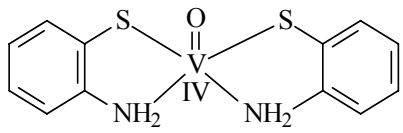

4 DMF

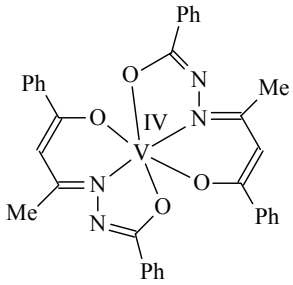

5 DMF

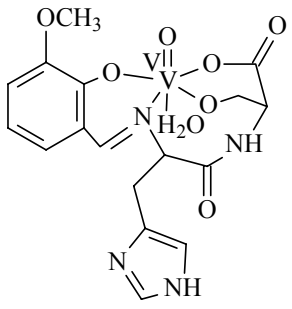

6 DMF

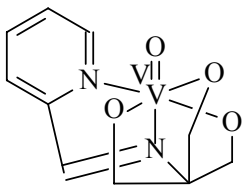

7 DMSO

Complexes **3** to **7** have been prepared by various methods. They are formulated on the basis of elemental analyses and a variety of physical measurements (see Experimental), and

the possible structures are listed in Table 4. Complexes **3**, **4**, and **5** are vanadium(IV), **6** and **7** vanadium(V) compounds.

Complex **3** has been synthesized in analogy to complex **1**. It is unstable in air in the solid state. Its color changes from green to dark green on exposure to air. Characteristics are the same as for complex **1**. The IR spectra of **3** show the stretching frequencies ν(NH) and ν(C=S) (3291, 3189, and 1162cm^{-1}), also present in the free ligand (3343, 3167, and 1185cm^{-1}), indicating the coordination of the ligand to vanadium out of the monoanionic tridentate ONS form. Solutions of complex **3** in THF show two species in the EPR spectrum. The ratio is, however, inverse with respect to compound **1** (see above), i.e. species (2) corresponding to the component with the larger coupling constant, **3**(L), is the major component (L = THF).

Complex **4** can be synthesized by using the ligand-exchange method in different kinds of solvents, starting with $VO(acac)_2$ and *o*-aminothiophenol. In addition to complex **4**, $V(acac)_3$ and diaminodiphenyldisulfide are formed in this reaction, indicating redox activity during the reaction. The formation of $V(acac)_3$, testified by a X-ray structure analysis, indicates that vanadium(IV) can be reduced by thiolate under mild conditions, which will be discussed later. The IR spectrum of complex **4** shows the stretching frequency ν(NH) (3210 cm^{-1}), indicating that a Schiff base ligand does not form during the reaction.

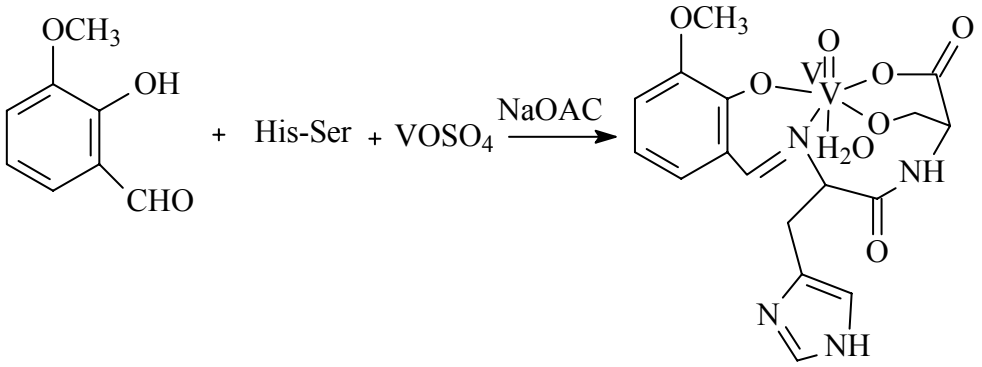

Fig. 22 Synthesis of complex **6**

The brown non-oxo vanadium complex **5** was prepared by reacting $VO(Phacac)_2$ (Phacac = phenyl-acetylacetoneate) and 2 equivalents of benzoyl hydrazide in dry methanol under N_2 atmosphere. It is air-stable in the solid, and lacks the characteristic ν(V=O) band in the IR spectrum. The small EPR coupling constant and g parameter ($A_0 = 69.9 \cdot 10^{-4}$ cm^{-1}, g_0 = 1.9177) may account for the non-oxo characteristics of this V^{IV} complex.

The green complex **6** was synthesized in a one-pot reaction (Fig. 22) in deoxygenated ethanol/water under N_2 from $VOSO_4$, *o*-vanillin and histidyl-serine. **6** is air-stable in the solid

state, and highly soluble in DMSO and DMF. In this reaction, vanadium has been oxided from the +IV to the +V state, possibly due to the alcoholic group in the dipeptide. The mediation of this kind of oxidations by alcohols is quite common in vanadium chemistry. The IR spectrum shows the stretching frequency ν(CONH) at 1676 cm^{-1}, indicating that the amide group is not coordinated. The ^{51}V NMR chemical shift (-529 ppm) is in accord with coordinated alkoxide.

Complex **7** was prepared by the reaction of $VO(acac)_2$ and pyridylidene-tris(methoxy)methylamine in dry CH_2Cl_2 under N_2 atmosphere. The dark green solid is air-stable, and soluble in DMSO and DMF.

1.2. Insulin-mimetic activity and toxicity tests of the vanadium complexes

1.2.1 Toxicity tests

Toxicity tests were carried out by incubating transformed fibroblasts from mice (cell line SV 3T3) with solutions of the vanadium complexes for 12, 24 and 36 h, followed by addition of trypan blue. This dye penetrates the membrane of dead cells only, and hence only dead cells adopt a bluish colour. SV transformed fibroblasts attain the physiological features of adipocytes, which effectively metabolise glucose. At vanadium concentrations, *c*(V), below 10 μM, practically none of the vanadium compounds was toxic. The presentation of results (Fig. 23) is hence restricted to *c*(V)=1000, 100 and 10 μM for these vanadium complexes.

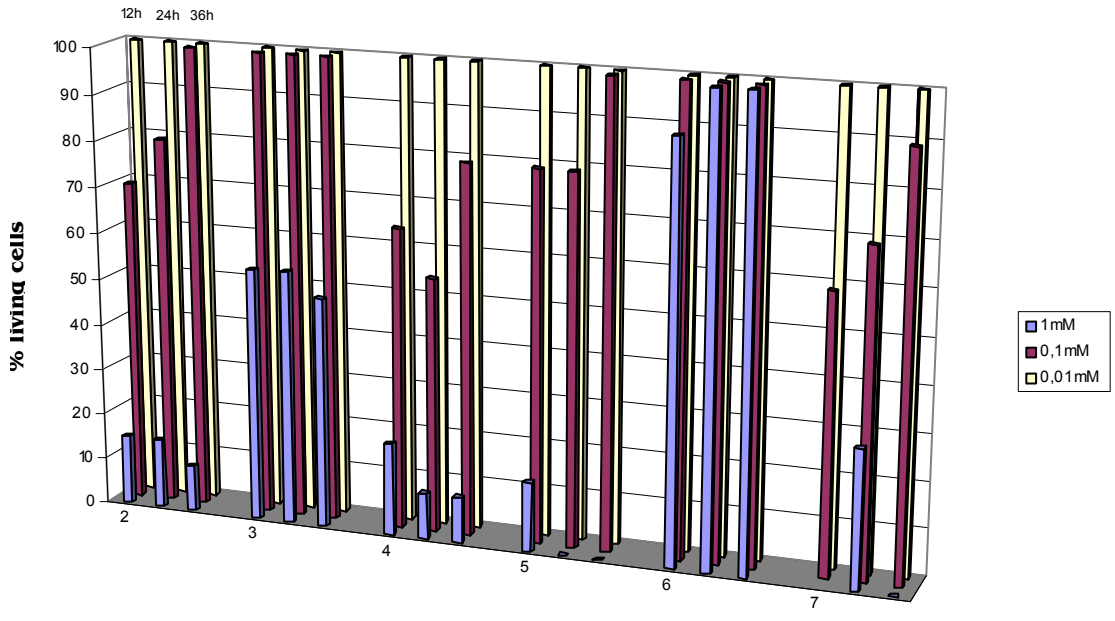

Fig. 23 Toxicity test

General trends can be summarized as follows.

1. Toxic effects increase with increasing exposure time of the cells to the vanadium compounds, suggesting that the compounds retain – at least to a certain extent – their identity.

2. Toxicity decreases with decreasing concentration.

3. Most of the vanadium compounds are toxic at *c*(V) = 1 mM. The only non-toxic compound at *c*(V) = 1 mM, even after 36 h of incubation, is VO(van-His) (**6**), a V^V complex containing a Schiff base ligand composed of *o*-vanillin and the dipeptide histidyl-serine. Most complexes are negligibly toxic or non-toxic at *c*(V) = 0.01 mM and below, i.e. at concentrations of physiological and pharmacological relevance.

4. There are no striking differences in cell toxicity between these vanadium compounds. However, in disagreement with what is generally believed, V^V complexes tend to be less toxic than V^{IV} complexes. It should, however, be emphasized that complexes with low toxicity do not necessarily belong to the family of more active compounds, as activity relates to the ability to induce glucose translocation into the cells.

1.2.2 Insulin-mimetic tests

The tests for the ability of vanadium compounds to trigger glucose intake into cells was carried out with transformed SV 3T3 fibroblasts from mice. Cells were grown to sub-confluence. The culture medium was then depleted of insulin for 72 h , and thereafter incubated for 4 h with the dissolved vanadium compound. The glucose intake was determined by a vitality test based on MTT, i.e. addition of yellow MTT, which is reduced in the mitochondrial respiratory chain to formazane blue by reduction equivalents stemming from glucose. The amount of MTT-fomazan blue was measured photometrically, the absorbance being related to the amount of glucose incorporated by the cell. The data are presented graphically in Fig. 24. The diagrams also contain the data for a control group (neither insulin nor vanadium compound added) and for a group where insulin was employed instead of vanadium. General trends can be summarized as follows:

(a) At *c*(V) = 1 mM, i.e. at a concentration where most vanadium compounds are toxic, there is no insulin-mimetic effect for most of the vanadium species, i.e. the absorbance is close to that of the control group.

(b) Maximum activity is found in the concentration range 0.1 to 0.001 mM. In the cell samples which were kept in insulin-free media for 72 h and incubated with vanadium thereafter, most of the compounds are clearly less effective than insulin.

(c) Except for the low efficacy at higher concentrations, there is no apparent correlation between toxicity and the extent of insulin-mimetic action. Thus, VO(py-tris) (**7**) is quite effective although comparatively toxic, while the non-toxic VO(van-Hisser) (**6**) is only moderately effective.

(d) Similarly, V^{IV} complexes (which are generally more toxic than V^{V}) tend to be more effective insulin-mimetics than V^{V} complexes. These observations corroborate the assumption that the complexes undergo speciation within the cell, thus giving rise to active species different from those originally employed.

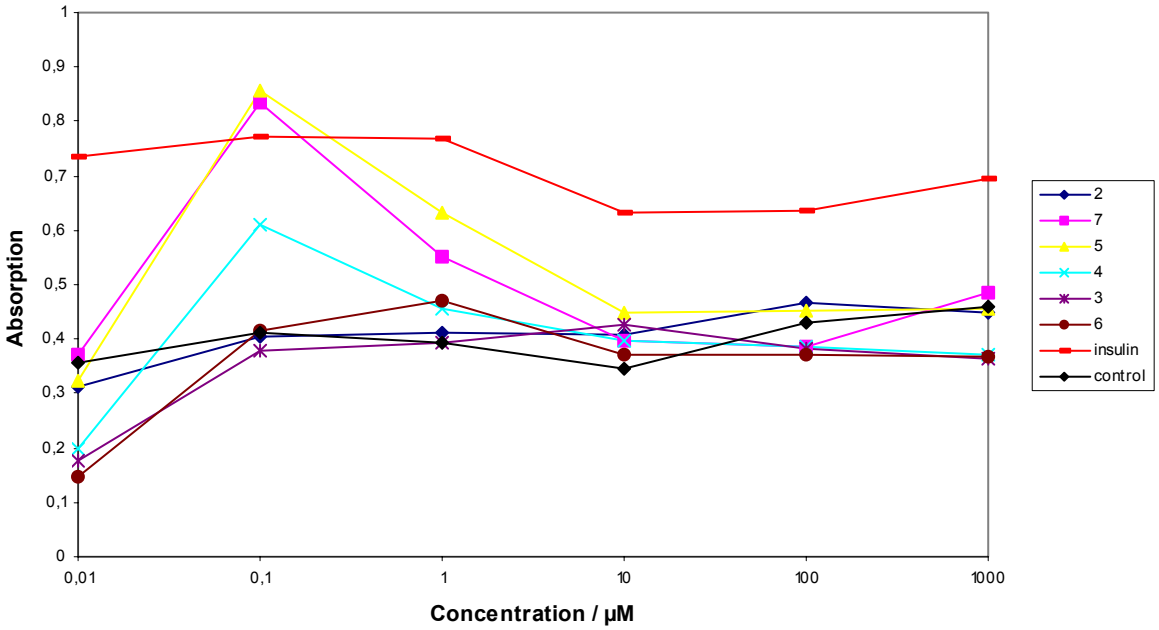

Fig. 24 Insulin-mimetic behavior of vanadium complexes; 72h incubation

2. Synthesis and characterization of vanadium complexes with thiolate and/or disulfide ligands.

Sulfur compounds play an important role in vanadium chemistry, due not only the fact that sulfide is constituent in vanadium nitrogenase, but also because they take part in the redox chemistry of vanadium under physiological conditions. V^{V} has been found to be reduced to vanadyl by glutathione in the intracelluar medium [105], and can be further reduced to V^{III} (see also above) with the concomitant formation of disulfide. Efforts have been undertaken to synthesize vanadium complexes with thiolates. No vanadium model complex with disulfide has been synzhesized until now. In order to understand the relationship between

vanadium and the organic substrates containing disulfide, $VCl_3(thf)_3$, $VOCl_2(thf)_2$ and ligands containing disulfide have been chosen as the starting materials to model their interaction.

2.1 VO{chloro-[N-(2-sulfidophenyl)thiosalicylideneaminate]} (**8**)

In order to avoid the isomerization of the Schiff base ligand with thiolate functions, **8** was prepared in a one-pot reaction from equivalent amounts of 2,2'-dithiodibenzaldehyde, $VCl_3(THF)_3$, and *o*-mercaptoaniline, and 5 equivalents of triethylamine dissolved in abs. THF by refluxing overnight under nitrogen atmosphere. The brown precipitate formed during the reaction was a mixture of complex **8** and $[NHEt_3]Cl$. The IR bands at 1582 and 930 cm^{-1} were assigned to ν(C=N) and ν(V=O), indicating the formation of the Schiff base, and the concomittant oxidation of vanadium during the reaction. In the far IR, there are two bands at 380 and 349 cm^{-1}, associated with the V-S and V-Cl stretching vibration.

8·C_5H_{12} was crystallized by diffusion of pentane to the filtrate of the reaction. The structure is illustrated in Figs. 25 and 26, while selected bonds length and angles are listed in Table 5. The vanadium atom is in a distorted square-pyramidal environment, consisting of a chloro ligand, an imine nitrogen, and two thiophenolate sulfurs in the basal plane, and the doubly bonded oxo group O1 of the vanadyl moiety occupying the apical position. The vanadium atom is 0.61 Å above the mean plane defined by the basal atoms. There is some distortion towards a trigonal bipyramid, quantified by a τ value of 0.345. The bicyclic system formed between the vanadium center and the tridentate ligand is slightly folded along the V1-

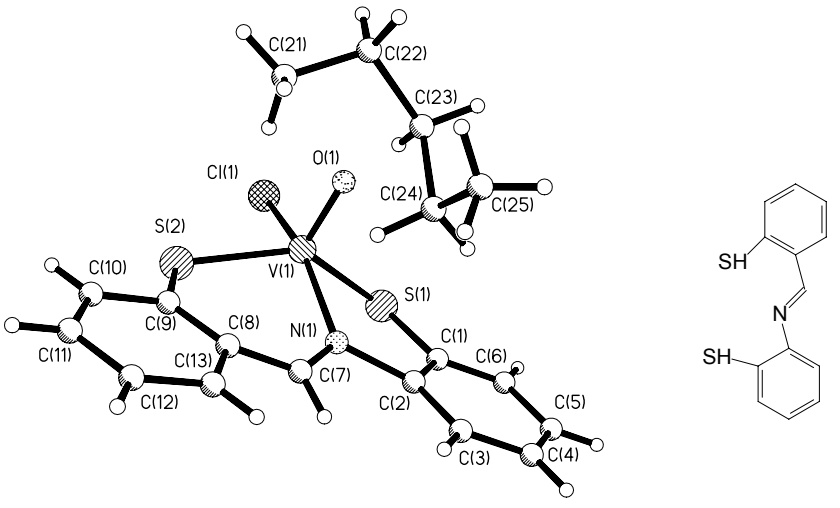

Fig. 25 Molecular structure of **8**·C_5H_{12} (30% probability level), and the corresponding ligand

N1 axis: The angle between the planes V1-S2-C9-C8-N1 and V1-N1-C2-C1-S2 amounts to 22.72°. The V-Cl band lengths is 2.340 Å, similar to **1**·Me_2CO. The V-S bond lengths [2.307(3), 2.288(3) Å] are significantly shorter than those in [$VOCl_2$([9]aneN_2S)] [106], where the d(V-S) are 2.634 and 2.470 Å, respectively; and in **1**·Me_2CO, where the V-S bond length is 2.358 Å. But they are similar to d(V-S) = 2.306 Å in [$V(ONS)_2$] [15] (cf. Fig. 2).

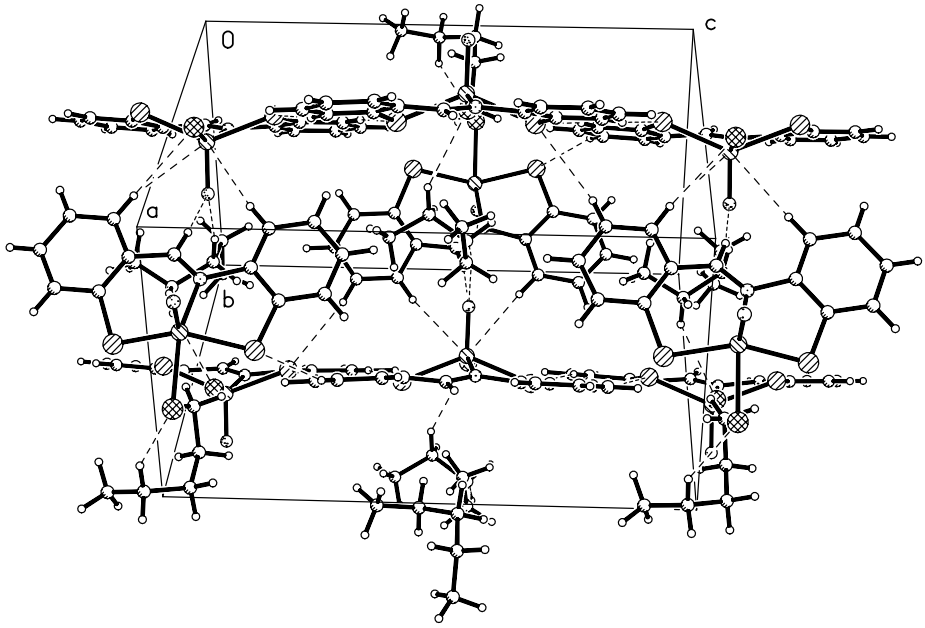

Fig. 26 Cell drawing of **8**·C_5H_{12}

Table 5. Bond lengths and bond angles of complexes **8** and **9**

Complex **8**		Complex **9**	
V-O1 1.626(4)		V(1)-O(2)	1.589(3)
V-N1 2.114(6)		V(1)-O(1)	1.925(3)
V-S1 2.307(3)		V(1)-O(3)	1.986(3)
V-S2 2.288(3)		V(1)-N(1)	2.117(4)
V-Cl 2.3383(15)		V(1)-Cl(1)	2.3690(14)
Cl-V-S2 85.39(9)		S(1)-S(2)	2.0699(17)
Cl-V-S1 84.27(9)		C(1)-S(1)-S(2)	100.30(16)
Cl-V-N1 156.17(17)		C(10)-S(2)-S(1)	98.95(16)
S1-V-S2 135.14(8)		N(1)-V(1)-Cl(1)	156.83(10)
N1-V-S1 79.08(17)		O(1)-V(1)-O(3)	142.55(13)
N1-V-S2 94.46(18)		C1S1S2/C10S2S1	72.14

2.2 VO[chloro{N,N'-[dithio-bis(phenylene)]bis(salicylideneiminate)} (**9**·3CH_2Cl_2)

Complex **9** was synthesized by the reaction of $VCl_3(THF)_3$ and the disulfide ligand N,N'-[dithio-bis(phenylene)]bis(salicylideneiminate) in dry CH_2Cl_2. The IR band at 1613 cm^{-1} associated with the two ν(HC=N) stretching frequencies of the free ligand is shifted to 1627 and 1607 cm^{-1} in the corresponding complex **9**, indicating that the two HC=N have different chemical environments, i.e. one of the HC=N coordinates to the vanadium atom while the other one remains uncoordinated, as also showed by the X-ray structural analysis (see below). The IR band at 992 cm^{-1} assigned to the ν(V=O) again indicates that vanadium had been oxidized during the reaction.

Crystals of **9** were obtained from the reaction solution by addition of CH_2Cl_2. The structure is illustrated in Figs. 27 and 28; selected bonds lengths and angles are listed in Table 5. In disagreement with complex **8**, the disulfide bridge remained intact during formation of complex **9** in spite of the oxidation of vanadium during the reaction. Although the dianionic ligand (Fig. 27) usually functions as a pentadentate ligand [20-23], it coordinates to the vanadium ion only with part of the functions; i.e. two phenolic oxygens and only one of the imine nitrogens, the other imine-N and the disulfide-S remaining uncoordinated. Vanadium is in a distorted tetragonal pyramidal environment with the doubly bonded oxo group O2 in the

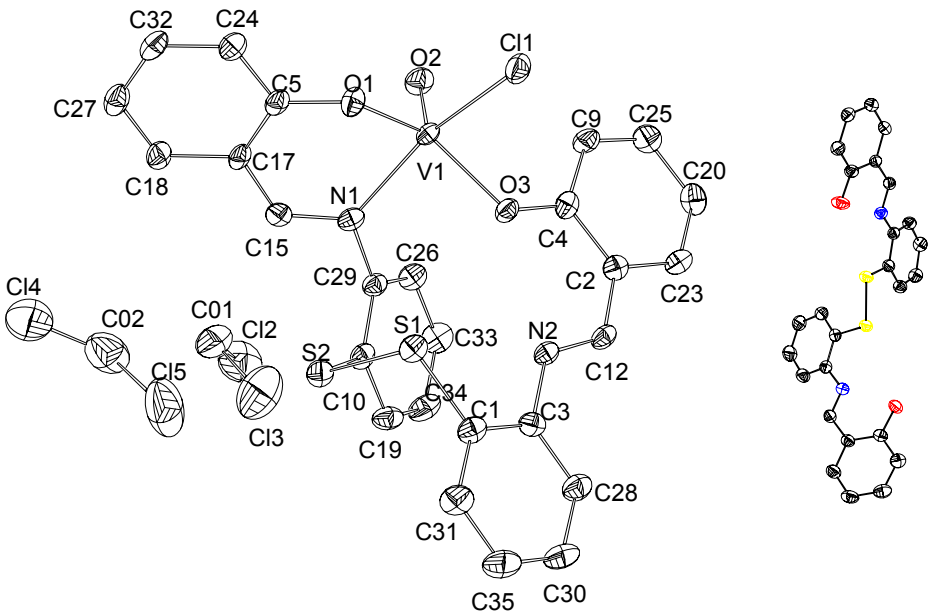

Fig. 27 Molecular structure of **9**, and its ligand

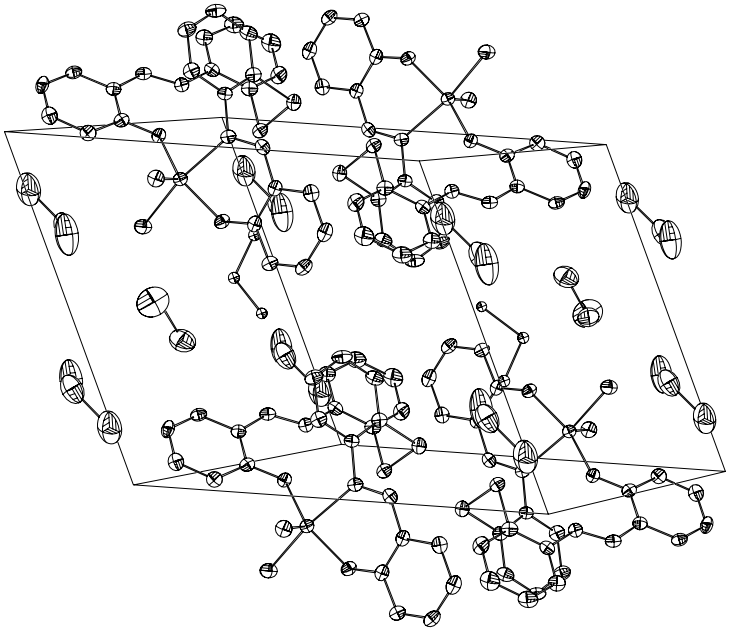

Fig. 28 Cell drawing of **9**

apical position. The chloro ligand, the two-phenolate functions and one of the imine nitrogen occupy the plane. Vanadium is only 0.0893 Å above the basal plane. There is a slight distortion towards a trigonal bipyramid, quantified by a τ value of 0.283. The V-$O_{phenolate}$ bond distances (1.925, 1.986 Å) in complex **9** are obviously longer than in the other vanadium(V) complexes [107]. The S-S distance in **9** is 2.0699 Å, which is in good agreement with the distance reported for other complexes containing disulfide ligands [20-23], but a little longer than in the ligand itself (2.026 Å). The angles at the sulfur atoms S1 and S2 [98.95(16) and 100.30(16)°] are obviously smaller than those in the ligand (105.0 ± 0.4°) and the mean values found for other disulfides (103.0 ± 0.4°). The dihedral angle C1,S1,S2/C10,S2,S1 for the complex, 72.14°, is significantly narrowed with respect to those of other disulfides (82.1 ± 5.4°) and the ligand (99.61°), but it is larger than in [Ni(dtpp)Cl] (55.4°) [20]. The distance V-Cl (2.369Å) is ~0.02Å longer than that in complexes **1** and **8**.

2.3 *{[VO(N-2-mercaptophenyl-2'-pyridinecarboxamide)]$_2$O}·(HNEt$_3$)(0.5NEt$_3$)* (**10**)

Complex **10** was synthesized by reacting equivalent amounts of $VOCl_2(THF)_2$ and the ligand N.N'-[dithiobis(phenylene)bis(pyridinecarboxamide)], and three equivalents of NEt_3 in dry THF. The green precipitate formed during the reaction was a mixture of complex **10** and

[$NHEt_3$]Cl. The IR band at 1690 cm^{-1} associated with the ν(CONH) stretching frequencies of the free ligand is shifted to 1626 and 1596 cm^{-1} in the corresponding complex **10**, indicating that the amide is deprotonated and coordinated to vanadium, and that the two vanadium centers are non-equivalent. The band at 990 cm^{-1} was assigned to ν(V=O).

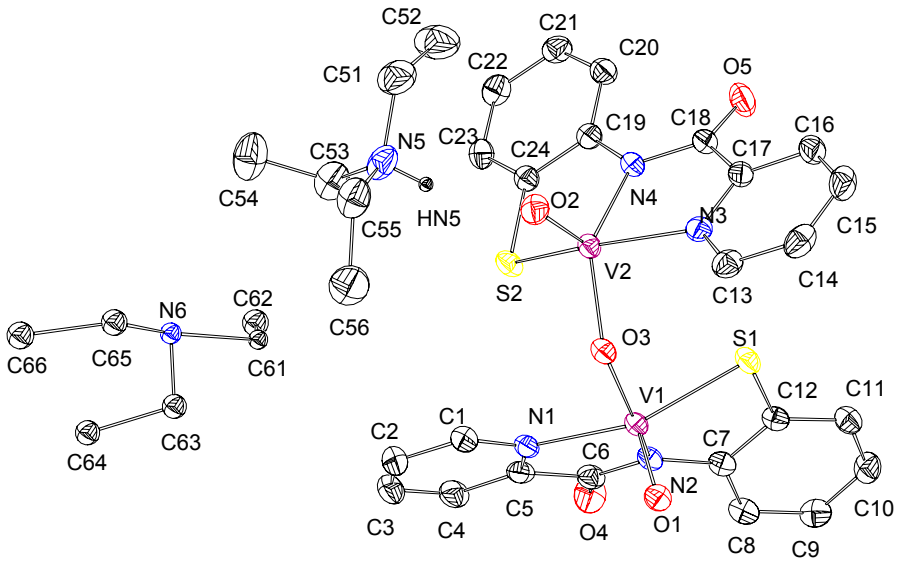

Fig. 29 Molecular structure of **10**

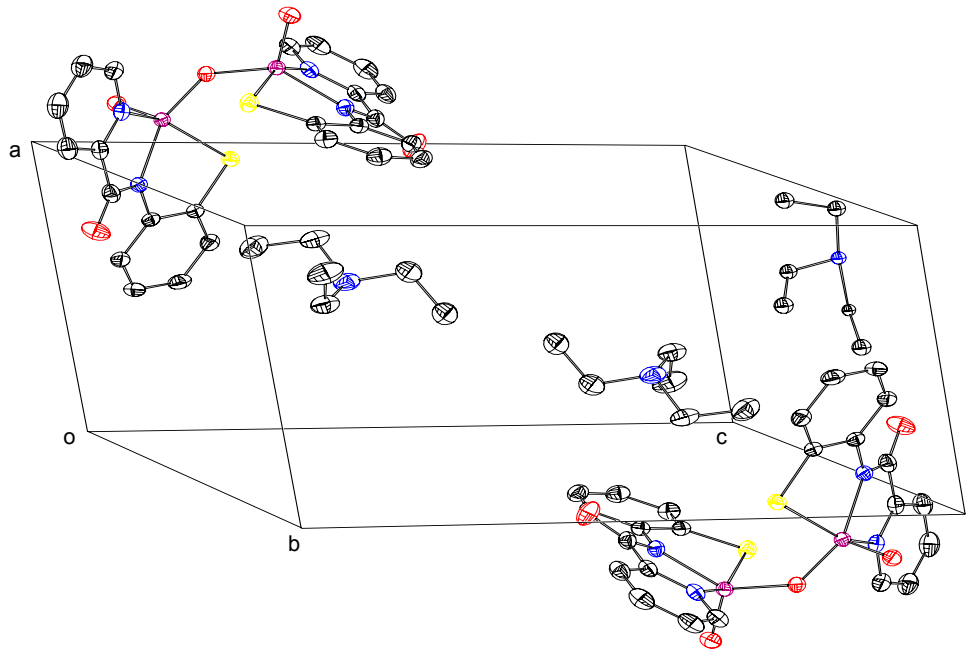

Fig. 30 Cell drawing of **10**

Crystals of **10** were obtained by dissolving the above precipitate in CH_2Cl_2, and keeping this solution at –20°C. The structure is illustrated in Figs. 29 and 30; selected bonds lengths and angles are listed in Table 6. Like complex **8**, the disulfide bridge of the ligand was broken during the reaction. **10** is an asymmetric, oxo- bridged dimer with the two oxo-bridged oxovanadium groups twisted with respect to each other. One of the vanadium centers [V(1)] is in an ideal tetragonal pyramidal environment with the doubly bonded oxo group O1 in the apical position, and the deprotonated carboxamido nitrogen, the bridging oxygen, the pyridine-N, and the thiolate-S occupying the basal plane. The other vanadium center [V(2)] is

Table 5. Bond lengths and bond angles of complexes **10** and **11**

Complex **10**		Complex **11**	
V(2)-O(2)	1.6111(18)	V(1)-N(2)	2.0582(18)
V(2)-O(3)	1.8657(17)	V(1)-N(4)	2.0777(18)
V(2)-N(4)	2.031(2)	V(1)-N(1)	2.1141(19)
V(2)-N(3)	2.097(2)	V(1)-N(3)	2.1141(18)
V(2)-S(2)	2.3458(7)	V(1)-S(1)	2.3481(7)
V(1)-O(1)	1.5991(18)	V(1)-S(2)	2.3868(7)
V(1)-O(3)	1.7496(17)	N(2)-V(1)-N(4)	173.52(7)
V(1)-N(2)	2.042(2)	N(1)-V(1)-S(1)	159.91(6)
V(1)-N(1)	2.092(2)	N(3)-V(1)-S(2)	153.63(6)
V(1)-S(1)	2.3307(7)	S(1)-V(1)-S(2)	103.47(3)
O(2)-V(2)-O(3)	111.64(9)		
O(3)-V(2)-N(4)	136.81(8)		
O(3)-V(2)-N(3)	87.99(8)		
N(3)-V(2)-S(2)	152.52(6)		
O(1)-V(1)-O(3)	109.01(9)		
O(3)-V(1)-N(2)	146.47(8)		
N(1)-V(1)-S(1)	145.45(6)		
V(1)-O(3)-V(2)	135.06(10)		

in a distorted tetragonal pyramidal environment. This distortion towards a trigonal bipyramid for V2 is quantified by a τ value of 0.26; vanadium is is 0.1161 Å above the basal plane. Of the four V-N bonds, the bonds to N2 [2.042(2) Å] and N4 [2.031(2) Å], the amide nitrogens, are a little longer than those of reported in the literature [mean $d(V\text{-}N_{am})$ = 2.014Å] [139],

while the bond lengths to N1 [2.092(2) Å] and N3 [2.097(2) Å], the pyridine nitrogens, are in the usual range for oxovanadium complexes containing V-N_{py} bonds [mean d(V-N_{py}) = 2.1Å] [107]. The V-S bond lengths [2.3307(7) for S1, 2.3458(7) Å for S2] are slightly longer than those in complex **8** [2.307(3), 2.288(3) Å], but shorter than those in [$VOCl_2$([9]aneN_2S)] [106], where the d(V-S) are 2.634 and 2.470 Å, respectively; and in **1**, where the V-S bond length is 2.358 Å. The V=O bond length of V2 [1.6111(18)Å] and V1 [1.5991(18)Å] are the same within the limit of the 3σ criterion. O2 is involved in hydrogen bonding interaction with N5 [d(N5···O2) = 2.856 Å]. The bond lenghths V1-O3 and V2-O3 [1.7496(17), and 1.8657(17) Å] differ significantly. The torsion angle [O1,V1,V2/V1,V2,O2 = 40.22°] in **10** is clearly smaller than those reported for comparable complexes in the literature (79.7°) [18], while the V-(μ-O)-V angle of **10** [135.06(10)°] is obviously larger [109.3(6)°] [18].

2.4 *{[V(N-2-mercaptophenyl-2'-pyridinecarboxamide)]$_2$}·(HNEt$_3$)* (**11**)

Complex **11** was synthesized by the reaction of equivalent amounts of $VCl_3(THF)_3$, the ligand N-2-mercaptophenyl-2'-pyridinecarboxamide ($PyPepSH_2$), and four equivalents of NEt_3 in dry THF. The red complex **11** was obtained from the filtrate after standing for a few weeks at –20°C. The IR band at 1690 cm^{-1} associated with the ν(CONH) stretching frequenciy of the free ligand is shifted to 1611 and 1586 cm^{-1} on complexation. The bands at 2976, 2672, 2498 cm^{-1} were assigned to stretching frequencies of the protonated triethylamine.

The structure of complex **11** is shown in Figs. 31 and 32, selected bonding parameters are collated in Table 6. The coordination geometry around vanadium is distorted octahedral, with two deprotonated carboxamido nitrogens, one pyridine-N, and a thiolate-S constituting the basal plane, while the other pyridine-N and the second thiolate-S occupy the axial positions. The two dianionic $PyPepS^{2-}$ ligands are coordinated in the *mer* fashion. The distances V(III)-N_{amid} (amid = carboxamido) are 2.0582(18) Å for N2, and 2.0777(18) Å for N4, which is a little longer than in complex **10**, and substantially longer than corresponding parameters reported in the literature [mean d(V-N_{am}) = 2.014 Å] [139]. The bond lengths of vanadium to N1 [2.1141(19) Å] and N3 [2.1141(18) Å], the pyridine nitrogens, are in the usual range for oxovanadium complexes containing V-N_{py} bonds [mean d(V-N_{py}) = 2.1 Å] [107]. The V-S bond lengths [2.3481(7) for S1, 2.3868(7) Å for S2] are slightly longer than those in complex **8** [2.307(3), 2.288(3) Å] and **11** [2.3307(7), 2.3458(7) Å].

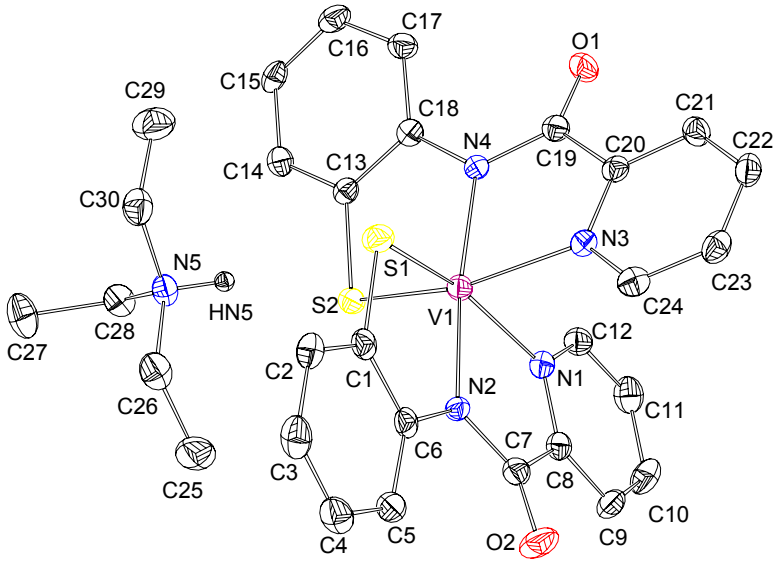

Fig. 31 Molecular structure of **11**

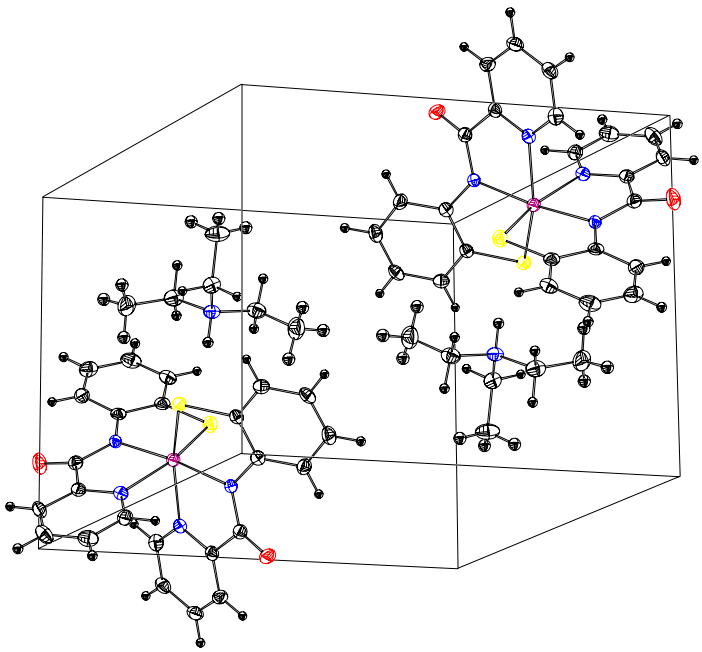

Fig. 32 Cell drawing of **11**

*2.5 VO{N,N'-[dithiobis(phenylene)]bis(5,6-benzosalicylideneiminate)}***(12)** *and VO{N,N'-[dithiobis(phenylene)]bis(3-methoxysalicylideniminate)}***(13)**

Reaction of equivalent amounts of diaminodiphenyldisulfide with VO(*o*-vanilin)$_2$ and VO(nap)$_2$, respectively, in abs. THF (reflux) overnight under nitrogen yields brown solutions,

from which brown products **12** and **13** were obtained by evaporation in vacuo. The complexes are air-stable in the solid state, and formulated on the basis of elemental analyses and physical measurements. The possible structures are shown in Fig. 33. A few characteristic infrared absorption frequencies of the starting material and the complexes **12** and **13** are listed in Table 6. The IR bands at 3373 and 3297 cm^{-1} associated with $\nu(NH_2)$ of the diaminodiphenyl-disulfide (ligand) and 1657 and 1686 cm^{-1} associated with ν(CHO) of VO(*o*-vanilin)$_2$ and VO(nap)$_2$, respectively, disappear in the new complexes **12** and **13.** The new band appearing at 1603 and 1617 cm^{-1} for complexes **12** and for **13** were assigned to ν(C=N); the (V=O) of VO(*o*-vanilin)$_2$ and VO(nap)$_2$ are shifted from 958 to 985 cm^{-1} for **12** and 978 to 982 cm^{-1} for **13**. The X-band EPR data are summarized in Table 7. The isotropic EPR spectra of the vanadium(IV) complexes **12** and **13** reveal eight resonances attributable to an $S = 1/2$ species in which the unpaired electron in a d_{xy} orbital is coupled to the nuclear spin of the vanadium nucleus [$I(^{51}V) = 7/2$]. Apparently, no redox reaction occured in these case.

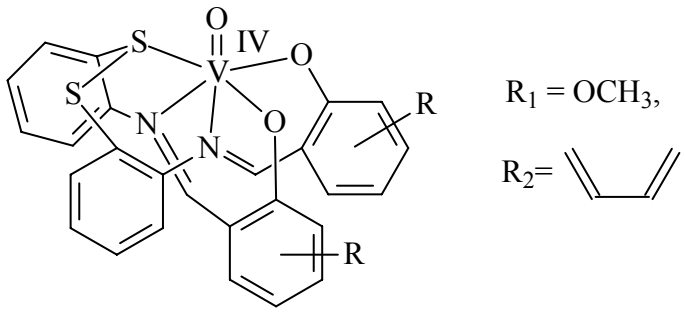

Fig. 33 Possible structure of complexes **12** and **13**

Table 7. Characteristic IR bands (cm^{-1}) and EPR data for the starting material and **12** and **13**

	ν(NH2)	ν(CHO)	ν(C=N)	ν(V=O)	EPR(A,$cm^{-1}\times10^{-4}$)	
VO(o-vanilin)$_2$		1657		958		
VO(nap)$_2$		1686		978		
ligand	3373,3297					
complex **12**			1603	985	g_0=1.9738	A_0=101.33
complex **13**			1617	982	g_0=1.9687	A_0=103.33

3. Polyoxometalates and cryptands

As already noted in the introduction, polyoxometalates have recently attracted interest in the context of oxidation catalysis [70] and their potential in medicinal applications [72]. The role of decavanadate, an isopolyoxometalate, as an inhibitor for phosphate-metabolising enzymes, has been documented in several instances [108]. Usually, decavanadate (partially protonated $V_{10}O_{28}^{6-}$) forms in mildly acidic solution and has been well characterized both in solution [109,110] and in the solid state [111-115]. It can accept up to three protons. The unprotonated, mono-, di- and triprotonated forms have been identified and studied in solution by ^{51}V- and ^{17}O-NMR spectroscopies [109,110]. In decavanadate, there are

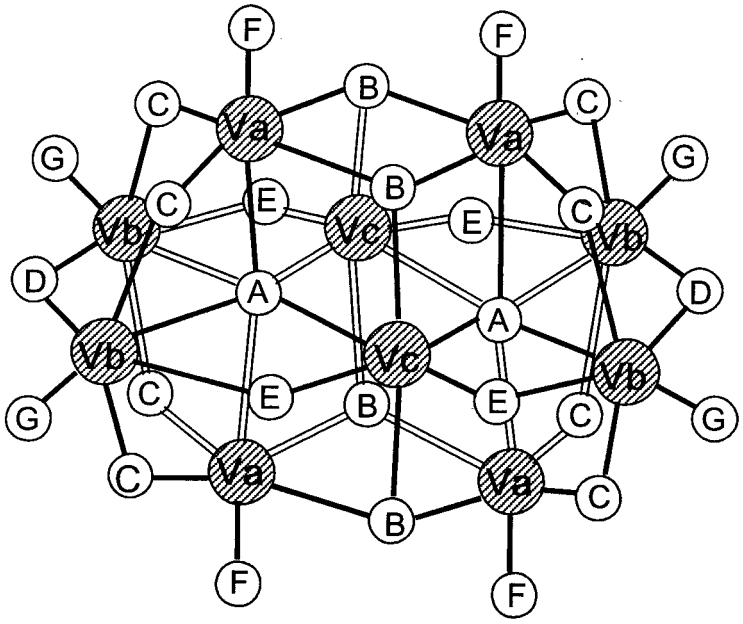

Fig. 34 Schematic drawing of the centrosymmetric dihydrogendecavanadate(4-)

three distinguishable vanadium centers, denoted as Va, Vb, Vc (Fig. 27), all of which are in a distorted octahedral array, differentiated by the binding mode of the oxo groups: **Va** = VO(μ_2-O)$_2$(μ_3-O)$_2$(μ_6-O), **Vb** = VO(μ_2-O)$_4$(μ_6-O) and **Vc** = V(μ_2-O)$_2$(μ_3-O)$_2$(μ_6-O)$_2$. There are seven different oxo groups, denoted as **A-G**, falling into four categories, namely terminal (F and G), μ_2 (C, D and E), μ_3 (B) and μ_6 (A). In agreement with calculations directed towards the basicity of the oxo ligands [90], the oxygen atoms C (μ_2 linking Va and Vb) and B (μ_3 linking two Va and a Vc centre) have been identified as protonation sites. Diprotonation may occur at two centrosymmetrically related C site [112,113,115], at two B sites [111] or at a C plus a B site [113].

The physiological function of decavanadate, at first sight, is a little surprising. Because decavanadate is unstable under physiological condition and nanomolar concentration, it should slowly hydrolyse to monovanadate [86], which will be reduced in the intracellular medium to VO^{2+}. Once administered, however, or formed at special cell sites, decavanadate may become inaccessible to hydrolysis. A possible explanation is that decavanadate reacts with biogenic macromolecules, such as ionophores, forming sandwich-like structures stable against hydrolytic and redox degradation [92, 93]. In order to further test this possibility, different cryptands and related ligands have been chosen in this work to model this interaction, which has also been extended to heteropolyoxometalates (such as $[PV_{14}O_{42}]^{9-}$ and $[PV_2W_{10}O_{40}]^{5-}$).

3.1 Synthesis and structural characterization of $[(H^+)_2C23]_2[(H^+)_2V_{10}O_{28}]\cdot 6H_2O$ (**14**) *and* $[(H^+)_2C211]_2(H_3O)^+_2[V_{10}O_{28}]\cdot 6H_2O$ (**15**)

Crystals of the title compounds have been synthesized by mixing a solution of decavanadate, which was obtained according to the literature [116], with a solution of C23 or C211, respectively. These mixtures were kept in the refrigerator for a few weeks. In order to avoid disturbance by Na^+ and K^+ ions, the pH values of the solution were adjusted with tetraethylammonium hydroxide and HCl to pH ~ 5.5.

3.1.1 Spectroscopy and crystallographic studies of compound **14**.

The IR spectrum of compound **14** is similar to that reported for other diprotonated decavanadates [110,117]: the bands in the range of ca. 900 to 1000 cm^{-1} can be assigned to the stretching vibrations of the terminal V=O groups. Bridging antisymmetric vibrations corresponding to V-O-V are in the range 860-730 cm^{-1}, while the symmetric bands are between 600-440 cm^{-1}. The peaks in the range 1500-1000 cm^{-1} can be assigned to the stretching vibrations of the cryptand C23, while the peaks in the range 2700-2300 cm^{-1} are assigned to the stretching vibrations of the protonated amine groups $(R_2NH_2)^+$ of C23. ^{51}V NMR spectroscopy of an aqueous solution of **14** showed three resonance at -425, -507, and -525 ppm. These signals are in the range reported previously for the decavanadate unit [110,117], indicating non-covalent bonding of C23 to the decavanadate ion in solution. The ^1H NMR spectrum of the compound **14** (Fig. 35) contains three sharp signals in the relative intensity ratio 1:1.5:1 [(Hb) 3.697 ppm, (Hc) 3.597 ppm, (Ha) 3.228 ppm], which are assigned

to the hydrogen atoms of cryptand C23. Compared with the ^{1}H NMR of the free C23 (Ha, 2.63 ppm; Hb, 3.47 ppm; Hc, 3.5145 ppm), the ^{1}H NMR

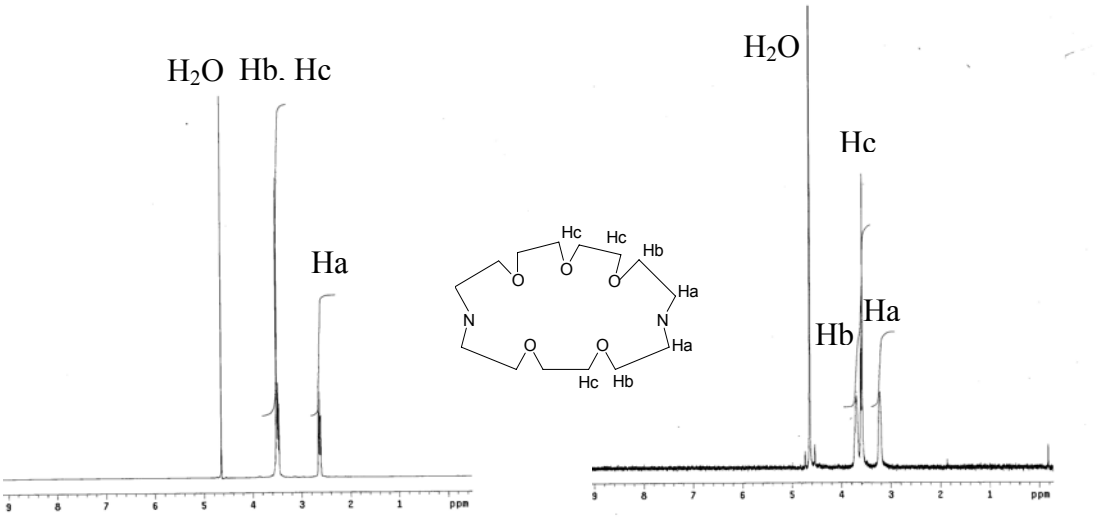

Fig. 35 ^{1}H NMR spectra of cryptand C23 (left) and complex **14** (right)

resonances of compound **14** have shifted to low field, especially so the proton Ha ($\Delta\delta$ = 0.60 ppm), due to the hydrogen-bonding interaction between decavanadate and the cryptands.

Complex **14** crystallizes as an aqua solvate of formula $[(H^+)_2C23]_2[(H^+)_2V_{10}O_{28}]\cdot 6H_2O$ in the centro-symmetric orthorhombic space group Pbca (Figs. 36 and 37). Figure 36 shows the structure and labeling scheme of the decavanadate anion, the water molecules and the

Table 8. Interatomic distances (Å) and angles (°) involving hydrogen-bonded atoms in **14**

N2 -- O2	2.948(3)	N2 -- HN2A -- O2	157(2)
N2 -- O16	2.808(3)	N2 -- HN2B -- O16	172(2)
O2 -- O17	2.736(3)	O2 -- H2O -- O17	168(2)
N1 -- O17	3.094(3)	N1 –HN1A – O17	130(2)
N1 -- O15	2.964(3)	N1 –HN1A – O15	135(3)
N1 – O6	3.137(3)	N1 –HN1B – O6	141(2)
N1 -- O12	3.316(3)	N1 –HN1B – O12	150(2)
O15 – O30	2.845(3)	O2 – H15A – O30	173(3)
O15 – O9	2.798(3)	O2 – H15B – O9	177.7(16)
O16 – O33	2.915(3)	O2 – H16A – O33	167(3)
O16 -- O15	2.821(3)	O2 – H16B -- O15	151(3)
O17 – O34	2.815(3)	O2 – H17B – O34	152(3)

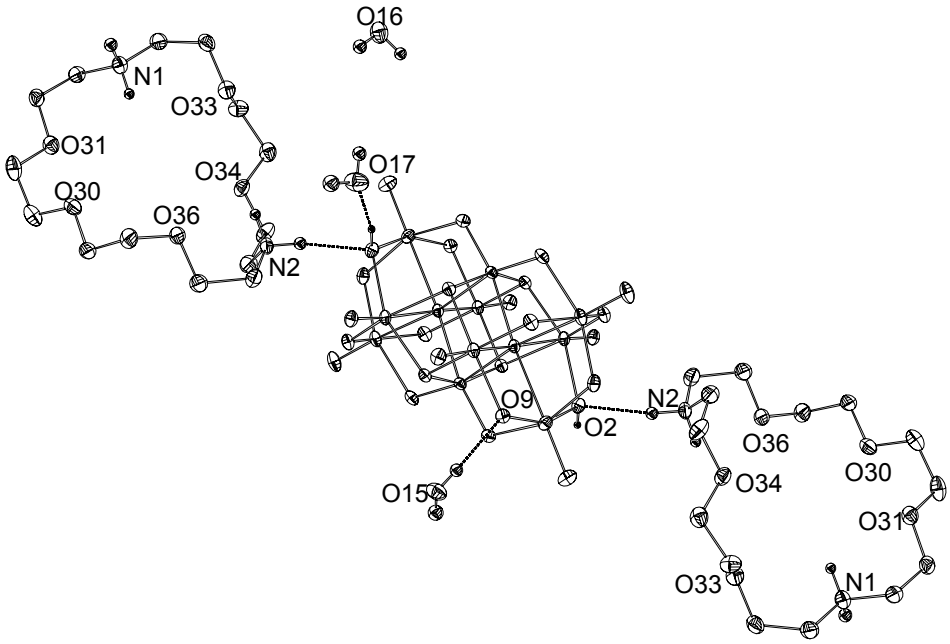

Fig. 36 Molecular structure of **14**

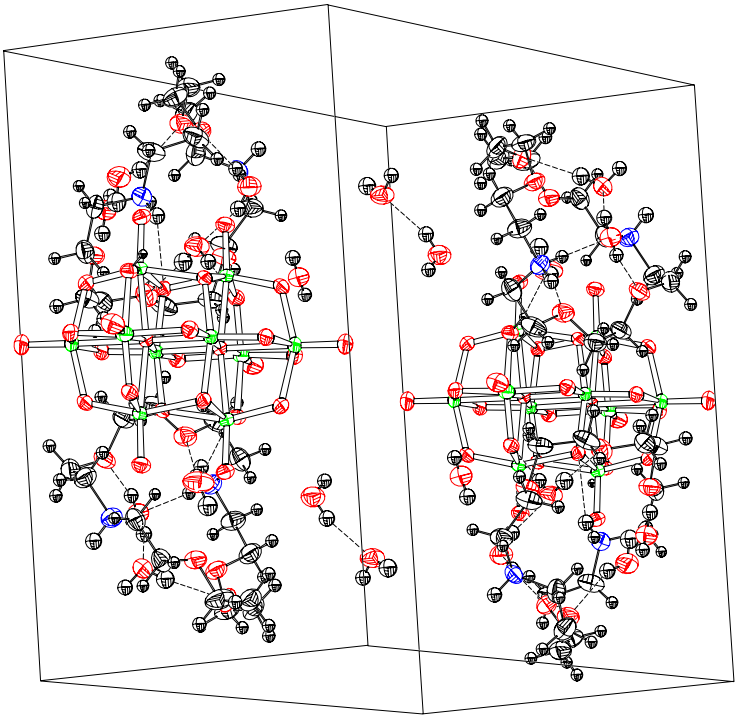

Fig.37 Cell drawing of **14**

diprotonated cryptands C23, as well as the main hydrogen-bonding interactions involving the three components (Table 8); selected bond lengths and bond angles of **14** are listed in Table 9. The $[(H^+)_2V_{10}O_{28}]^{4-}$ anion consists of an an octahedrally packed aggregation of 10 VO_6 octahedra sharing edges. The bond angles and distances observed for the $[V_{10}O_{28}]^{4-}$ unit indicate that the geometry is quit similar to that found in previously reported structures of decavanadates [91,110-114,117], i.e. ten distorted octahedra are edge-linked via bridging oxygen atoms (Fig. 36). The distortion mainly concerns the V-O bonds *trans* to the terminal, doubly bonded oxo groups. The decavanadate anion core includes two hydrogen atoms at doubly bridging oxo groups (O2 and O2') to give a total charge for the anion of -4. The protonation sites are consistent with the location of the H atoms found in the Fourier

Table 9. Selected bond lengths (Å) and bond angles (°) for **14**

	V1(a)	V2(c)	V3(a)	V4(b)	V5(b)
O1(G)				1.5998(18)	
O2(C)			1.9708(18)		
O3(F)			1.6064(16)		
O4(G)					1.5971(18)
O5(E)		1.6873(17)			
O6(F)	1.6055(17)				
O7(D)				1.8468(18)	1.8204(18)
O8(C)			1.7461(17)		
O9(C)	1.9096(17)			1.7796(16)	
O10(B)	1.9280(17)		2.0583(17)		
O11(A)	2.2717(15)	2.1040(17)		2.3143(16)	2.3298(17)
O12(B)	2.0145(16)	1.9588(16)	1.9132(16)		
O13(E)		1.6919(17)		1.9951(18)	
O14(C)	1.7881(17)				1.8656(17)

V1 – O14 – V5	115.07(9)	V2 – O11 – V5	170.22(8)
V2 – O13 – V4	111.01(9)	V1 – O11 – V4	84.87(5)
V2 – O12 – V1	108.32(7)	V2 – O11 – V4	86.93(6)
V3 – O12 – V1	99.51(7)	V2 – O11 – V1	94.73(6)
V3 – O12 – V2	106.29(7)	V1 – O10 – V3	97.51(7)
V4 – O11 – V5	83.29(5)	V4 – O9 – V1	113.98(8)
V1 – O11 – V5	84.12(5)	V5 – O7 – V4	115.49(9)

difference maps. Table10 summaries the $\sum s$ values thus calculated from *d*(VO). For most of the oxygen atoms, the values range between 1.74 and 1.90, i.e. they are close to the expected bond order 2 for oxygen. The low *s* values for the oxygen atom O2 and O2' ($\sum s$ = 1.135) definitely indicate that these two oxygens carry a proton. Furthermore, the protonation sites

Table 10. V-O valence bond orders $\sum s$ for compounds **14** and **15**

$[(H^+)_2C23]_2[(H^+)_2V_{10}O_{28}]\cdot 6H_2O$(**14**)		$[(H^+)_2C211]_2(H_3O)^+_2[V_{10}O_{28}]\cdot 9H_2O$(**15**)	
μ_2 - O(C)		μ_2 – O(C)	
O2 - (V3, V4_$1)	1.135	O14(V2, V3)	1.519
O8 - (V3, V5_$1)	1.791	O17(V3, V4)	1.795
O9 – (V1, V4)	1.749		
O14 – (V1, V5)	1.810		
μ_2 - O(D)		μ_2 – O(D)	
O7 – (V4, V5)	1.792	O15(V2, V4)	1.809
μ_2 - O(E)		μ_2 – O(E)	
O5 – (V2, V5_$1)	1.867	O12(V1, V2)	1.877
O13 – (V2, V4)	1.909	O19(V1_$1, V4)	1.854
μ_3 - O(B)		μ_3 – O(B)	
O10 – (V1, V3, V2_$1)	1.884	O11(V1, V3, V3_$3)	1.770
O12 – (V1, V2, V3)	1.890		
μ_6 - O(A)		μ_6-O(A)	
O11 – (V1, V2, V4, V5)	2.007	O10(V1,V2,V3,V4)	2.024
Terminal O(F, G)		Terminal O(F,G)	
(O1-V4, O3-V3, O4-V5)	~1.75	O13-V2, O16-V3, O18-V4	~1.7

agree with those of structurally characterized decavanadate anions previously synthesized [117]. The relatively low $\sum s$ of the other oxygen atoms (except of μ_6-O11) might be indicative of their participation in an extended hydrogen-bonding network between water molecule, the anion $[(H^+)_2V_{10}O_{28}]^{4-}$ and the diprotonated cryptand $[C23(H^+)_2]^{2+}$.

The oxygen atoms of the cryptands are oriented inwards toward the cryptand cavity in a symmetrical manner. Except of the interaction with water molecules, they do not participate in any other H-bonding interactions. There are [relatively weak, *d*(O2---N2) = 2.948 Å] hydrogen-bonding interaction between the protonated μ_2-O2 of the decavanadate and one of the protonated nitrogen atoms of the cryptand cation. Oxygen atoms of the decavanadate also

interact with water molecules [*d*(O9---O15 = 2.798 Å; *d*(O2---O17) = 2.736 Å] through hydrogen bonds. The involvement of O2 is in accord with both experimental and theoretical predications regarding the basicity of oxygen sites in decavanadate [90,110,118].

3.1.2 Crystallographic studies of complex **15**

The IR spectrum is similar to that reported for other hexaanionic decavanadates [110,117]. Although ^{51}V NMR spectroscopy of an aqueous solution of **15** also showed three resonances at -560, -573 and -580 ppm, the pattern differs from that

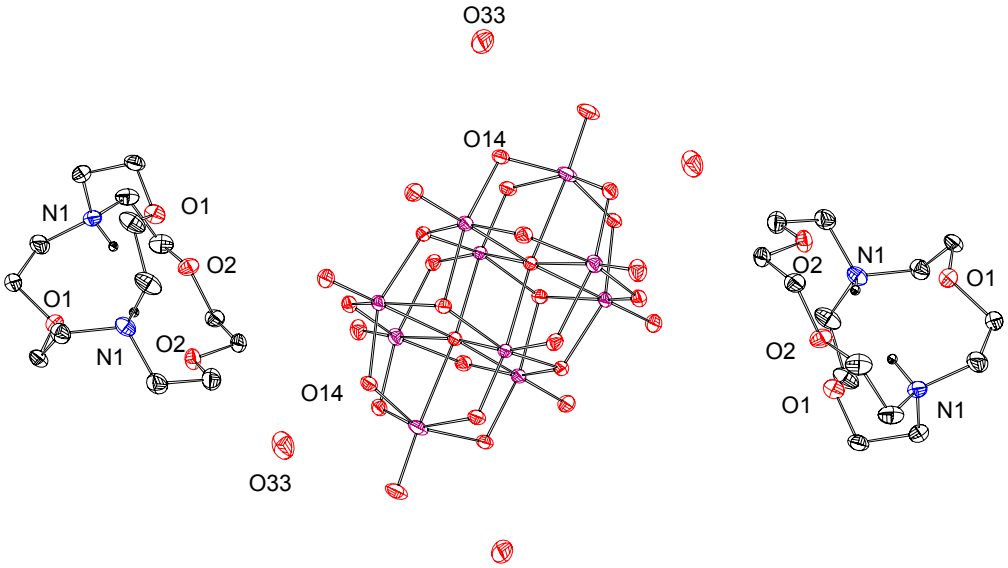

Fig. 38 Molecular structure of **15**

reported for the decavanadate unit [110,117], but corresponds to mono-, di- and tetravanadate [119], indicating that **15** has hydrolyzed under the test condition in solution.

15 crystallizes as an aqua solvate of formula $[(H^+)_2C211]_2(H_3O)^+_2[V_{10}O_{28}]\cdot 9H_2O$ in the centro-symmetric monoclinic space group C2/m (Figs.38, 39). Fig.38 shows the structure and labelling scheme. Selected bond lengths and bond angles of **15** are listed in Table 11. The bond lengths and bond angles observed for the $[V_{10}O_{28}]^{6-}$ unit indicate also that the geometry is similar to that found in previously reported structures of the hexaanionic complexes [91,110-114,117]. The $\sum s$ values for the oxygen atoms are all in the range 1.51-2.04 (Table 10), showing qualitatively that there are no protonated oxygen atoms present in the decavanadate; this result is also in accord with that of the Fourier difference map. Two-

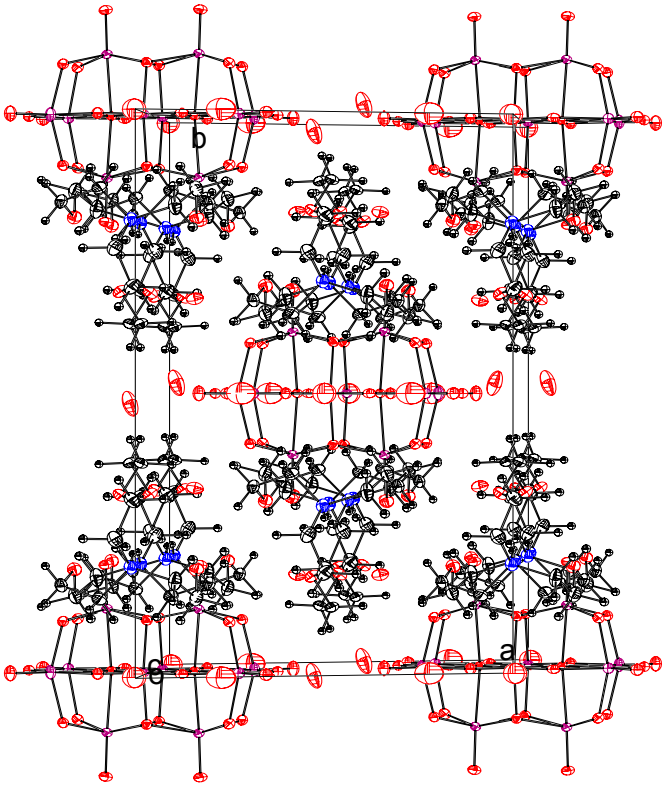

Fig. 39 Cell drawing of **15**

Table11. Selected bond lengths (Å) and bond angles (°) for **15**

	V1(c)	V2(b)	V3(a)	V4(b)
O10(A)	2.063(3)	2.266(3)	2.25986)	2.3151(3)
O11(B)	1.9294(19)		2.0167(19)	
O12(E)	1.670(3)	2.089(3)		
O13(F)		1.594(3)		
O14(C)		1.8826(19)	1.8958(19)	
O15(D)		1.820(3)		1.832(3)
O16(F)			1.609(2)	
O17(C)			1.778(2)	1.8889(19)
O18(F)				1.602(3)
O19(E)				1.991(3)

V1 – O10 – V3	94.56(7)	V3 – O17 – V4	115.38(10)
V1 – O10 – V2	89.04(9)	V3 – O10 – V4	85.29(7)
V1 – O10 – V4	172.72(13)	V4 – O15 – V2	113.64(14)
V1 – O11 –V3	107.20(9)	V4 – O10 – V2	83.68(9)
V1 – O12 – V2	107.27(14)	V2 – O14 – V3	113.60(10)
V2 – O10 – V3	88.62(6)		

diprotonated C211 sandwich the anion, the oxygen atoms of the cryptand are oriented inwards towards the cryptand cavity in a symmetrical manner, the protons form an inter-cavity hydrogen-bonding network.

Hydrogen-bonding interaction between the decavanadate anion and $C211(H^+)_2$, if any, is very weak, as documented by the interatomic cation-anion contacts. The closest contacts, 3.5 Å, are those between N1 and O11 (B type oxygen). $[(H^+)_2C211]_2(H_3O)^+_2[V_{10}O_{28}]$ further contains nine water molecules in the unit cell, four of them are linked to the doubly bridging atoms of the decavanadate anion by hydrogen bonding, i.e. O31/O15(D) and O33/OO14(C).

3. 2 Complexes between heteropolyoxometalates and cryptands

Although several isopoly compounds, such as polyvanadate, have been found to have medicinal potential, heteropoly compounds are more numerous and their structural and electronic properties are easier to modify synthetically than those of the isopoly compounds. Heteropoly compounds therefore dominate the medically oriented research on POMs to date, especially the Keggin structures, $[XM_{12}O_{40}]^{x-}$ (M is usually V, Mo or W; the charge x depends on M and the heteroatom X) with M = W have been found to be very effective antiviral agents. In disagreement with decavanadate, most of the heteropoly compounds, except of the reduced ones, can only exist under very strong acidic condition, i.e. they are thermodynamically unstable in water at physiological pH and degrade into a mixture of inorganic products immediately. Their protection by biogenic macromolecules is a probable

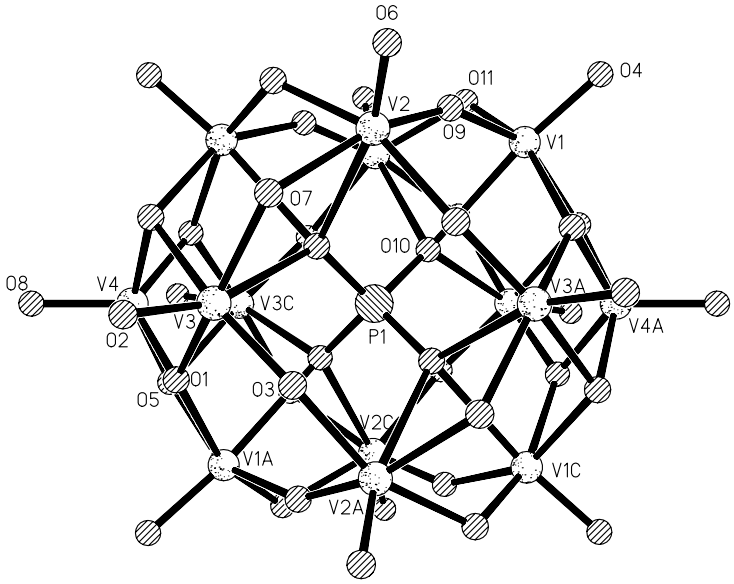

Fig. 40 Schematic prepresentation of $[PV_{14}O_{42}]^{9-}$

way to prevent degradation. In order to testify this possibility, the heteropoly compound $[PV_{14}O_{42}]^{9-}$(Fig. 40) has been chosen to react with the cryptands C22 and C221 to yield $[C22(H^+)_2]_2NEt_4[H_4PV_{14}O_{42}]\cdot 8H_2O$ (**16**) and $[C221(H^+)_2]_2$ $[H_5PV_{14}O_{42}]\cdot 8H_2O$ (**17**).

The compound **16** and **17** were obtained by slow diffusion of an aqueous solution of phosphovanadate into a gel prepared by adding tetramethylsilane to an aqueous solution (pH 3.6) of the cryptand [*c*(cryptand) = 10mM, 15% $Si(OMe)_4$]. The phosphovanadate was prepared according to the literature [120]. In order to avoid the degradation of the compound, the pH of the solution was adjusted to 3.6. Compound **16** was crystallized in the form of red blocks, while **17** was obtained as blue block-like crystals. Both compounds are stable in air.

3.2.1 Studies of compound **16**

Although there are two VO^{3+} caps in addition to the Keggin structure, the IR spectra are not obviously different from those of the Keggin ions themselves. The bands at 1065, 946, 874 and 805 cm^{-1} are assigned to ν_{as}(P-O10), ν_{as}(V=Ot), ν_{as}(V-Ob-V), and ν_{as}(V-Oc-V), respectively (Ot = terminal oxygen, Ob = bridging oxygen of two octahedra sharing a corner,

Table12. Selected bond lengths (Å) and bond angles (°) for **16**

	V1	V2	V3	V4	P
O1			1.9555 (18)	1.8264 (18)	
O2			1.6003(20)		
O3			1.7186 (19)		
O4	1.6005 (22)				
O5				1.9080 (18)	
O6		1.6018 (19)			
O7		2.0129 (19)	1.9262 (19)		
O8				1.6025 (31)	
O9	1.8947 (19)	1.7311 (19)			
O10	2.3869(18)				1.5455(17)
O11	1.7278 (18)				

O(4)-V(1)-O(11)	101.27(10)	O(2)-V(3)-O(3)	103.89(10)
O(4)-V(1)-O(9)	102.91(10)	O(2)-V(3)-O(7)	97.55(9)
O(11)-V(1)-O(9)	95.61(9)	O(3)-V(3)-O(7)	98.50(9)
O(4)-V(1)-O(10)	170.08(9)	O(2)-V(3)-O(1)	99.50(9)
O(11)-V(1)-O(10)	77.45(7)	O(3)-V(3)-O(1)	91.71(8)
O(9)-V(1)-O(10)	87.01(7)	O(7)-V(3)-O(1)	157.40(8)
O(6)-V(2)-O(9)	104.32(10)	O(8)-V(4)-O(1)	116.54(6)
O(6)-V(2)-O(7)	95.22(9)	O(8)-V(4)-O(5)	103.56(6)
O(9)-V(2)-O(7)	160.43(8)	O(5)-V(4)-O(1)	83.74(8)
O(5)_$C-V(4)-O(5)	152.89(12)	O(1)_$C-V(4)-O(1)	126.92(12)

and Oc = bridging oxygen of edge-sharing octahedra). Features at 2815, 1454, 1374, 1354, 1124, and 1106 cm^{-1} are characteristic of cryptand C22.

16 crystallizes as an aqua solvate of formula $[C22(H^{+})_2]_2NEt_4[H_4PV_{14}O_{42}]\cdot 8H_2O$ in the centro-symmetric orthorhombic space group Pban (Fig. 41 and Fig. 42). In addition to the two diprotonated C22 and $[H_4PV_{14}O_{42}]^{4-}$, the unit cell contains eight water molecules and one ammonium ion. Figure 41 shows the structure and labeling scheme of **16** and the hydrogen-bonding interactions involving the tetradecavanadaphosphate anion and cryptand C22. Selected bond lengths and bond angles of **16** are listed in Table 12. The bond angles and distances observed for the $[H_4PV_{14}O_{42}]^{4-}$ unit indicate that the geometry is similar to that previously reported [121]. In the $[H_4PV_{14}O_{42}]^{4-}$ anion, the central PO_4 tetrahedron shares its oxygen atoms with four V_3O_{13} groups, each of which is made up of three edge-sharing VO_6 octahedra. Four V_3O_{13} units are connected to each other by shared corners. The four P-O10 distances (1.545 Å) are a little longer than the value reported in literature (1.529 Å) [121]. This part is the well-known α-Keggin structure having idealized T_d symmetry. There are two A sites which are "pits" on a Keggin molecule, for further coordination of two VO^{3+} units, forming trigonal-pyramidal caps. The metal-oxygen bonds in the VO_6 octahedra are not equivalent; the variation of V-O bond lengths in the VO_6 octahedra correlates with the coordination number of the oxygen: the longest V-O10 (μ_4-O) distances (ca. 2.36Å) and the shortest V=O (terminal) distances (ca. 1.60Å) are the limiting cases.

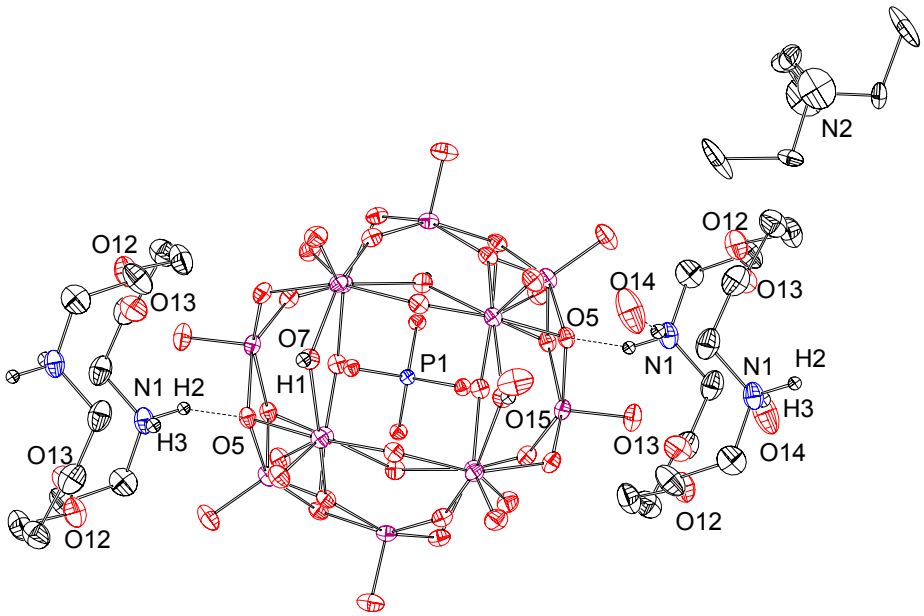

Fig. 41 Molecular structure of **16**

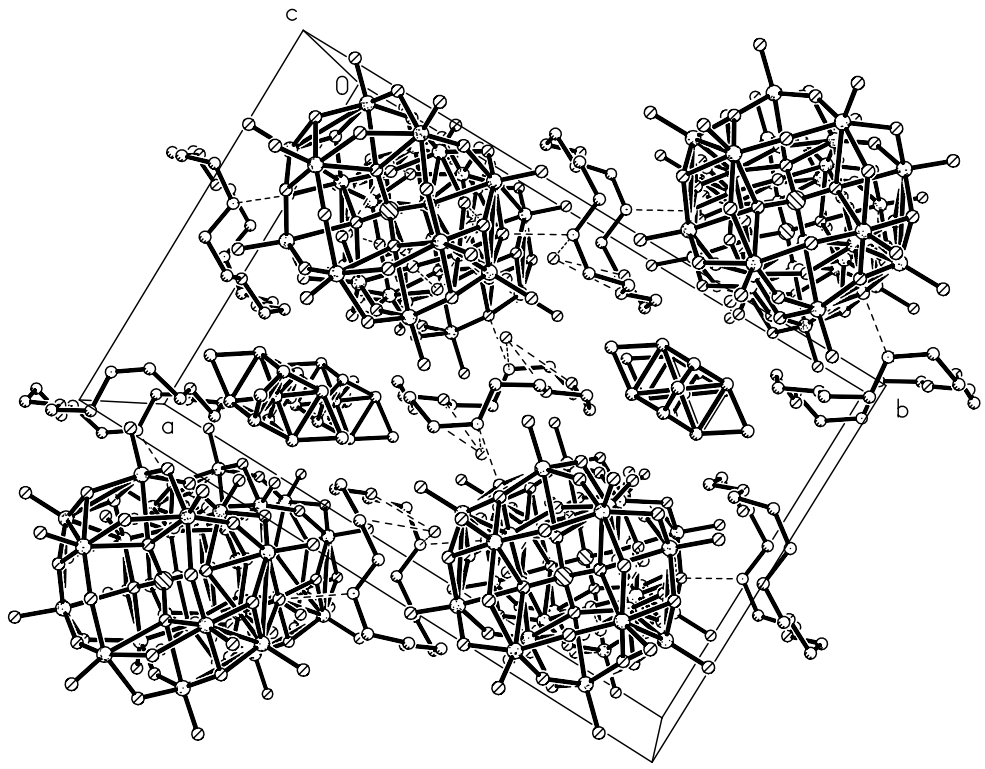

Fig. 42 Cell drawing of **16;** the disorder of the NEt_4 cation has been included

The capping vanadium V4 is bound to five oxygen atoms in a distorted trigonal-bipyramidal arrangement. The vanadium atom forms is in-plane with the three equatorial oxygen atoms (O1, O1_$3, O8). The two axial oxygens (O5 and O5A) are out of line with the

Table13. V-O valance bond orders $\sum s$ for compounds **16** and **17**

$[C22(H^+)_2]_2NEt_4[H_4PV_{14}O_{42}]\cdot 8H_2O$ (**16**)		$[C221(H^+)_2]_2\ [H_5PV_{14}O_{42}]\cdot 8H_2O$ (**17**)	
μ2-O		μ2-O	
O3 (V3, V2_$1)	1.89	O53(V7, V10)	1.27
O7 (V3, V2)	1.23	O55(V1, V3)	1.24
O9 (V1, V2)	1.93	O58(V2, V3)	1.31
O11(V1, V2_$2)	1.865	O72(V3, V12)	1.22
μ3-O		O89(V8, V10)	1.27
O1(V3, V4, V1_$1)	2.04	μ3-O	
O5 (V4, V1_$1, V3_$3)	1.81	O79(V2, V12, V14)	1.39
μ-O (Terminal)		μ-O (Terminal) and	
O2, O4, O6, O8	~1.77	other oxygen atoms	1.7~2.02

Table 14. Interatomic hydrogen-bonding for **16**.

O2 →	H2	2.779	O3 →	O9	2.595
	H3	2.958		O7	2.694
	O15	2.998		O6	2.719
	O14	3.043		O15	2.903
O5 →	H2	1.870		O10	2.959
	O10	2.572	O12→	H3	2.608
	O4	2.716		O14	2.910
	O2	2.740	O13→	O14	2.914
	O7	2.772	O14→	H3	1.930
	O11	2.784		N1	2.906
O15→	H1	1.854		O15	2.920
N1 →	O5	2.803	O7 →	O15	2.741
	O12	2.945			

vanadium atom, the angel O5-V4-O5_$1 is 152.86° (bent towards the center of the compound and thus smaller than the value reported in the literature, 157.4°). The *d*(V-O) to the apical oxygens, *d*(V4-O5) = 1.908 Å, is relatively weak. The high negative charge would prevent the formation of a normal Keggin anion $[PV_{12}O_{40}]^{15-}$, whereas the bicapped Keggin anion $[PV_{14}O_{42}]^{9-}$ is stabilized by the two capping VO^{3+} units.

The phosphovanadate anion core includes four hydrogen atoms at doubly bridging oxygen atoms (O7) to give a total charge of -5. The protonation sites are consistent with the location of H atoms in the Fourier difference maps and consideration based on the valence bond orders summations. The valence bond orders $\sum s$ are listed in Table 13. Except of O7 ($\sum s$ = 1.23), all of the values are in 1.7 - 2.04 range.

The three components of **16** are in contact with each other through hydrogen bonding to afford a three dimensional layered structure (Fig. 42). The interatomic distances and angles regarding hydrogen bonding are listed in Table 14. Each two-protonated nitrogen atoms of the cryptand dication forms a hydrogen bonds with the trebly bridging O5 of the phosphovanadate anion as a hydrogen acceptor to provide a two-dimensional layer structure, which, like sandwich, possily protects the phosphovanadate anion against degradation. Through the hydrogen bonding interaction with the water molecule O15, the phosphovanadate anion connect with each other to give a one dimensional structure, which connect also with the layer structure formed by phosphovanadate anion and diprotonated cryptand to form a

three dimensional structure. (N1--O5 = 2.803 Å, H2--O5 = 1.87 Å). The water molecules in complex **16** act both as a proton acceptor and a proton donor, classified into two types: The type 1 water molecules (O14) as a proton donor bind to opposite sites of one cryptand via O12 and O13 (Fig. 42) (O14--O12 = 2.910 Å, O14--O13 = 2.914 Å). The type 2 water molecules (O15) as a proton acceptor interact with the protonated oxygen of the phosphovanadate anion (O15---O7 = 2.741 Å). The basicity of the bridging oxygen atoms has been examined by ^{17}O and ^{51}V NMR as well as by *ab initio* MO calculations of decavanadates, and the increasing order in the basicity is as following: trebly> doubly > terminal oxygen atoms [90,110,118]. The X-ray crystallographic structure of **16** shows that the hydrogen bonding occurs between the organic molecule and the triply bridging oxygen atoms, and is in good agreement with both experimental and theoretical predictions regarding the basicity of oxygen sites on the vanadate decamer. Thus, the triply bridging oxygen atoms prefer proton acceptors to the doubly and terminal oxygen atoms. This trend is not the exception in **16**.

3.2.2 Studies of compound **17**

17 crystallizes as an aqua solvate of formula $[C221(H^+)_2]_2[H_5PV_{14}O_{42}]\cdot 8H_2O$ in the triclinic space group P1(bar) (Figs. 43 and 44). Selected bond distances and angles are given

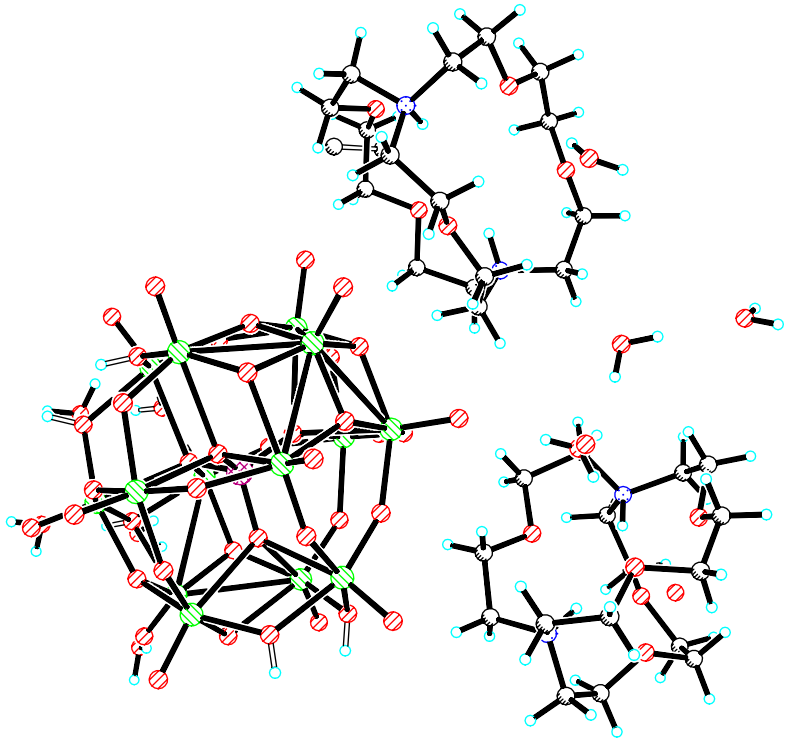

Fig. 43 Molecular structure of **17**

Table15. Selected bond lengths (Å) and bond angles (°) for **17**

	V2	V5	V14	P
O59	1.6152(17)			
O65		1.8109(16)		
O77				1.5301(16)
O78	1.6907(16)			
O79	2.1046(16)		2.0866(16)	
O80		1.9006(16)		
O82			1.8193(15)	
O83	2.3737(16)			1.5565(16)
O87			1.6049(17)	
O88		1.6013(17)		
O92			1.7705(16)	

O(77)-P(1)-O(85)	110.21(9)	O(74)-P(1)-O(83)	108.73(9)
O(61)-V(5)-O(80)	152.94(7)	O(88)-V(5)-O(65)	116.71(8)
O(92)-V(14)-O(79)	154.74(7)	O(82)-V(14)-O(62)	123.09(7)
O(58)-V(2)-O(82)	158.78(7)	O(78)-V(2)-O(79)	155.90(7)

In Table 15. Like **16**, compound **17** consists of twelve MO_6 octahedra, one PO_4 tetrahedron and two VO caps. In **17**, however, the PO_4 tetrahedron is distorted; the P-O distances are in the range of 1.5301 -1.5565 Å, the O-P-O angles vary from 108.73(9) to 110.21(9)°. The two capping vanadium atoms are bound to five oxygen atoms in a distorted trigonal-bipyramidal arrangement. The V5 is in the same plane as the three equatorial oxygen atoms (O51, O65, O88), and the two apexes of the trigonal-bipyramida are out of line with the vanadium atom (O61-V5-O80 = 152.94°). V14 is out of the equatorial plane (O62, O82, O87) by 0.1767 Å; the angle O79-V14-O92 is 154.75°. The distance V14-O79 is slightly longer than V5-O61, and V5-O80 due to the protonation of the oxygen atom O79. Unlike compound **16**, there is no ammonium counterion in the unit cell of compound **17**, and the $[H_5PV_{14}O_{42}]^{4-}$ ion is fivefold protonated, which has been testified not only by structural refinement, but also by valence bond orders. The $\sum s$ values have been listed in Table 13. There are six protonation sites in **17,** each with occupancy of ~ 80%, thus giving rise to an effective number of five protons.

Contrasting **16**, there is no hydrogen-bonding interaction between the phosphovanadate ions and the two diprotonated cryptands. There is, however, a manifold of hydrogen bonds between water molecules, water molecules and cryptands and between

water molecules and the phosphovanadate anion. Examples are OA2 --OA3 = 2.774(3) Å, OA3-- OA5 = 2.801(5) Å; OA3--O41 = 3.043(4) Å, OA3--O42 = 3.149(4) Å; OA1-- O56 = 2.760(3) Å, OA2-- O51 = 2.912(2) Å.

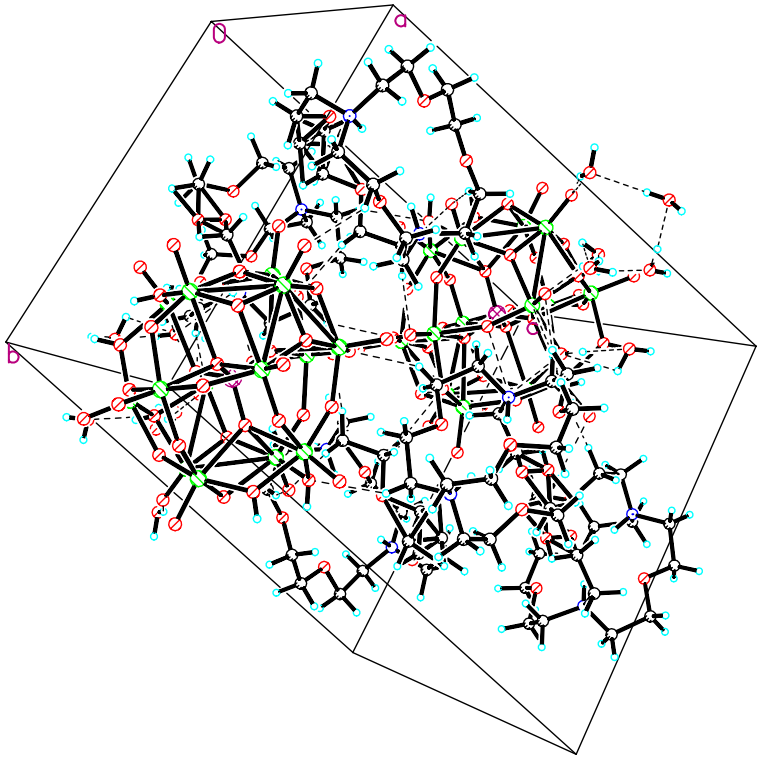

Fig. 44 Cell drawing of **17**

3.3 Synthesis and characterizing of $[(H^+)_2C22]_{2.5}[PV_2W_{10}O_{40}]\cdot 11H_2O$ (18)

Compound **18** was prepared by the low-temperature-freezing-diffusion method in a Dewar (see experimental part) from C22 and $K_6[PV_3W_9O_{40}]\cdot xH_2O$, prepared according to the literature [123]. The pH was kept below 3.0 in order to avoid the degradation of $[PV_3W_9O_{40}]^{6-}$. Complex **18** forms red block-like crystals and is air-stable. Although the anion of **18**, compared with the known $[PV_3W_9O_{40}]^{6-}$, lacks one vanadium atom possibly due to the change of the solution pH, the IR spectrum of **18** is similar to that of $[PV_3W_9O_{40}]^{6-}$ [123], possibly indicating that two vanadium atoms and one tungsten atom coexist in the same three positions, which is also verified by the structural analysis. The IR of **18** is different from that of γ-$Cs_5[PV_2W_{10}O_{40}]$ [124], where the frequency of the ca. 900 cm^{-1} band, generally ascribed

to M-O-M corner vibrations, decreases and overlaps with the 800 cm^{-1} M-O-M edge vibrations.

18 crystallizes as an aqua solvate of formula $[C22(H^+)_2]_{2.5}[PV_2W_{10}O_{40}]\cdot 11H_2O$ in the triclinic space groups P-1 (Figs. 45 and 46). The X-ray crystal structure of compound **18** reveals the presence of water molecules of crystallization, the cryptand dication $[(H^+)_2C22]$, and the $[PV_2W_{10}O_{40}]^{5-}$ anion. Figure 45 shows the structure and labeling scheme of the compound. Selected bond distances and angles are given in Table 16.

Table 16. Selected bond lengths (Å) and bond angles (°) for **18**

	P	W1	W10(V1)	W12(V2)
O1		1.691(9)		
O10			1.611(9)	
O12				1.660(10)
O13	1.545(9)	2.393(8)		
O15	1.522(9)		2.395(8)	
O16				2.385(9)
O31		1.899(9)		
O29 O38			1.857(9) 1.863(10)	

O(15)-P(1)-O(16)	110.3(5)	O(15)-P(1)-O(13)	107.9(5)
O(31)-W(1)-O(17)	156.9(4)	O(25)-W(1)-O(22)	157.1(4)
O(38)-W(10)-O(39)	158.5(4)	O(29)-W(10)-O(23)	157.5(4)
O(39)-W(12)-O(34)	157.3(4)	O(36)-W(12)-O(32)	157.1(4)

The polyanion consists of 12 octahedra and one PO_4 tetrahedron. For PO_4, the P-O distances are in the range of 1.522(9)-1.545(9) Å, while the O-P-O angles vary from 107.9(5) to 110.3(5)°. The tungsten atoms exhibit typically distorted octahedral coordination with short W=O (terminal) bonds, 1.667-1.739Å, (except W10, W11, W12, which will be discussed below), long W-O(phosphate) bonds, 2.393-2.409 Å, and intermediate W-O-W bonds, 1.839-1.945 Å, for the bridging oxygen atoms.

Compared with the molecular mass of tungsten, the molecular mass of vanadium is small, and the sites of the vanadium atoms in complex **18** could not be determined exactly. A reasonable approach is to conclude that there are 2/3 vanadium and 1/3 tungsten atoms in the

positions 10, 11, and 12. That is to say, two vanadium and one tungsten atoms coexist in these three sites. This is also evident from the bond lengths W/V(10,11,12)-Ot: 1.611 Å, 1.653 Å and 1.660 Å. With increasing site occupancy by V, the bond becomes shorter.

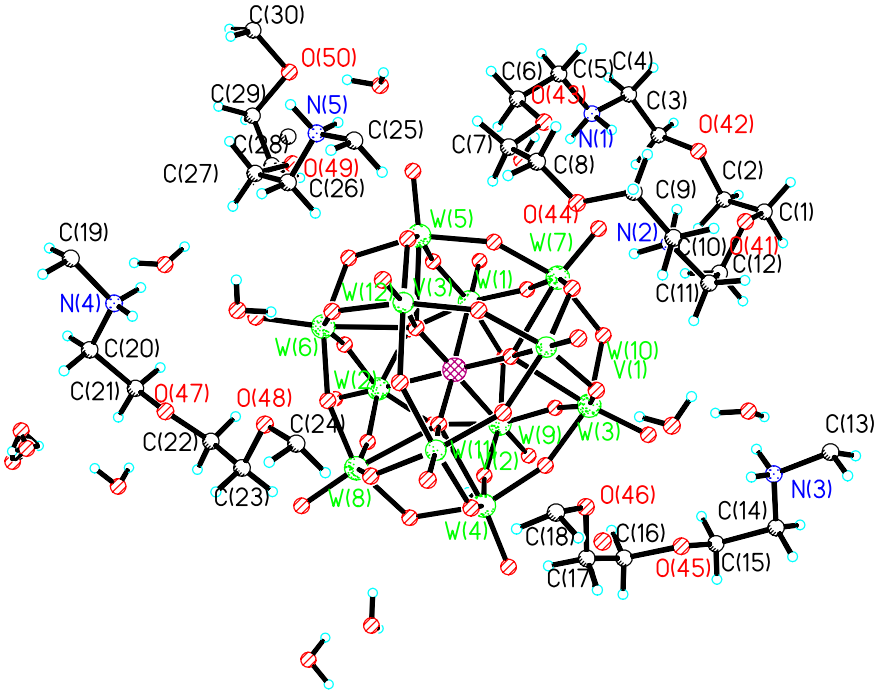

Fig. 45 Molecular structure of **18**

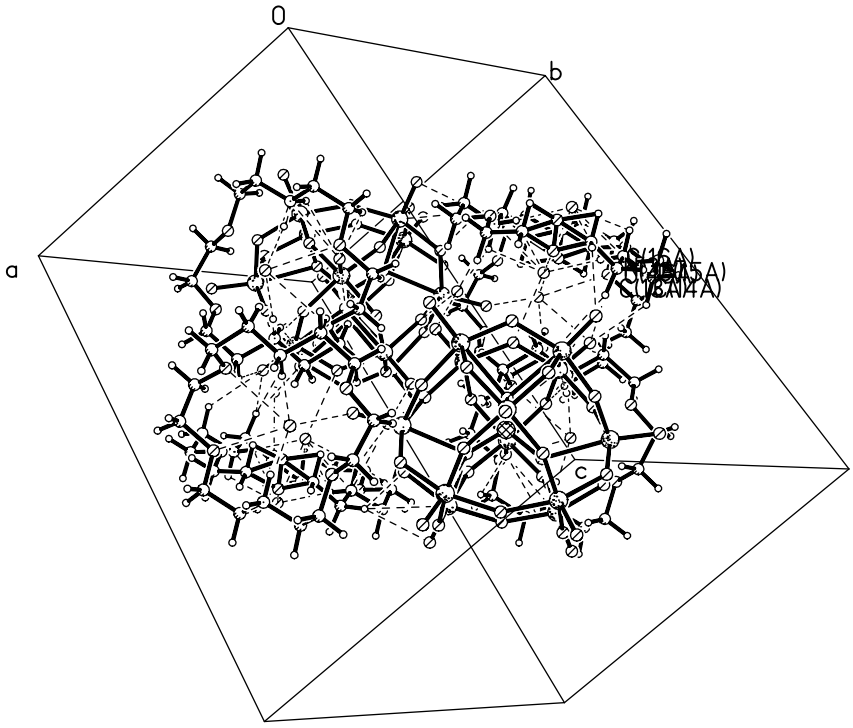

Fig. 46 Cell drawing of **18**

4. Summary/Zusammenfassung

4.1. Summary

The objective of the present work was to synthesize vanadium coordination compounds which model the biological role of vanadium and/or are of potential interest in medicinal applications. Three differing fields of investigation have been dealt with in this context:

(1) The preparation and characterization of potentially insulin-mimetic vanadium compounds as orally administered remedies for diabetes mellitus;

(2) Model investigations towards the interaction (coordination and redox chemistry) of vanadium with sulfur-containing compounds (thiolates and disulfides) under physiological conditions;

(3) Stabilization of decavanadates, and phospho- and tungsto-polyoxovanadates by cryptands and related macrocyclic ligands.

(1) Potentially insulin-mimetic vanadium coordination compounds

Seven oxovanadium(IV) and -(V) complexes containing *ONO*, *SN* or *ONS* donor sets haven been synthesized and characterized, where *O* is phenolate, alkoxide or carboxylate, *N* is imine, aromatic or aliphatic amine, and *S* is thioamide or thiolate. Two of these complexes have also been structurally characterised by X-ray diffraction, viz. a chloro-oxovanadium(IV) complex containing a thiosemicarbazone ligand, **1**·acetone (Fig. I), and a dimeric oxovanadium(V) complex, **2**·4DMF (Fig. I), containing a Schiff base ligand based on 2-hydroxynaphthalene-1-carbaldehyde and tris(ethanol)methylamine. In **1**, the thiosemicarbazone ligand coordinates out of its thioketonic tautomeric form. Specific structural features of **2**, which has an inversion centre, are the asymmetrically alkoxo-bridged *anti*-VO^{3+} moities, and the dangling alcoholic groups.

Figure I: ORTEP drawings of the structures of complexes **1** and **2**

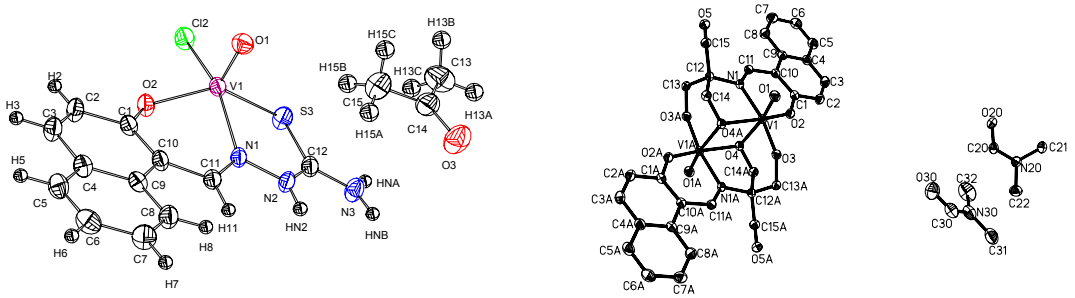

1 **2**

In vitro tests with these compounds have been carried out, using simian virus transformed fibroblasts from mice. Most of the compounds are cytotoxic at concentrations of 1 mM, and non-toxic (over an incubation period of three days) at concentrations of 0.01 mM and below. They show insulin-mimetic effects in that they stimulate the glucose intake by cells, which are comparable to the effect of insulin itself. VO(py-tris) [py-tris is the Schiff base from pyridine-2-carbaldehyde and tris(ethanol)methylamine], although comparatively toxic, is the most effective compound, while VO(van-hisser) (van-hisser is the Schiff base derived from *o*-vanillin and histidylserine), although non-toxic even at 1 mM concentrations, is only marginally effective.

(2) Model reactions for the interaction of vanadium complexes with thiolates and disulfides

The reaction between vanadyltrichloride and disulfides results in the reductive splitting of the disulfide and coordination of the resulting thiolate to $V^{V}O^{3+}$; cf. reactions (a). In the case of **8**, an auxillary ligand fragment, *o*-mercaptoaniline is necessary to provide a stable complex [eqn. (a)]. In the anionic complex **11**, formed in the reaction between VCl_3 and picolinic acid-(*o*-mercapto)anilide [eqn. (b)], the ligand coordinates through the pyridine-N, the deprotonated amide-N and the thiolate. Similarily, the disulfide bond is ruptured as vanadyldichloride is reacted with the disulfide employed in eqn. (c). In the resulting complex **10** [eqn. (c)], the same coordination mode is attained as in **11**. **10** is a dimeric oxo-bridged complex, in which the two VO moieties of the mixed valence (IV and V) complex are about perpendicular to each other.

Eqns. (a), (b) and (c)

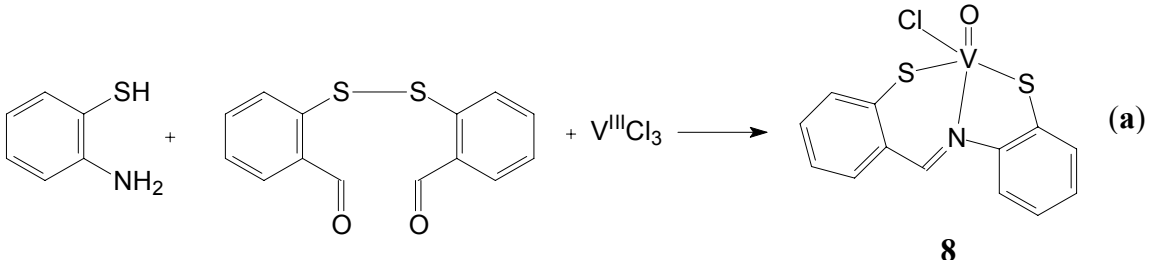

(**a**)

8

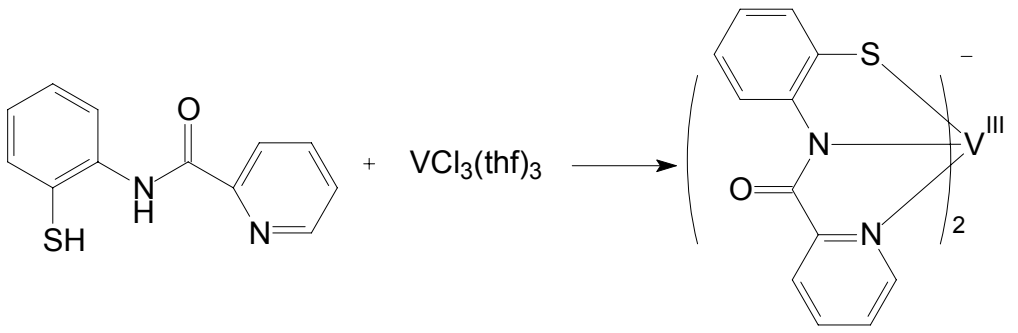

(**b**)

11

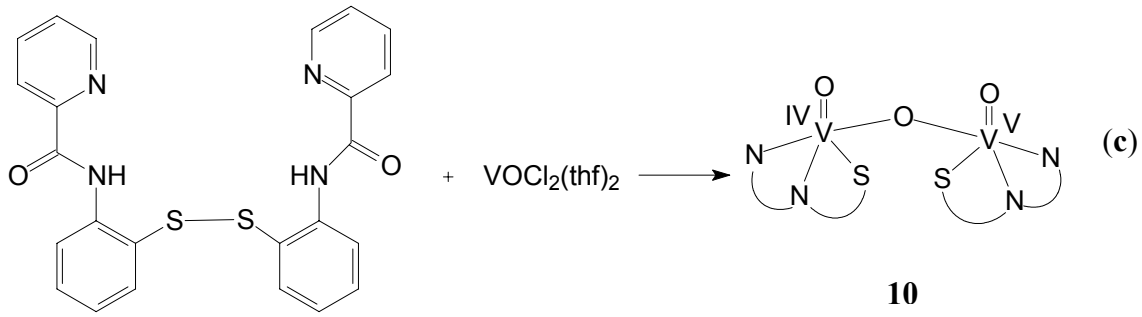

10

Retention of the disulfide bond is observed in the reactions between VCl_3 and a bis(Schiff base) ligand having a disulfide linkage [eqn. (d)], and in the reaction between VO(*o*-vanillin)$_2$ and bis(*o*-aniline)disulfide [eqn. (e)]. The formation of complex **9** according to eqn. (d) is again accompanied by an oxidation of the vanadium centre, here a two-electron oxidation of V^{III} to $V^{V}O^{3+}$. Complexes **8**·pentane, **9**·CH_2Cl_2, [$HNEt_3$]**10**·0.5NEt_3 and [$HNEt_3$]**11** have been characterised by X-ray diffraction analysis.

Eqns. (d) and (e)

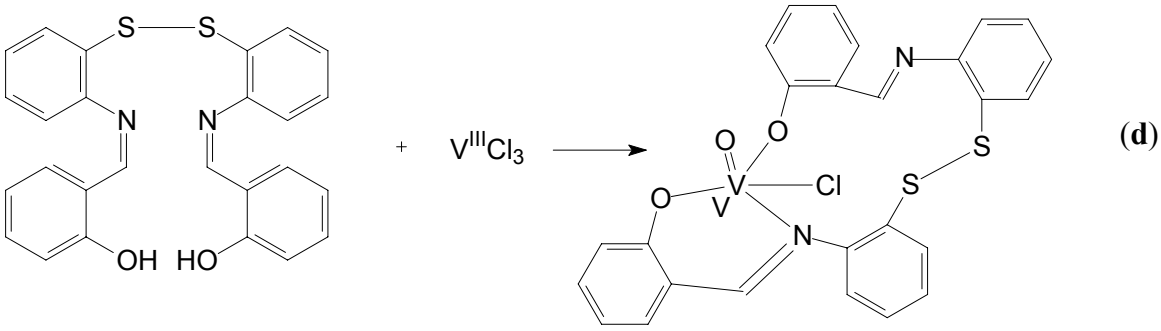

9

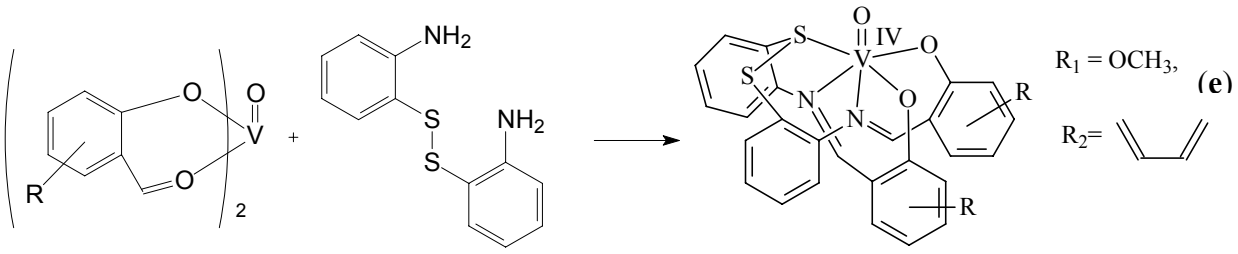

(3) Stabilization of polyoxovanadates

12, **13**

The following iso- and hetero-polyoxovanadates have been obtained and chracterised by X-ray diffraction spectrometry: $[(H^+)_2C23]_2[(H^+)_2V_{10}O_{28}]\cdot 6H_2O$ (**14**) and $[(H^+)_2C211]_2(H_3O)^+_2[V_{10}O_{28}]\cdot 6H_2O$ (**15**);
$[C22(H^+)_2]_2NEt_4[H_4PV_{14}O_{42}]\cdot 8H_2O$ (**16**) and $[C221(H^+)_2]_2[H_5PV_{14}O_{42}]\cdot 8H_2O$ (**17**),
$[(H^+)_2C22]_{2.5}[PV_2W_{10}O_{40}]\cdot 11H_2O$ (**18**).

Fig. II

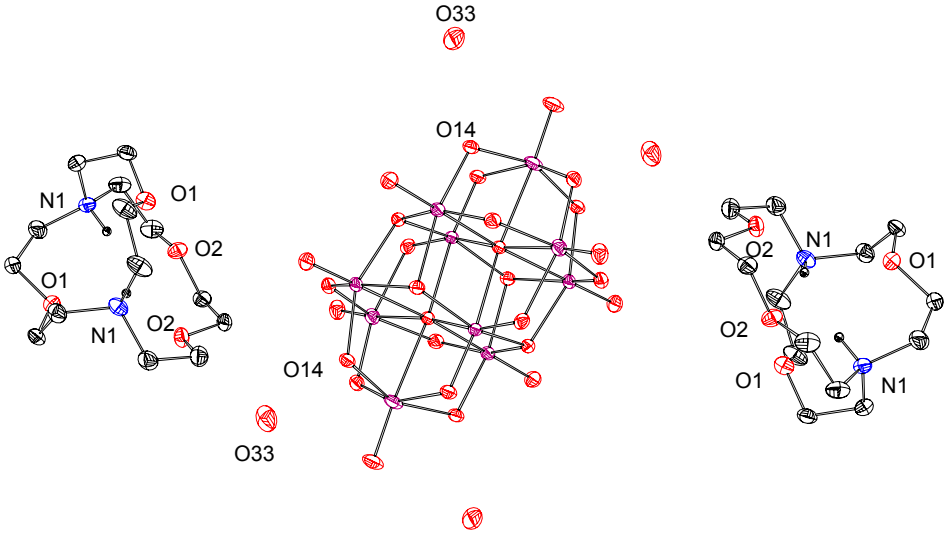

15

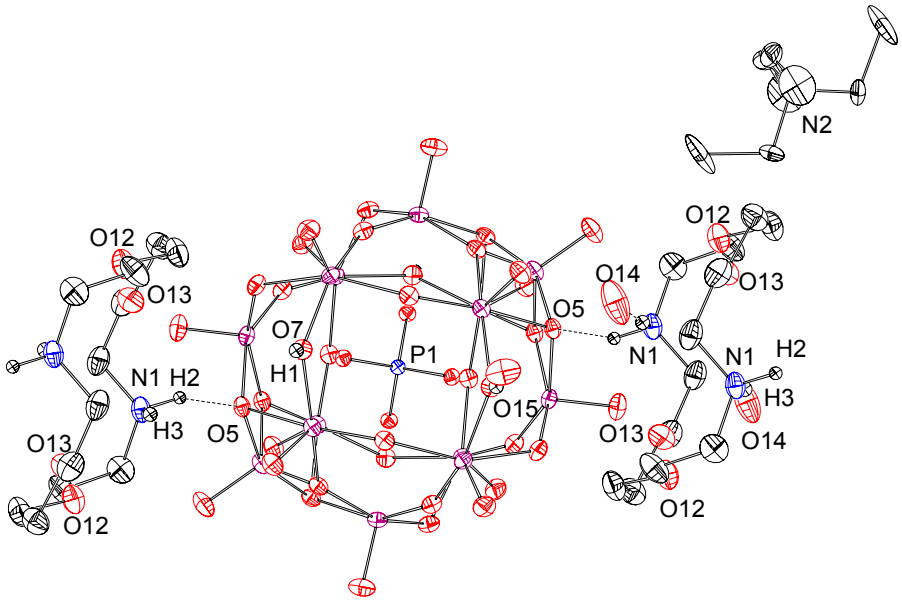

16

Fig. III

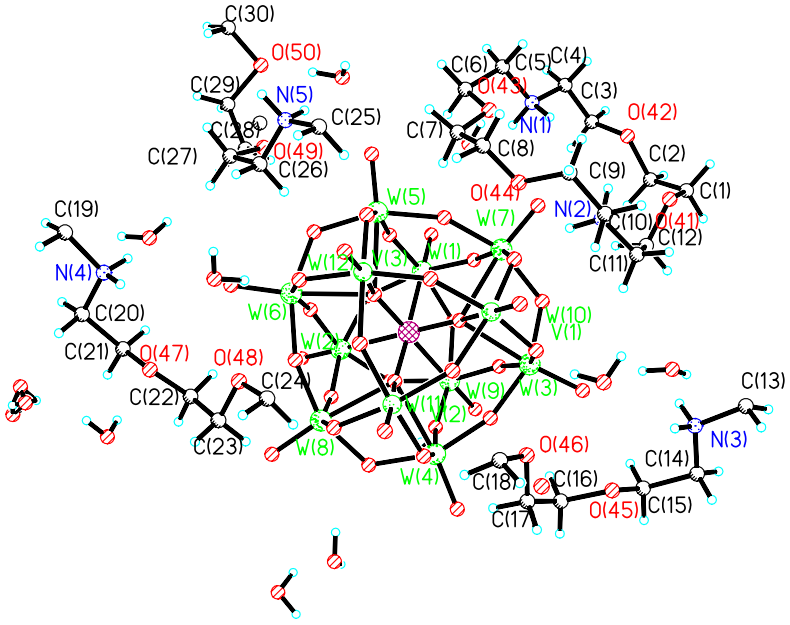

18

For the macrocyclic ligands see Fig. II, for the structures of decavanadate (**14** and **15**), the VO^{3+} bi-capped α-Keggin-phosphovanadate (**16**, **17**) and the phospho-vanadopolyoxotungstate **18** see Fig. III. While the dihydrogendecavanadate in **14**, linked by hydrogen bonds to the diprotonated C23, is stable in water (^{51}V NMR evidence), this is not the case for the unprotonated decavanadate in **15**, where such hydrogen bonding interaction does not exist. Protonation sites in **14** are two doubly bridging (*C*-type) oxygens. The protonation sites have been found in the Fourier difference map and are also evident from the valence bond sums $\Sigma s = 1.13$ (in contrast to 1.7 to 2 for non-protonated oxygens). Hydrogen bonding between the anion and the cation, in addition to electrostatic attraction, is also present in the phosphovanadate **16**, but not in **17**. Another striking difference between **16** and **17** is the number of protonation sites: Four such sites are present in **16**, allowing for a highly symmetric arrangement, i.e. ideal tetrahedral symmetry for the central phosphate and equivalent trigonal-bipyramidal environments for the capping VO^{3+} fragments. In contrast, the symmetry is lifted in **17**, where there are six protonation sites of 80% occupancy each (i.e. five protons present), leading to distortions in the central phosphate and in one of the capping oxovanadium groups.

Apart from the hydrogen bonds between mycrocylic ligand cation and polyoxovanadate anion in **14** and **16**, there is a manifold of hydrogen bonding interactions between water molecules (of crystallization) and water molecules, and water molecules and cations. Noteworthy are the two types of H_2O molecules in **16**: Type one act as donors for cryptand-O and -N, type two are acceptor molecules for the protonated oxo sites in the anion. Further there are intra-cavity hydrogen bonds in the cryptand cations.

An extended hydrogen-bonding network is also present in the tungstate **18**. Here, three adjacent positions of the original Keggin-type phosphotungstate $[PW_{12}O_{40}]^{3-}$ are occupied by 2/3 vanadium ions, leading to an overall composition $[PV_2W_{10}O_{40}]^{5-}$. The five negative anionic charges are counter-balanced by 2.5 diprotonated C22. The partial occupation of tungsten sites by vanadium is in accord with the metal to terminal oxygen bond lengths, which are 1.653-1.660 Å for W=O and 1.611 Å for W/V=O.

4.2. Zusammenfassung

Ziel der vorliegenden Arbeit war die Synthese von Koordinationsverbindungen des Vanadiums mit Modellcharakter für dessen biologische Funktion und/oder potenzieller Anwendung von Vanadiumverbindungen im medizinischen Bereich. In diesem Zusammenhang sind drei unterschiedliche Forschungsfelder behandelt worden:

(1) Darstellung und Charakterisierung potenziell insulinmimetischer Vanadiumverbindungen für die orale Applikation bei Diabetes mellitus;

(2) Modelluntersuchungen in Hinblick auf die Wechselwirkung (Koordination und Redoxchemie) von Vanadium mit schwefelhaltigen Verbindungen (Thiolaten und Disulfiden) unter physiologischen Bedingungen;

(3) Stabilisierung von Dekavanadat sowie Phospho- und Wolframatophospho-vanadaten mittels Cryptanden und vergleichbarer makrozyklischer Liganden.

(1) Potenziell insulinmimetische Koordinationsverbindungen des Vanadiums

Sieben Oxovanadium(IV) und -(V) Komplexe mit *ONO*, *SN* oder *ONS* Donorsätzen wurden synthetisiert und characterisiert. Hierin steht *O* für Phenolat, Alkoxid oder Carboxylat, *N* für Imin, aromatisches oder aliphatisches Amin, und *S* für Thioamid oder Thiolat. Zwei dieser Komplexe wurden auch durch Röntgenstrukturanalyse abgesichert: ein Chloro-oxovanadium(IV)-Komplex mit einem Thiosemicarbazonliganden, **1**·Aceton (Abb. I), und ein dimerer Oxovanadium(V)-Komplex, **2**·4DMF (Abb. I), der einen Schiffbase-Liganden aus 2-Hydroxynaphthalin-1-carbaldehyde und Tris(ethanol)methylamin enthält. In **1** koordiniert das Thiosemicarbazon aus seiner tautomeren Thioketonform heraus. Besondere Strukturmerkmale von **2**, das inversionssymmetrisch ist, sind die unsymmetrisch alkoxoverbrückten, *anti* stehenden VO^{3+}-Einheiten, und die nicht koordinierten alkoholischen Funktionen.

Abbildung I: ORTEP Zeichnungen der Strukturen der Komplexe **1** und **2**

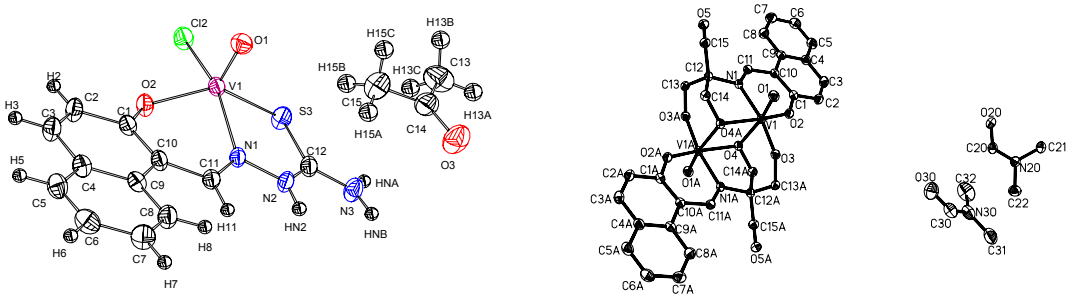

1 **2**

An diesen Verbindungen wurden *in vitro* Tests mit Simianvirus transformierten Mäuse-Fibroblasten durchgeführt. Die meisten Verbindungen sind bei Konzentrationen von 1 M cytotoxisch, unterhalb 0.01M aber bei einer Inkubationszeit von 3 Tagen nicht toxisch. Sie zeigen insulinmimetische Eigenschaften in Hinblick auf die Befähigung, die Aufnahme von Glucose durch die Zellen zu stimulieren. Die durch die Vanadiumverbindungen bewirkten

Effekte sind dabei ähnlich der Wirkung des Insulins selbst. VO(py-tris) [py-tris ist die Schiffbase aus Pyridine-2-carbaldehyd und Tris(ethanol)methylamin], obwohl vergleichsweise giftig, zeigt den ausgeprägtesten insulinmimetischen Effekt, während VO(van-hisser) (van-hisser ist die sich von *o*-Vanillin und Histidylserin herleitende Schiffbase) nur einen geringen Effekt zeigt, obwohl der Komplex bereits bei Konzentrationen von 1 mM ungiftig ist.

(2) Modellreaktionen für die Wechselwirkung von Vanadiumkomplexen mit Thiolaten und Disulfiden

Die Reaktion zwischen Vanadiumtrichlorid und Disulfiden führt zur reduktiven Spaltung der Disulfidbindung und Koordination des resultierenden Thiolats an $V^{V}O^{3+}$; Gl. (a). Im Falle der Verbindung **8** bedarf es eines Hilfsliganden - *o*-Mercaptoanilin - um einen stabilen Folgekomplex zu generieren [Gl. (a)]. Im anionischen Komplex **11**, gebildet aus VCl_3 und Picolinsäure-(*o*-mercapto)anilid [Gl. (b)] koordiniert der Ligand über den deprotonierten Amid-N, Pyridin-N und Thiolat. In ähnlicher Weise wird auch die Disulfidbrücke in dem in Gl. (c) eingesetztem Disulfid gespalten, wenn dieser potenzielle Ligand mit Vanadyldichlorid umgesetzt wird. Im resultierenden Komplex **10** [Gl. (c)] ist dieselbe Koordinationsweise realisiert wie in **11**. **10** ist ein zweikerniger, oxoverbrückter Komplex, in dem die beiden VO Einheiten des gemischt-valenten (IV und V) Komplexes annähernd senkrecht zueinander stehen.

Gleichungen (a), (b) und (c)

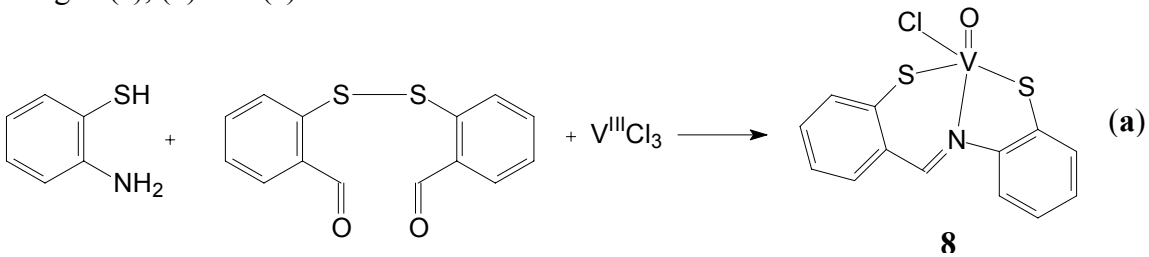

(**a**)

8

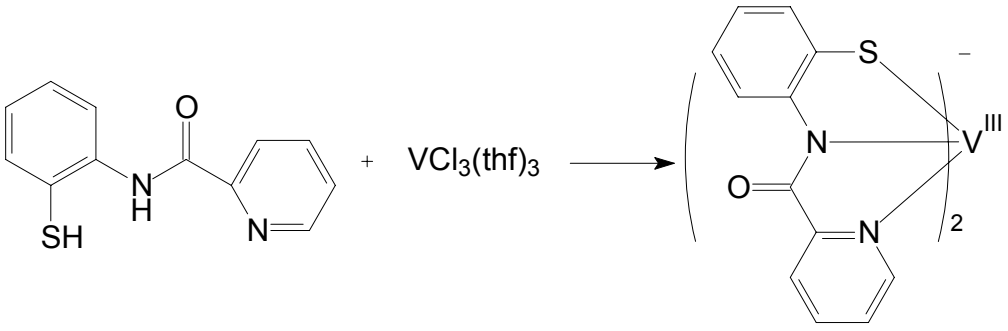

(**b**)

11

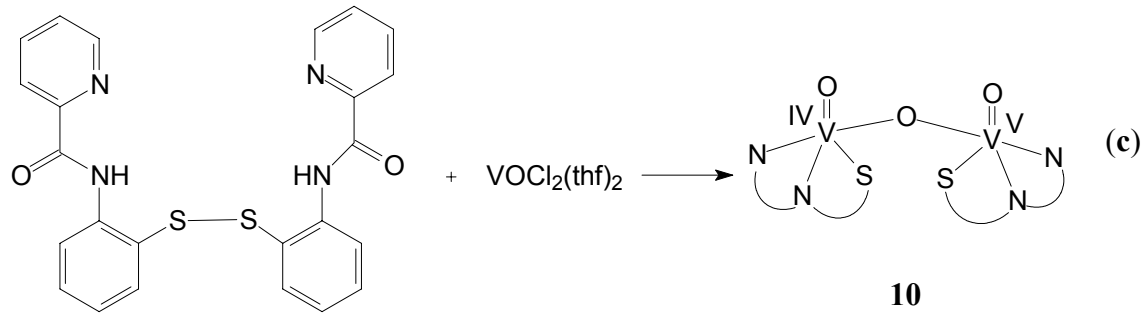

10 (**c**)

Erhalt der Disulfidbindung wird in der Reaktion zwischen VCl_3 und einem Bis(Schiffbase)-Liganden mit einer Disulfid-Brücke [Gl. (d)], sowie in der Reaktion zwischen VO(*o*-vanillin)$_2$ und Bis(*o*-Anilin)disulfid [Gl. (e)] beobachtet. Die Bildung des Komplexes **9** gemäß Gl. (d) wird wieder durch eine Oxidation des Vanadiumzentrums begleitet, hier durch eine Zweielektronen-Oxidation von V^{III} zu $V^{V}O^{3+}$. Die Komplexe **8**·Pentan, **9**·CH_2Cl_2, [$HNEt_3$]**10**·0.5NEt_3 und [$HNEt_3$]**11** wurden durch Röntgendiffraktometrie charakterisiert.

Gleichungen (d) und (e)

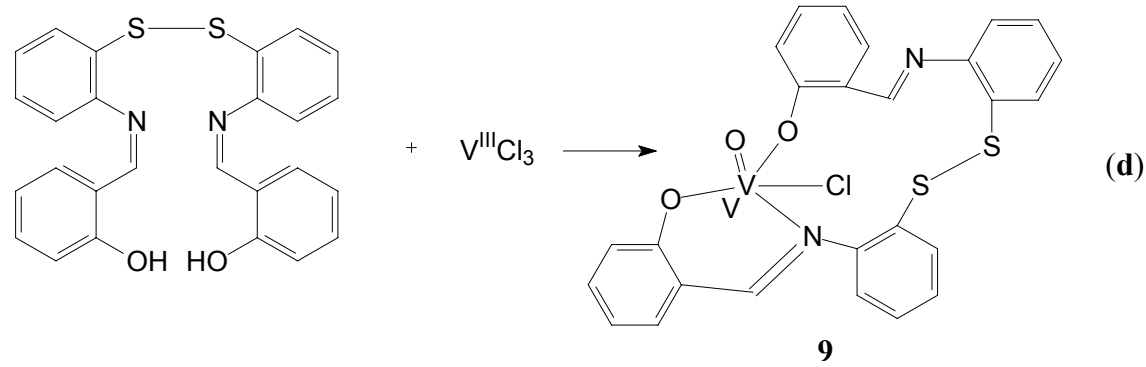

9 (**d**)

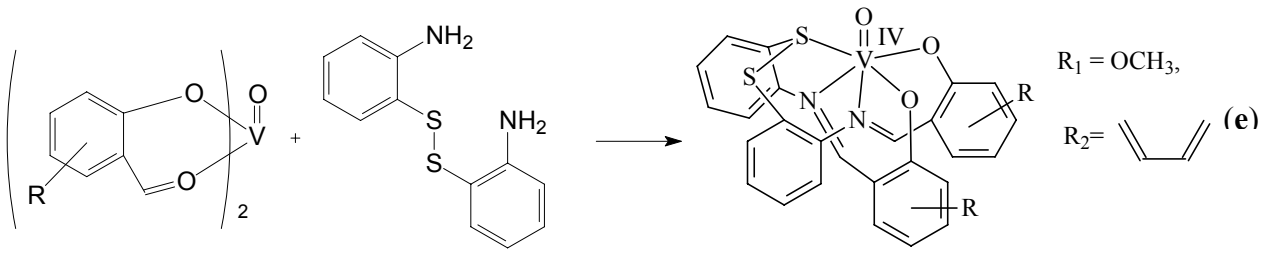

12, **13** (**e**)

(3) Stabilisierung von Polyoxovanadaten

Die folgenden Iso- und Heteropolyoxovanadate wurden synthetisiert und durch Röntgendiffraktometrie charaktersiert: $[(H^+)_2C23]_2[(H^+)_2V_{10}O_{28}]\cdot 6H_2O$ (**14**) und $[(H^+)_2C211]_2(H_3O)^+_2[V_{10}O_{28}]\cdot 6H_2O$ (**15**);
$[C22(H^+)_2]_2NEt_4[H_4PV_{14}O_{42}]\cdot 8H_2O$ (**16**) und $[C221(H^+)_2]_2[H_5PV_{14}O_{42}]\cdot 8H_2O$ (**17**),
$[(H^+)_2C22]_{2.5}[PV_2W_{10}O_{40}]\cdot 11H_2O$ (**18**).

Abbildung II

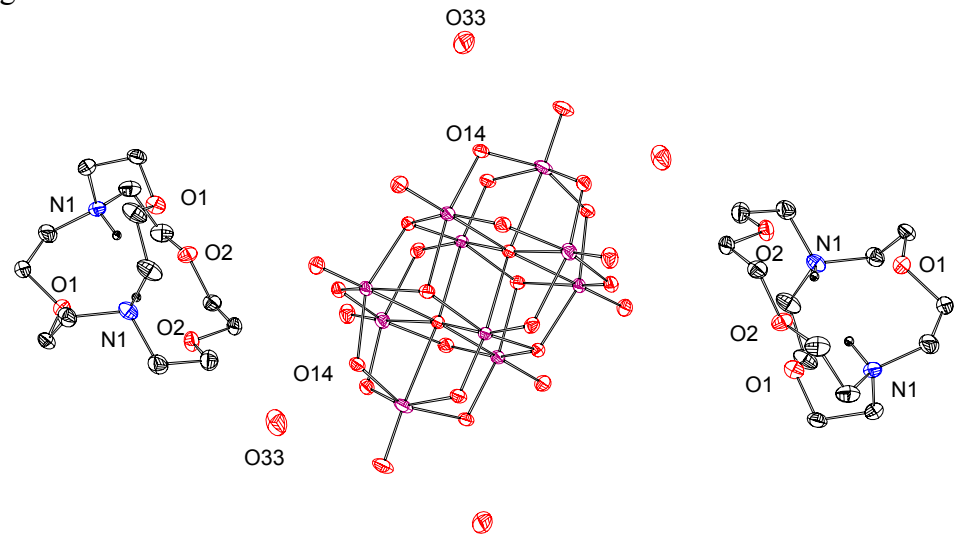

15

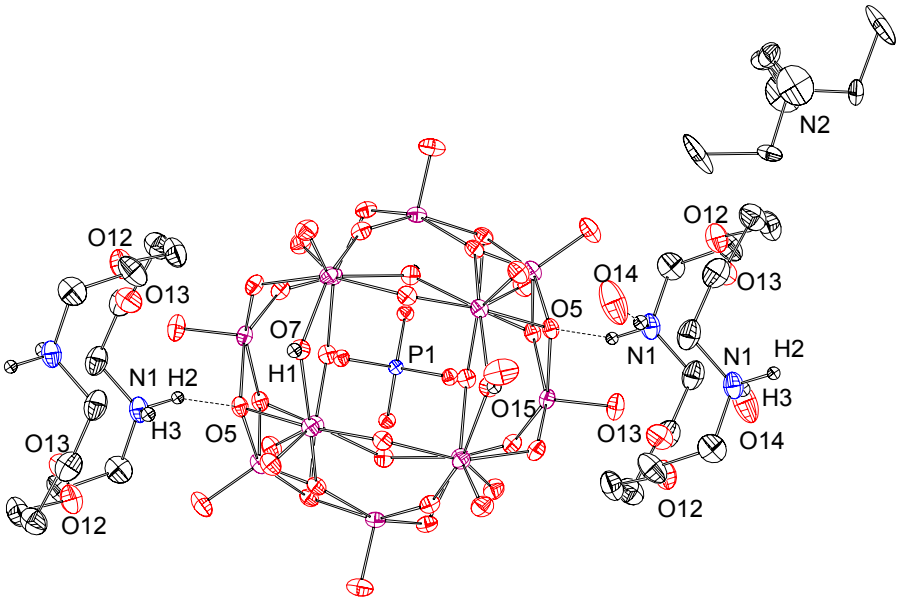

16

Abbildung III

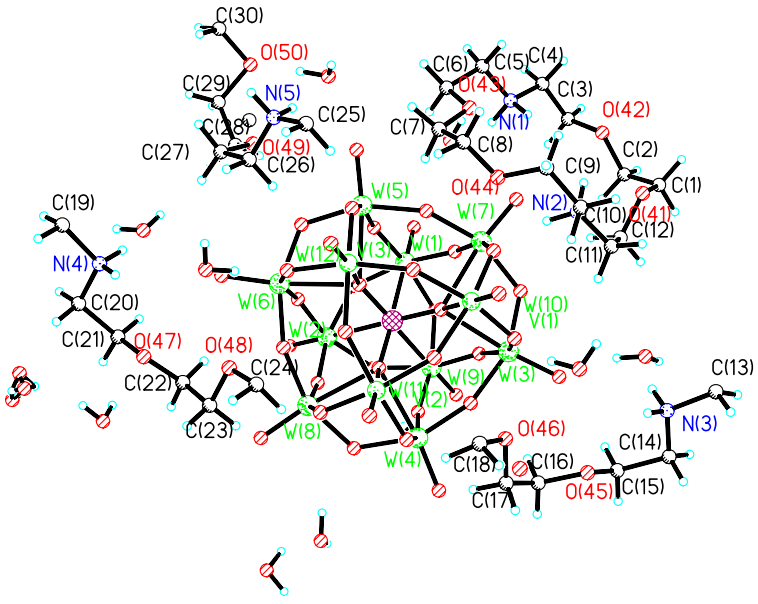

18

Die makrozyklischen Liganden sind in Abb. II, die Strukturen von Dekavanadat (**14** und **15**), der VO^{3+}-verkappten α-Keggin-Phosphovanadate (**16** und **17**) sowie des Phosphovanadatowolframats **18** in Abb. III zusammengestellt.
Während das Dihydrogendecavanadat in Verbindung **14**, verknüpft durch eine Wasserstoffbrückenbindung mit dem zweifach protonierten C23, in Wasser - wie ^{51}V NMR-Spektren zeigen - stabil ist, ist dies im Falle des nicht protonierten Dekavanadats der Verbindung **15**, in der eine solche Wasserstoffbrücke fehlt, nicht der Fall.
Protonierungsstellen in **14** sind zwei doppelt verbrückende (*C*-Typ) Oxo-Liganden. Die Wasserstoffatome wurden in der Fourier-Differenz-Mappe gefunden; ihre Existenz wird aber auch durch die Valenzbindungssummen $\Sigma s = 1.13$ (gegenüber 1.7 bis 2 für nicht-protonierte Oxo-Liganden) gestützt. Wasserstoffbrüchen-Bindungen zwischen Kation und Anion, zusätzlich zu elektrostatischer Wechselwirkung, liegen auch im Phosphovanadat **16**, nicht aber in **17** vor. Ein weiterer auffälliger Unterschied zwischen **16** und **17** ist die Anzahl der Protonierungsstellen: Vier solcher Protonierungsstellen liegen in **16** vor. Hierdurch wird eine hohe Symmetrie ermöglicht, nämlich ideale Tetraedersymmetry für das zentrale Phosphat, und äquivalente trigonal-bipyramidale Umgebungen für die beiden verkappenden VO^{3+}-Fragmente. Im Gegensatz dazu wird die hohe Symmetrie in **17** aufgehoben durch insgesamt sechs Protonierungsstellen mit jeweils ca. 80% Besetzung; effektiv liegen hier also fünf Protonen vor. Dies führt zu einer Verzerrung der Geometrie für das zentrale Phosphat und einer der verkappenden Oxovanadiumgruppen.

Neben den Wasserstoffbrücken-Bindungen zwischen dem makrozyklischen, kationischen Liganden und dem Polyoxovanadatanion in **14** und **16** gibt es eine Vielzahl von Wasserstoffbrücken-Wechselwirkungen zwischen Kristallwasser-Molekülen und Wasser plus Kation. Erwähnenswert sind zwei unterscheidbare Typen von Wassermolekülen in **16**: Typ 1 ist ein H-Donor für *O*- und *N*-Funktionen im Kryptanden, Typ 2 ist ein H-Akzeptor für protonierte Oxoanionen des Polyoxovanadats. Darüberhinaus finden sich intramolekulare H-Brücken in den Kryptanden.

Ein ausgedehntes Wasserstoffbrücken-Netzwerk findet sich schließlich auch im Wolframat **18**. Hier sind drei benachbarte Positionen des ursprünglichen Keggin Phosphowolframats $[PW_{12}O_{40}]^{3-}$ besetzt durch 2/3 Vanadium, was zu der Zusammensetzung $[PV_2W_{10}O_{40}]^{5-}$ führt. Den fünf negativen Ladungen des Anions stehen 2.5 zweifach protonierte C22 gegenüber. Die partielle Besetzung von Wolframpositionen durch Vanadium manifestiert sich auch in den Bindungslängen der Metallionen zu den endständigen Oxoliganden; sie betragen 1.653-1.660 Å für W=O und 1.611 Å für W/V=O.

5 Experimental Sections

5.1 Physical Measurements

5.1.1 Elemental analysis

All elemental analyses (C, H, N) were carried out on a Heraeus CHN-O-Rapid analyser in the microanalytical laboratory of the Institut für Anorganische und Angewandte Chemie der Universität Hamburg.

5.1.2 IR-spectroscopy

IR spectra were recorded on a Perkin-Elmer 1720 spectrometer, using KBr pellets for solid samples or nujol spreadings between KBr crystal plates for liquid samples.

5.1.3 NMR- spectroscopy

The ^{1}H spectra were recorded on a Varian Gemini 200 Hz spectrometer (chemical shift range 0–15ppm). The samples were prepared in deuterated solvents in 5 mm vials. TMS (δ= 0 ppm) was used as an internal standard.

The ^{51}V spectra were recorded on a Bruker 360 spectrometer. The samples were prepared in deuterated solvent in 10mm vials and referenced against external $VOCl_3$ at sweep widths of 125 KHz (time domain 8200K) and pulse angles of 60°.

5.1.4 EPR-spectroscopy

EPR spectra were measured with a Bruker ESP 300E spectrometer at 9.74 GHz in 4mm vials and concentrations of 1-5mM.

5.1.5 Cyclic voltammetric measurement

Cyclic voltammetry was carried out with an Anel-System 5000 potentiostate (with the software Easy Scan) under nitrogen atmosphere. A platium wire was used as working electrode, and a platium disk as auxiliary electrode. Ag/AgCl was used as the reference electrode. All potentials were referenced against Fc/Fc^{+}.

5.1.6 X-ray crystallography

X-ray structure analyses were carried out in the θ/2θ scan mode either with a Hilger & Watts Y 290 diffractometer with monochromated Mo-K_α irradiation (λ= 0.71073 Å) or with an Enraf-Nonius CAD4 diffractometer with monochromated Cu-K_α irradiation (λ = 1.54178 Å). Calculations were carried out with the following programs.

ANALYSES	Calculation of the molar weight and the coefficient of absorption (126)
Y290	Steuerung Hilger & Watts Y 290 (127)
WATSHEL	Data reduction and transformation of the data, which were measured by Y290, into SHELX(s) forms (128)
XPREP	Determination of the space group (129)
SHELXS	Structure solution by Patterson and direct methods (130)
SHELXL	Structure refinement (131)
PLUTON	Drawing of molecules (132)
XP	Drawing of molecules (133)
PLATON 95	for molecule picture, symmetry and absorption correction (134)

The factors, which were used for structural analysis, were defined as following:

$$R1 = \frac{\sum_h \left\| F_0(h) \right| - \left| F_c(h) \right\|}{\sum_h \left| F_0(h) \right|}$$

$$wR2 = \sqrt{\frac{\sum_h w\left[F_0(h)^2 - F_c(h)^2\right]^2}{\sum_h w\left[F_0(h)^2\right]^2}}$$

$$Good = \sqrt{\frac{\sum_h w\left[F_0(h)^2 - F_c(h)^2\right]^2}{(n-p)}}$$

U(eq) is defined as one third of the trace of the orthogonalized Uij tensor.

$$U_{eq} = \frac{1}{3}\sum_i \sum_j U_{ij} a_i^* a_j^* \alpha_i \alpha_j$$

5.2 General working method, solvents and starting materials

5.2.1 General working method

All manipulations had to be carried out under a strict inert atmosphere of pure nitrogen by making extensive use of familiar Schlenk techniques (except of the polyoxometalates and cryptands, which were handled in air). The products will be dried under high vacuum and kept under nitrogen.

5.2.2 Solvents

All reagent pure solvents have been dried before using:

THF has been dried over $LiAlH_4$ for 48h, distilled, and then kept under nitrogen.

Dichloromethane has been dried over CaH_2 for 24h, distilled, and then kept under nitrogen.

Ethanol and methanol have been dried over magnesium shavings.

Acetonitrile has been dried over CaH_2 for 24h, distilled, and then kept under nitrogen.

DMF has been dried over CaH_2 for 24h, distilled, and then kept under nitrogen.

Toluene has been dried over Na for 24h, distilled, and then kept under nitrogen.

Triethylamine was dried over CaH_2 for 24h, distilled, and then kept under nitrogen.

5.2.3 Cell cultures and biological test

Tests were performed on Simian virus transformed Swiss 3T3 mice fibroblasts (cell line SV 3T3). The SV 3T3 fibroblasts were maintained in monolayer cultures in T80 plastic tissue culture bottles at 37°C under a humidified atmosphere containing 5% CO_2. Dulbecco's modification of Eagle's medium (DMEM, Sigma) was employed, containing 4.5 g/L of glucose and L-glutamine, supplemented with 10% of fetal calf serum (cytogen), 50 units of penicillin (Sigma) and 50μg of streptomycin (Sigma) per mL. For further treatment, cells were removed with 0.05% trypsin (Sigma) in saline solution. See also [104].

In all tests, an insulin group (cells incubated with insulin instead of the vanadium compound) and a control group (neither insulin nor vanadium compound present) were included, and all tests were carried out in three-fold.

Vanadium complexes were dissolved in the solvents indicated in Table 4.

For toxicity tests, cells were grown in 96 multi-well plates to sub-confluency, and the cells were incubated with the vanadium complexes for 12, 24 and 36h in DMEM. The supernatant medium was removed. Trypane blue (0.2%w/v) in phosphate buffered saline solution was added to the cells and the ratio of stained to non-stained cells was determined after 5 min of incubation time. The counts were related to the overall amount of the cells present (= 100%). The mean error was ca. 10%.

Tests for insulin-mimetic activity were based on the MTT-reduction essay. The yellow, soluble MTT (3-[4,5-dimethylthiazol-2-yl]-2,5-diphenyltetrazolium bromide, Sigma) is reduced by dehydrogenases of living cells in the mitochondrial electron transfer chain to the insoluble purple formazan blue. Cells with an increased level of glucose attain a higher

reduction rate in comparison to a control group. The amount of formazan blue was measured at 570 nm in a multi-well reader (SLT 340 ATC).

Cells were grown to sub-confluency on 96 multi-well plates. The supernatant medium was removed and exchanged for serum-free DMEM without phenol red, supplemented with selenium (5µg/L), glucose (3.5g/L), transferring (5mg/L), hydrocortisone (0.4 mg/L), glutamine (200mg/L), streptomycin (501g/L) and 50 units of penicillin per mL (all Sigma grade chemicals). The cells were incubated in this (insulin-free) medium for 72h. The supernatant medium was removed, and DMEM (without phenol red, as specified) supplemented with MTT (0.5 g/L), and the solutions of the vanadium complex were added to the cells. The cells were incubated at 37°C in a 5% CO_2 atmosphere. After 4h, the supernatant was poured off, and the reaction stopped with 0.5 M HCl in 2-propanol. Photometric measurements were carried out before and after extraction of the dye with HCl/2-propanol. In most cases, the two data sets essentially paralleled each other. The data for the 2-propanol extracts have been used in this presentation, because they are more reliable since they are free of possible inferences caused by colored vanadium compounds. Mean errors for the absorbance are around 0.005 (0.001-0.012).

5.2.4 Starting materials

All required chemicals were obtained from Merck, Aldrich and Fluka, respectively, except the following chemicals, which have been synthesized according to the literature:

N.N'-[dithiobis(phenylene)bis(salicylidenimine)](125)	VCl_3 (thf) $_3$(136)
2,2'-dithiodibenzaldehyde(137)	$VOCl_2$ (thf) $_2$(135)
Decavanadate solution (125)	$K_6(PV_3W_9O_{40})\cdot xH_2O$(123)
N.N'-[dithiobis(phenylene)bis (pyridinecarboxamide)] (138)	$Na_5H_4PV_{14}O_{42}\cdot xH_2O$(120)
N-2-mercaptophenyl-2'-pyridinecarboxamide (138)	$VO(Phacac)_2$(140)

5.3 Synthesis of specific compounds

5.3.1 Synthesis of ligands and starting materials:

1. 2-Hydroxynaphthalene-1-carbaldehyde thiosemicarbazone (TSCnap) (L1)

To a hot solution of 2.25g (25mmol) of thiosemicarbazone in 20ml of ethanol was added 4.305(25mmol) of 2-hydroxynaphthalene-1-carbaldehyde in 20 ml ethanol, the mixture

was then slowly refluxed for 4 h, then was cooled down to room temperature. The precipitate was collected by filtration, washed with ethanol and ether, and dried in vacuum.
Yield: 3.68g (60%)
IR (KBr)[cm^{-1}]: 3045 ν(O-H); 3263 ν(NH_2); 3165 ν(NH); 3051 ν(C-Har.); 1626 ν(C=N); 1192 ν(C=S)
^{1}H NMR (THF-d8) [ppm]: 7.1-8.2 (m, 6H, Har.); 9.026 (s, 1H, CH=N); 10.56 (s, 2H, $CSNH_2$); 10.712(s, 1H, CSNH)
Elemental analysis: M($C_{12}H_{11}N_3OS$) = 245.30g/mol: C, 58.76(58.44); H, 4.52(4.63); N, 17.14(17.09).

2. 3-Methoxy-salicylaldehyde (*o*-vanillin) thiosemicarbazone (L2)

To a hot solution of 4.5g (50mmol) thiosemicarbazone in 20 ml of ethanol was added 7.6g (50mmol) of *o*-vanillin in 10ml ethanol and the mixture then slowly refluxed for 2 h. The mixture was then cooled down to room temperature. The precipitate was collected by filtration, washed with ethanol thoroughly and dried in vacuum. (Prepared according to literature 141)
Yield: 8.33g (74%).
IR (KBr)[cm^{-1}]: 3060 ν(O-H); 3342ν(NH_2); 3166 ν(NH); 3032 ν(C-Har.); 2974 ν($C\text{-}H_{methoxy}$); 1622 ν(C=N); 1185 ν(C=S)
Elemental analysis: M($C_9H_{11}N_3O_2S$) = 225.06 g/mol: C, 47.99(47.60); H, 4.90(5.22); N, 18.66(18.21).

3. 2-Hydroxynaphthalene-1-carbaldehyde-tris(hydroxymethyl)aminomethane (L3)

4.30g (25mmol) 2-hydroxynaphthalene-1-carbaldehyde and 3.02g (25mmol) tris(hydroxymethyl)aminomethane was dissolved in a 100mL mixture of ethanol/toluene (1/1), refluxed for 1h, and then cooled down to room temperature. The precipitate was collected by filtration, washed with ethanol and ether, and dried in vacuum. (Prepared according to literature 142)
Yield: 5.5g (80%).
IR (KBr)[cm^{-1}]: 3032 ν(C-Har.); 2968 ν(-CH_2-); 1636 ν(C=N)
Elemental analysis: M($C_{15}H_{17}NO_4$) = 275.3g/mol: C, 65.44(64.41); H, 6.22(6.50); N, 5.09(5.28)

4. [VO(*o*-vanilline)$_2$]

7.6g (0.05mol) *o*-vanillin, 6.32g (0.025mol) $Na_2SO_4 \cdot 5H_2O$ and 6.8g (0.05mol) $NaOAc \cdot 3H_2O$ were dissolved in 80mL deoxygenated water/ethanol (1.25/1). The solution was stirred for 2h at room temperature. The green precipitate was collected by filtration, washed with ethanol and ether, and then dried in vacuum.

Yield: 14.7g (80%).

IR (KBr)[cm^{-1}]: 3032 ν(C-Har.); 978 ν(C=O)

5. [VO(2-hydroxynaphthalene-1-carbaldehyde)$_2$]

8.6g (0.05mol) 2-hydroxynaphthalene-1-carbaldehyde, 6.32g (0.025mol) $Na_2SO_4 \cdot 5H_2O$ and 6.8g (0.05mol) $NaOAc \cdot 3H_2O$ were dissolved in 80mL deoxygenated water/ethanol (1.25/1). The solution was stirred for 4h at room temperature. The green precipitate was collected by filtration, washed with ethanol and ether, and then dried in vacuum.

Yield: 14.3g (70%).

IR (KBr)[cm^{-1}]: 3050 ν(C-Har.); 982 ν(C=O)

5.3.2 Synthesis of vanadium complexes:

1. VO{chloro-[5,6-benzosalicylidene-thiosemicarbazonato} (**1**)

To a stirred solution of 0.25g (1.0mmol) L1 in abs. THF was added 0.28g (1.0mmol) of $VOCl_2(thf)_2$ in 15ml abs.THF, and the resulting green solution was stirred at room temperature for 2h. The green compound that separated was filtered, washed with abs. THF and n-pentane, and then dried in vacuum.

Yield: 0.2g (50%).

Elemental analysis: M($C_{12}H_{10}N_3O_2SVCl \cdot$ ¾ THF) = 400: C, 44.96(44.74); H, 4.02(4.26); N, 10.48(10.32); V, 12.71(12.68).

IR (KBr)[cm^{-1}]: 3313, 1541 ν(N-H); 1618 ν(C=N); 976 ν(V=O).

Crystals of **1**·$OCMe_2$ suitable for an X-ray analysis were obtained by allowing an acetone solution to slowly concentrate at room temperature.

IR (KBr)[cm^{-1}]: 1696 ν(C=O actone);

EPR(thf)($10^{-4}cm^{-1}$): $g_0 = 1.979$; $A_o^{(1)} = 98.7$, $A_o^{(2)} = 101.1$ (for the redissolved crystal)

2. [V_2O_2\{naphthalylidene[hydroxymethyl-bis(oxymethyl)]aminomethane\}$_2$] (**2**)

1.31g (5mmol) $VO(acac)_2$ and 1.35g (5mmol) L3 were dissolved in 30mL of absolute ethanol and the mixture heated for 4h. The resulting pale green precipitate was filtered off,

washed twice with ethanol and then with ether, and dried in vacuum. Crystals suitable for an X-ray analysis were obtained from DMF.

Yield: 1.07g (60%)

Elemental analysis: M($C_{15}H_{15}NO_5V \cdot H_2O$) = 358.05g/mol; C, 50.29(49.48); N, 3.91(4.03); H, 4.78(5.49); V, 14.22(14.03).

IR (KBr)[cm^{-1}]: 1618 ν(C=N); 974 ν(V=O)

Crystals of **2**·DMF suitable for X-ray analysis were obtained by recrystallization from DMF.

Elemental analysis: $C_{15}H_{14}NO_5V \cdot DMF$ (M=412.32$gmol^{-1}$) C, 52.44(52.22); N, 6.71(6.71); H, 5.13(5.14).

IR (KBr)[cm^{-1}]: 1618 ν(C=N); 952 ν(V=O)

^{51}NMR(DMSO-d6/DMSO): δ=-533pm

3. VO{chloro-(*o*-vanalin-thiosemicarbazonato)}(**3**)

To a stirred solution of 0.23g (1.0mmol) L2 in abs. THF was added 0.28g (1.0mmol) of $VOCl_2(thf)_2$ in 15ml abs. THF, and the resulting green solution was stirred at room temperature for 2h. The green compound that separated was filtered, washed with abs. THF and n-pentane, and then dried in vacuum.

Yield: 0.18g (50%).

Elemental analysis: M($C_9H_{10}N_3O_3SVCl \cdot 1/2THF \cdot 1/2H_2O$) = 370.99 g/mol: C, 35.53(35.38); H, 4.07(4.06); N, 11.33(11.14).

IR (KBr)[cm^{-1}]: 33186 ν(N-H); 1605 ν(C=N); 980 ν(V=O).

EPR(CH_2Cl_2)($10^{-4}cm^{-1}$): g_0 = 1.971; $A_o^{(1)}$ = 94.3, $A_o^{(2)}$ = 100.7

4.VO-(*o*-aminothiophenolate)$_2$ (**4**)

265mg (1mmol) $VO(acac)_2$ was dissolved in 20mL of absolute ethanol and treated with a solution of 250mg (2mmol) *o*-aminothiophenol dissolved in 20mL of ethanol. The mixture was refluxed for 4h, filtered and kept at room temperature for 2 days; a silvery precipitate was formed, filtered and washed with ether, then dried under high vacuum.

Yield: 90mg (30%).

Elemental analysis: $C_{12}H_{12}N_2O_2S_2V$ (M=315.19$gmol^{-1}$), C, 45.71(45.72); H, 3.84(3.97), N, 8.88(8.82).

IR(KBr)[cm^{-1}]: 3434.3, 3210.9 ν(NH_2); 3059.0 ν(C-Harm.); 984 ν(V=O).

EPR(thf)($10^{-4}cm^{-1}$): g_0 = 1.9259; A_o = 88.9.

5. V(phenylacetylacetonato-benzoylhydrazone)$_2$ (**5**)

VO(Phacac)$_2$ (390mg, 1mmol) and benzoylhydrazine (270mg, 2mmol) were dissolved in 40 mL of absolute methanol and refluxed for 4h. The mixture was then cooled to room temperature and filtered; the precipitate was washed with methanol and ether and dried in vacuum.

Yield: 630mg (80%)

Elemental analysis. M($C_{34}H_{28}N_4O_4V$) = 607.53gmol^{-1}; C, 67.22(66.85); N, 9.22(9.14); H, 4.65(4.76); V, 8.38(8.68).

IR (KBr)[cm^{-1}]: 3065 ν(C-Harm.); 1599, 1586 ν(C=N).

EPR (thf)(10^{-4}cm^{-1}): g_0 = 1.9177, A_o = 69.9.

6. VO[N-(2-oxido-3-methoxysalicylidene)-histidyl-serine](H_2O) (**6**)

60.5mg (0.25mmol) L-Histidyl-L-serine and 68mg (0.5mmol) sodium acetate trihydrate dissolved in 1mL of deoxygenated water were treated with a solution of o-vanillin (38.05mg, 0.25mmol) in 1.25mL of deoxygen ethanol. To this mixture, 54mg (0.25mmol) $VOSO_4 \cdot 5H_2O$ dissolved in 0.4mL of deoxygen water was slowly added, after 2h of stirring, a light green precipitate had formed, which was filtered off, washed with cold ethanol and ether, and dried in high vacuum.

Yield: 68.5mg (60%)

Elemental analysis: M($C_{17}H_{17}N_4O_7V \cdot H_2O$) = 459.31gmol^{-1}; C, 44.46(44.34); H, 4.39(4.43; N, 12.20(12.10)

IR(KBr)[cm^{-1}]: 1678 ν(CONH); 1618 ν(C=N); 969 ν(V=O).

^{51}NMR(DMSO-d6/DMSO): δ=-529ppm

7. VO{pyrididene-tris(methoxy)methylamine} (**7**)

121mg (1mmol) Tris(hydroxymethyl)aminomethane and 123mg (1mmol) pyridine-2-carbaldehyde were dissolved in 50mL of ethanol and refluxed for 2h, the solvent was removed in vacuum. The residue (Schiffbase ligand) was redissolved in 50 mL of CH_2Cl_2. To this solution, 265mg (1mmol) VO(acac)$_2$ was added. After 4h of stirring at room temperature, a black green precipitate was filtered off, washed with pentane and dried under vacuum.

Yield: 13mg(50%).

Elemental analysis. ($C_{10}H_{11}N_2O_4V \cdot 4H_2O$) = 226.23gmol^{-1}: C 34.69(34.22); H, 5.53(5.55); N, 8.09(8.03); V, 14.71(14.41)

IR(KBr)[cm^{-1}]: 1606 ν(C=N), 984 ν(V=O).

^{51}NMR(DMSO-d6/DMSO): δ=-518ppm (relative to $VOCl_3$)

8. VO{Chloro-[N-(2-sulfidophenyl)thiosalicylideneaminate]} (**8**)

0.635g (1.7mmol) [$VCl_3(THF)_3$], 0.466g (1.7mmol) 2,2'-dithiodibenzaldehyde, and 0.463 g (3.4 mmol) *o*-mercaptoaniline were dissolved in 60 mL of abs. THF. 0.405g (4mmol) triethylamine was added, and the solution was refluxed overnight under nitrogen. The resulting brown precipitate was filtered off and washed with chloroform and pentane, and dried in vacuum.

Yield: 0.25g (80% with respect to [$VCl_3(THF)_3$])

IR (KBr)[cm^{-1}]: 1582 ν(C=N); 930 ν(V=O); 380 ν(V-S); 349 ν(V-Cl).

^{1}H NMR (DMSO-d6) [ppm]: 9.45 (s, HC=N)

Crystals of **8**·C_5H_{12} suitable for X-ray structure analysis were obtained by slow diffusion of *n*-pentane to the filtrate of the above reaction.

9. VO[{chloro-{N,N'-[dithiobis(phenylene)]bis(salicylideniminate)}] (**9**)

457mg (1mmol) N, N'-[dithiobis(phenylene)bis(salicylidenimine)], 373mg (1mmol) [$VCl_3(THF)_3$] were dissloved in 100ml absolute CH_2Cl_2, 0.405g (4mmol) triethylamine was added, and the solution was refluxed over night under nitrogen. After filtering, the filtrate was cooled to -20°C for two month to give the crystals, suitable for X-ray analysis.

IR(KBr)[cm^{-1}]: 1627, 1606 ν(C=N), 992 ν(V=O).

10. {[VO(N-2-mercaptophenyl-2'-pyridinecarboxamide)]$_2$O}·(H^+NEt_3)·0.5(NEt_3) (**10**)

282mg (1mmol) $VOCl_2(thf)_2$, 458mg (1mmol) N, N'-[dithiobis(phenylene)bis (pyridinecarboxamide)] and 303mg (3mmol) NEt_3 were dissolved in 100mL abs. THF. The solution was refluxed overnight under N_2, and then filtered. The precipitate was a mixture of complex **10** and NEt_3·HCl.

IR(KBr)[cm^{-1}]: 1626, 1596 ν(C=O); 989 ν(V=O).

Crystal of **10** was obtained by redissolving the precipitate in CH_2Cl_2, and keeping the solution at -20°C.

11. [$HNEt_3$][V(N-2-mercaptophenyl-2'-pyridinecarboxamide)$_2$] (**11**)

373mg (1.0mmol) [$VCl_3(THF)_3$], and 231mg (1.0mmol) N-2-mercaptophenyl-2'-pyridinecarboxamide were dissolved in 60 mL of abs. THF. 0.405g (4mmol) triethylamine was added, and the solution was refluxed overnight under nitrogen. The resulting brown

precipitate was filtered off and the filtrate was kept in the refrigerator. The microcrystalline product was collected by filtration and dried under vacuum.

Yield: 0.25g (80% with respect to $[VCl_3(THF)_3]$)

IR (KBr)[cm^{-1}]: 3044 ν(C-Hpyridine); 2976, 2672, 2498 ν(H^+NEt_3); 1611, 1586 ν(C=O); 363 ν_{as}(V-S); 320 ν_s(V-S).

Crystals of **12** suitable for an X-ray structure analysis were obtained by recrystallization in CH_2Cl_2.

12. [VO{N, N'-[dithiobis(phenylene)]bis(3-methoxysalicylideneiminate)}] (**12**)

0.248g (1mmol) diaminodiphenyldisulfide and 0.369g (1mmol) VO(*o*-vanillin)$_2$ were dissolved in 100 mL absolute THF. The solution was refluxed overnight under N_2, and then filtered. The filtrate was dried under vacuum.

Yield: 630mg (80%)

Elemental analysis. M($C_{28}H_{22}N_2O_5S_2V$) = 581.05 g/mol; C, 57.83(58.48); N, 4.82(4.67); H, 3.81(4.46); S, 11.03 (10.84).

IR (KBr)[cm^{-1}]: 3054 ν(C-Harm.); 2998, 2831 ν(OCH_3); 1603 ν(C=N); 984 ν(C=O)

EPR (thf)($10^{-4}cm^{-1}$): g_0 = 1.9738, A_o = 101.33

13. [VO{N,N'-[dithiobis(phenylene)]bis(5,6-benzosalicylideneiminate)}] (**13**)

0.248g (1mmol) diaminodiphenyldisulfide and 0.41g (1mmol) VO(2-hydroxynaphthalene-1-carbaldehyde)$_2$ were dissolved in 100mL absolute THF. The solution was refluxed over night under nitrogen, filtered, and then the filtrate was dried under vacuum.

Yield: 630mg (80%)

Elemental analysis. M($C_{34}H_{22}N_2O_3S_2V$) = 621.05 g/mol; C, 65.69(64.89); N, 4.51(4.38); H, 3.57(4.42); S, 10.31 (10.71).

IR (KBr)[cm^{-1}]: 3055 ν(C-Harm.); 1617 ν(C=N); 982ν(C=O)

EPR (thf)($10^{-4}cm^{-1}$): g_0 = 1.9687, A_o = 103.33.

14. $\{[(H^+)_2C23]_2[(H^+)_2V_{10}O_{28}]\}\cdot 6H_2O$. (**14**)

An aqueous solution (20mL) of 0.061g (0.2mmol) C23 was added to the rapidly stirred orange solution of 20mL (10mM) decavanadate over a period of 20 min. The resulting mixture was stirred overnight at room temperature. After two months at 4 °C, orange crystals suitable for study by means of X-ray diffraction were obtained.

IR(KBr)[cm^{-1}]: 2950-2872cm^{-1} ν(-CH_2-); 2700-2300cm^{-1}ν(H^+NR_2); 1500-1000cm^{-1} ν(C-O C-N); 1000-420cm^{-1} ν(V=O, V-O-V).

^{1}HNMR(H_2O-d_2/H_2O)(ppm): 3.697(b, 8H, RNC**H**$_2$), 3.597(b, 8H, **H**$_2$COR), 3.228 (d, 12H, ROC**H**$_2$C**H**$_2$OR, J = 5.6Hz)

^{51}NMR(H_2O-d_2/H_2O)(ppm): δ=-425, -507, and -525

The solution of decavanadate was prepared according to the literature [125].

15. {(C211)$_2$[$(H_3O)^+$][$(H^+)_2V_{10}O_{28}$]}·9H_2O (**15**)

The complex **15** was synthesized by the addition of 20mL 0.058g (0.2mmol) of an aqueous solution of C211 to the solution of decavanadate in analogy to complex **14**. After four months at 4 °C, orange-red crystals suitable for an X-ray diffraction studies were obtained

IR(KBr)[cm^{-1}]: 1500-1000cm^{-1} ν(C-O; C-N); 1000-420cm^{-1} ν(V=O, V-O-V).

^{51}NMR(H_2O-d2/H_2O)(ppm): δ= -560, -573, -580

16. [C22$(H^+)_2$]$_2$$NEt_4$[$H_4PV_{14}O_{42}$]·8$H_2O$ (**16**)

The complex was prepared by diffusion of an aqueous solution of phosphatevanadate (0.1mM, 20mL, pH 3.6) into a gel prepared by adding 3mL of tetramethoxisilane to an aqueous solution (17mL, pH 3.6) of the cryptand C22 (0.0525g, 0.2mmol). (see Fig. 48)

IR(KBr)[cm^{-1}]: 1500-1000cm^{-1}ν(C-O; C-N); 1065cm^{-1}ν(P-O); 1000-420cm^{-1}ν(V=O, V-O-V).

17. [C221$(H^+)_2$]$_2$[$H_5PV_{14}O_{42}$]·8H_2O (**17**)

The complex was also prepared in analogy to complex **16** by using cryptand C221 (0.0665g, 0.2mmol).

IR(KBr)[cm^{-1}]: 1500-1000cm^{-1}ν(C-O; C-N); 1055cm^{-1}ν(P-O); 950-420cm^{-1}ν(V=O, V-O-V).

18. [$(H^+)_2$C22]$_{2.5}$[$PV_2W_{10}O_{40}$]·11H_2O (**18**)

20 mL aqueous solution of 589.4mg 1.4.9-K_6[$PV_3W_9O_{40}$]·H_2O, prepared according to the literature, was put into a Schlenk and frozen, afterwards 15mL distilled water was added and frozen two times. Finally, a 20mL aqueous solution of C22 (52.47mg) was added and frozen. The Schlenk was kept in a liquefied N_2 filled dewarand and lift in room temperature. **18** was obtained by increasing of the solution temperature slowly. In order to avoid the degradation, the pH value of these solutions was kept under 3. (See Fig. 49)

IR(KBr)[cm^{-1}]: 1455-1000cm^{-1}ν(C-O; C-N); 1085cm^{-1}ν(P-O).

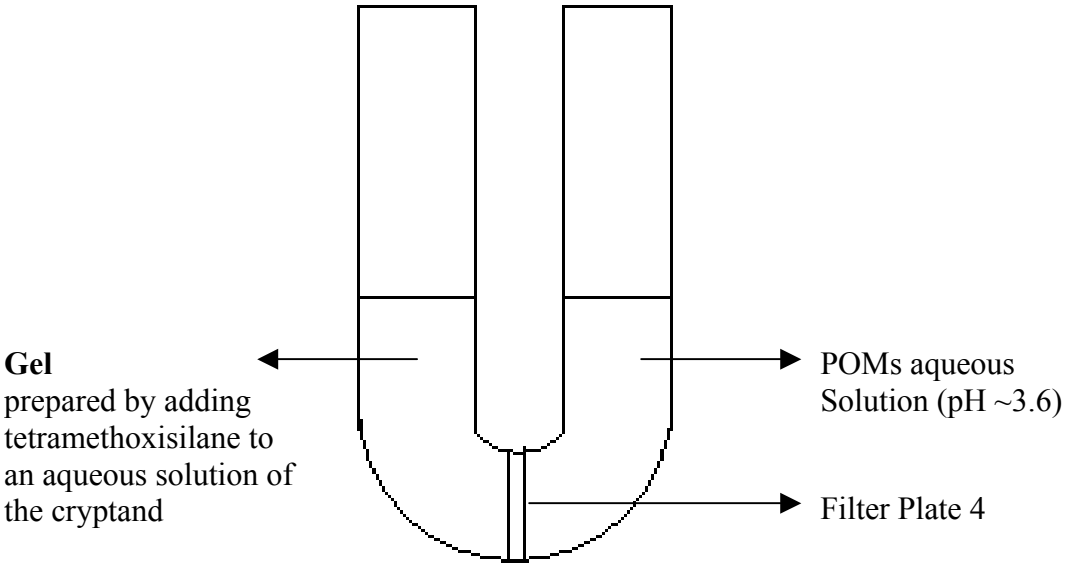

Fig. 48 used for synthesis of **16** and **17**

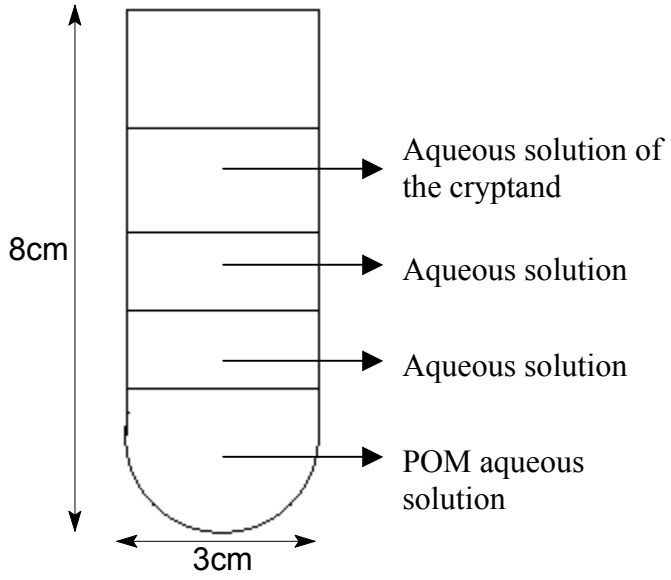

Fig. 49 used for synthesis of **18**

5.4 Crystal data

5.4.1. [**1**·$OCMe_2$]

Table 1: Crystal data and structure refinement for VO{Chloro-[5,6-benzosalicylidene-thiosemicarbazonato}·$OCMe_2$

Empirical formula	$C_{15}H_{16}ClN_3O_3SV$	
Formula weight	404.76	
Temperature	173(2) K	
Wavelength	1.54178 Å	
Crystal system, space group	monoclinic, P2(1)/c	
Unit cell dimensions	a = 7.7413(17) Å	alpha = 90°.
	b = 13.219(2) Å	beta = 98.28(2) °.
	c = 17.044(4) Å	gamma = 90°.
Volume	1725.9(7) $Å^3$	
Z, Calculated density	4, 1.558 g/cm^3	
Absorption coefficient	7.532 mm^{-1}	
F(000)	828	
Crystal size	0.60 x 0.30 x 0.20 mm	
Theta range for data collection	4.25 to 76.32 deg	
Index ranges	-9<=h<=3, 0<=k<=16, -21<=l<=21	
Reflections collected / unique	3937 / 3626 [R(int) = 0.0307]	
Completeness to 2theta = 76.32	95.7%	
Max. and min. transmission	0.3142 and 0.0931	
Refinement method	Full-matrix least-squares on F^2	
Data / restraints / parameters	3626 / 3 / 233	
Goodness-of-fit on F^2	0.688	
Final R indices [I>2sigma(I)]	R1 = 0.0561, wR2 = 0.1446	
R indices (all data)	R1 = 0.0650, wR2 = 0.1577	
Extinction coefficient	0.0011(3)	
Largest diff. peak and hole	1.205 and -1.224 e. $Å^{-3}$	

Table 2: Atomic coordinates (x 10^4) and equivalent isotropic displacement parameters ($Å^2$ x 10^3) for **1**·OCMe2. U(eq) is defined as one third of the trace of the orthogonalized Uij tensor

	x	y	z	U(eq)
V(1)	2674(1)	2034(1)	2544(1)	23(1)
Cl(2)	2483(1)	1761(1)	1178(1)	33(1)
S(3)	4719(1)	3315(1)	2395(1)	31(1)
O(1)	853(3)	2513(2)	2676(1)	31(1)
O(2)	2688(3)	602(2)	2713(1)	26(1)
N(1)	3969(3)	2090(2)	3705(2)	23(1)
N(2)	4988(4)	2936(2)	3934(2)	26(1)
N(3)	6424(4)	4348(2)	3590(2)	33(1)
C(1)	2379(4)	121(2)	3367(2)	23(1)
C(2)	1549(4)	-840(2)	3256(2)	29(1)
C(3)	1196(4)	-1390(2)	3884(2)	30(1)
C(4)	1650(4)	-1033(2)	4677(2)	26(1)
C(5)	1254(4)	-1615(2)	5322(2)	31(1)
C(6)	1631(5)	-1263(3)	6082(2)	33(1)
C(7)	2423(5)	-315(3)	6215(2)	34(1)
C(8)	2812(4)	276(2)	5600(2)	29(1)
C(9)	2465(4)	-74(2)	4808(2)	24(1)
C(10)	2843(4)	508(2)	4132(2)	23(1)
C(11)	3795(4)	1436(2)	4261(2)	23(1)
C(12)	5423(4)	3551(2)	3374(2)	26(1)
O(3)	3051(4)	5951(2)	4759(2)	49(1)
C(14)	2393(5)	5598(3)	4127(2)	37(1)
C(13)	2626(6)	6097(4)	3367(2)	50(1)
C(15)	1329(6)	4664(3)	4097(3)	53(1)

5.4.2 [**2**·4 DMF]

Table 1: Crystal data and structure refinement for V_2O_2\{naphthalylidene[hydroxymethyl-bis(oxymethyl)]aminomethane\}$_2$·4 DMF

Empirical formula	$C_{42}\ H_{56}\ N_6\ O_{14}\ V_2$
Formula weight	970.80
Temperature	173(2) K
Wavelength	0.71073 Å
Crystal system, space group	monoclinic, P2(1)/c
Unit cell dimensions	a = 13.2418(4) Å alpha = 90°.
	b = 8.1132(2) Å beta = 106.5420(10) °.
	c = 21.9466(6)Å gamma = 90 °.
Volume	2260.21(11) $Å^3$
Z, Calculated density	2, 1.426 g/cm^3
Absorption coefficient	0.486 mm^{-1}
F(000)	1016
Crystal size	0.50 x 0.40 x 0.40 mm
Theta range for data collection	1.94 to 27.50 deg
Index ranges	-17<=h<=17, -10<=k<=9, -28<=l<=26
Reflections collected / unique	14020 / 5173 [R(int) = 0.0225]
Completeness to 2theta = 27.50	92.9%
Absorption correction	SADABS
Max. and min. transmission	0.8294 and 0.7932
Refinement method	Full-matrix least-squares on F^2
Data / restraints / parameters	5173 / 1 / 308
Goodness-of-fit on F^2	1.026
Final R indices [I>2sigma(I)]	R1 = 0.0295, wR2 = 0.0764
R indices (all data)	R1 = 0.0352, wR2 = 0.0796
Largest diff. peak and hole	0.338 and -0.410 e. $Å^{-3}$

Table 2: Atomic coordinates (x 10^4) and equivalent isotropic displacement parameters ($Å^2$ x 10^3) for **2**·4 DMF U(eq) is defined as one third of the trace of the orthogonalized Uij tensor.

	x	y	z	U(eq)
V(1)	5612(1)	6150(1)	4573(1)	15(1)
O(1)	5966(1)	8018(1)	4507(1)	23(1)
O(2)	5492(1)	5321(1)	3754(1)	21(1)
O(3)	6843(1)	5196(1)	4961(1)	19(1)
O(4)	4876(1)	3620(1)	4693(1)	17(1)
O(5)	2064(1)	9170(1)	3937(1)	23(1)
N(1)	4010(1)	6796(1)	4188(1)	16(1)
C(1)	4787(1)	5342(2)	3189(1)	18(1)
C(2)	5102(1)	4632(2)	2675(1)	24(1)
C(3)	4421(1)	4608(2)	2079(1)	25(1)
C(4)	3385(1)	5279(2)	1946(1)	22(1)
C(5)	2687(1)	5246(2)	1321(1)	27(1)
C(6)	1690(1)	5877(2)	1192(1)	29(1)
C(7)	1349(1)	6579(2)	1687(1)	28(1)
C(8)	2008(1)	6635(2)	2298(1)	25(1)
C(9)	3047(1)	5984(2)	2450(1)	19(1)
C(10)	3775(1)	5995(2)	3086(1)	18(1)
C(11)	3432(1)	6644(2)	3605(1)	18(1)
C(12)	3511(1)	7526(2)	4658(1)	16(1)
C(13)	2707(1)	6324(2)	4784(1)	17(1)
C(14)	4425(1)	7733(2)	5268(1)	18(1)
C(15)	3004(1)	9219(2)	4449(1)	20(1)
O(20)	9444(1)	3586(2)	490(1)	31(1)
N(20)	10775(1)	1753(2)	560(1)	26(1)
C(20)	9978(1)	2385(2)	738(1)	25(1)
C(21)	11087(1)	2436(2)	24(1)	31(1)
C(22)	11336(2)	311(2)	877(1)	44(1)
O(30)	10974(1)	4186(2)	3515(1)	48(1)
N(30)	11918(1)	2607(2)	3014(1)	37(1)
C(30)	11774(2)	3444(2)	3503(1)	36(1)
C(31)	12913(2)	1780(3)	3049(1)	54(1)
C(32)	11074(2)	2457(3)	2429(1)	60(1)

5.4.3 [**8**· Pentan]

Table 1: Crystal data and structure refinement for
VO{Chloro-[N-(2-Sulfidophenyl)thiosalicylideneaminate]}·Pentan

Empirical formula	C18 H21 Cl N O S2 V
Formula weight	417.87
Temperature	153(2) K
Wavelength	0.71073 A
Crystal system, space group	Orthorhombic, Pna2(1)
Unit cell dimensions	a = 13.5994(4) A alpha = 90° .
	b = 9.6053(3) A beta = 90° .
	c = 16.3449(4) A gamma = 90°.
Volume	2135.07(11) A^3
Z, Calculated density	4, 1.300 Mg/m^3
Absorption coefficient	0.790 mm^{-1}
F(000)	864
Crystal size	0.70 x 0.15 x 0.05 mm
Theta range for data collection	2.46 to 27.49 deg.
Limiting indices	-17<=h<=17, -12<=k<=12, -21<=l<=21
Reflections collected / unique	45954 / 4903 [R(int) = 0.0598]
Completeness to theta = 27.49	99.9 %
Absorption correction	Semi-empirical from equivalents
Max. and min. transmission	0.9616 and 0.6080
Refinement method	Full-matrix least-squares on F^2
Data / restraints / parameters	4903 / 0 / 202
Goodness-of-fit on F^2	1.069
Final R indices [I>2sigma(I)]	R1 = 0.0802, wR2 = 0.2382
R indices (all data)	R1 = 0.0975, wR2 = 0.2502
Absolute structure parameter	0.31(7)
Largest diff. peak and hole	0.964 and -0.523 $e.A^{-3}$

Table 2: Atomic coordinates (x 10^4) and equivalent isotropic displacement parameters (A^2 x 10^3) for **8**·Pentan. U(eq) is defined as one third of the trace of the orthogonalized Uij tensor

	x	y	z	U(eq)
V(1)	4784(1)	1117(1)	549(13)	37(1)
Cl(1)	6117(1)	-424(2)	530(13)	57(1)
S(1)	4543(2)	274(3)	1851(13)	64(1)
S(2)	4464(2)	316(3)	-744(13)	51(1)
O(1)	5285(3)	2658(4)	572(14)	67(1)
N(1)	3313(4)	1739(6)	767(13)	55(2)
C(1)	3568(4)	1234(6)	2223(13)	48(2)
C(2)	2941(5)	1873(7)	1666(13)	66(3)
C(3)	2139(5)	2636(8)	1943(14)	99(4)
C(4)	1964(4)	2759(8)	2778(14)	124(6)
C(5)	2590(5)	2120(8)	3335(13)	98(4)
C(6)	3392(4)	1357(7)	3058(13)	69(3)
C(7)	2690(5)	2077(7)	221(13)	46(1)
C(8)	2830(4)	2079(6)	-608(13)	49(2)
C(9)	3495(4)	1361(6)	-1097(13)	48(2)
C(10)	3382(4)	1358(6)	-1942(13)	64(3)
C(11)	2603(5)	2073(7)	-2298(13)	68(3)
C(12)	1938(4)	2790(8)	-1809(13)	103(4)
C(13)	2051(4)	2793(7)	-964(13)	97(4)
C(21)	5239(10)	5392(10)	-989(14)	94(4)
C(22)	5675(10)	5930(8)	-220(14)	93(4)
C(23)	5059(8)	5457(7)	540(15)	89(3)
C(24)	3889(8)	5629(8)	575(16)	98(3)
C(25)	3626(9)	7184(10)	503(16)	112(4)
V(2)	4302(8)	22(12)	398(14)	80(4)
S(21)	4785	1187	-777	101(7)

5.4.4 [**9**·$3CH_2Cl_2$]

Table 1: Crystal data and structure refinement for

VO[{Chloro-{N,N'-[dithiobis(phenylene)]bis(salicylideniminate)}] ·$3CH_2Cl_2$

Empirical formula	$C_{29}H_{24}Cl_7N_2O_3S_2V$
Formula weight	540.93
Temperature	153(2) K
Wavelength	0.71073Å
Crystal system, space group	triclinic, P-1
Unit cell dimensions	a = 11.9662(9)Å alpha = 62.1500(10)°.
	b = 13.2090(10)Å beta = 84.3960(10)°.
	c = 13.7553(10)Å gamma = 65.9500(10)°.
Volume	1743.9(2) A^3
Z, Calculated density	2, 1.030 Mg/m^3
Absorption coefficient	0.500 mm^{-1}
F(000)	552
Crystal size	0.60 x 0.30 x 0.29 mm
Theta range for data collection	1.69 to 25.00°.
Limiting indices	-11<=h<=14, -15<=k<=15, -16<=l<=14
Reflections collected / unique	9640 / 6036 [R(int) = 0.0283]
Completeness to theta = 25.00	98.0 %
Max. and min. transmission	0.8687 and 0.7537
Refinement method	Full-matrix least-squares on F^2
Data / restraints / parameters	6036 / 5 / 395
Goodness-of-fit on F^2	1.108
Final R indices [I>2sigma(I)]	R1 = 0.0709, wR2 = 0.1715
R indices (all data)	R1 = 0.0790, wR2 = 0.1789
Largest diff. peak and hole	1.106 and -1.099 $e.A^{-3}$

Table 2: Atomic coordinates (x 10^4) and equivalent isotropic displacement parameters (A^2 x 10^3) for **9**·3CH_2Cl_2. U(eq) is defined as one third of the trace of the orthogonalized Uij tensor.

	x	y	z	U(eq)
V(1)	1250(1)	2662(1)	2226(1)	18(1)
Cl(1)	2854(1)	667(1)	3304(1)	28(1)
S(1)	-127(1)	3741(1)	4752(1)	23(1)
S(2)	-1154(1)	5534(1)	3515(1)	23(1)
O(1)	2413(3)	3334(3)	2207(3)	23(1)
O(2)	1166(3)	2719(3)	1055(3)	26(1)
O(3)	88(3)	1996(3)	3157(2)	20(1)
N(1)	-137(3)	4457(4)	1871(3)	18(1)
N(2)	-1344(3)	2156(4)	4753(3)	19(1)
C(1)	-1304(4)	3417(4)	5571(4)	23(1)
C(2)	-1137(4)	837(4)	3929(4)	20(1)
C(3)	-1804(4)	2669(4)	5490(4)	21(1)
C(4)	-284(4)	1181(4)	3176(4)	20(1)
C(5)	2345(4)	4490(4)	1560(4)	21(1)
C(9)	104(4)	613(4)	2485(4)	23(1)
C(10)	-1947(4)	5152(4)	2796(4)	21(1)
C(12)	-1607(4)	1327(4)	4673(4)	20(1)
C(15)	52(4)	5479(4)	1400(3)	19(1)
C(17)	1215(4)	5550(4)	1153(3)	19(1)
C(18)	1214(5)	6765(4)	492(4)	23(1)
C(19)	-3160(4)	5299(5)	3014(4)	26(1)
C(20)	-1165(5)	-546(5)	3248(4)	26(1)
C(23)	-1550(4)	-36(4)	3946(4)	23(1)
C(24)	3444(4)	4663(5)	1286(4)	23(1)
C(25)	-329(5)	-217(5)	2517(4)	27(1)
C(26)	-2024(4)	4265(5)	1634(4)	24(1)
C(27)	2299(5)	6900(5)	216(4)	27(1)
C(28)	-2725(5)	2417(5)	6142(4)	27(1)
C(29)	-1386(4)	4645(4)	2091(4)	19(1)
C(30)	-3130(5)	2925(5)	6858(4)	33(1)
C(31)	-1727(5)	3915(5)	6297(4)	30(1)
C(32)	3405(5)	5841(5)	618(4)	24(1)
C(33)	-3213(5)	4401(5)	1871(4)	29(1)
C(34)	-3785(5)	4926(5)	2547(4)	31(1)
C(35)	-2645(5)	3675(6)	6938(4)	36(1)
C(01)	-4699(6)	8480(7)	-1309(6)	53(2)
Cl(2)	-5977(2)	8585(2)	-1913(2)	66(1)
Cl(3)	-4637(2)	7797(2)	125(2)	84(1)
C(02)	-2646(8)	9335(7)	25(6)	65(2)
Cl(4)	-1657(3)	10082(2)	-260(2)	88(1)
Cl(5)	-2699(3)	8525(2)	1465(2)	95(1)
C(03)	-4359(6)	-1739(7)	5338(6)	57(2)
Cl(6)	-5293(4)	-2454(4)	5934(3)	51(1)
Cl(7)	-5149(4)	-2790(4)	5868(3)	46(1)

Cl(8)	-3283(4)	-2451(5)	4527(4)	62(1)
Cl(9)	-3089(7)	-2365(7)	4802(6)	60(2)
Cl(10)	-3579(14)	-1679(17)	4285(12)	101(4)

5.4.5 [**10**·(H^+NEt_3)·(0.5·NEt_3)]

Table 1: Crystal data and structure refinement for
{[VO(N-2-mercaptophenyl-2'-pyridinecarboxamide)]$_2$O}·(H^+NEt_3)·(0.5·NEt_3)

Empirical formula	C24 H16 N4 O S2 V	
Formula weight	526.92	
Temperature	153(2) K	
Wavelength	0.71073Å	
Crystal system, space group	triclinic, P-1	
Unit cell dimensions	a = 8.7500(4)Å	alpha = 90.6780(10)°.
	b = 10.8826(5)Å	beta = 102.9900(10)°.
	c = 18.4756(8)Å	gamma = 96.9840(10)°.
Volume	1700.16(13) A^3	
Z, Calculated density	2, 1.029 Mg/m^3	
Absorption coefficient	0.510 mm^{-1}	
F(000)	536	
Crystal size	0.41 x 0.24 x 0.14mm	
Theta range for data collection	1.13 to 25.00 deg.	
Limiting indices	-10<=h<=10, -12<=k<=12, -21<=l<=21	
Reflections collected / unique	32275 / 5982 [R(int) = 0.0377]	
Completeness to theta = 25.00	99.9 %	
Refinement method	Full-matrix least-squares on F^2	
Data / restraints / parameters	5982 / 0 / 433	
Goodness-of-fit on F^2	1.107	
Final R indices [I>2sigma(I)]	R1 = 0.0368, wR2 = 0.1006	
R indices (all data)	R1 = 0.0423, wR2 = 0.1114	
Largest diff. peak and hole	0.889 and -0.295 $e.A^{-3}$	

Table 2: Atomic coordinates (x 10^4) and equivalent isotropic displacement parameters (A^2 x 10^3) for **10**·H^+NEt_3·0.5·NEt_3. U(eq) is defined as one third of the trace of the orthogonalized Uij tensor

	x	y	z	U(eq)
V(2)	6910(1)	-1878(1)	6703(1)	19(1)
V(1)	9263(1)	144(1)	7970(1)	18(1)
S(1)	10638(1)	260(1)	7024(1)	23(1)
S(2)	7759(1)	-3268(1)	7624(1)	24(1)
O(4)	12747(2)	-1114(2)	9618(1)	37(1)
O(5)	9299(3)	-2823(2)	5130(1)	37(1)
O(3)	7499(2)	-511(2)	7370(1)	21(1)
O(1)	9083(2)	1526(2)	8209(1)	23(1)
O(2)	5017(2)	-2225(2)	6467(1)	26(1)
N(1)	8718(3)	-898(2)	8843(1)	21(1)
N(2)	11431(2)	-150(2)	8582(1)	20(1)
N(3)	7269(2)	-684(2)	5858(1)	22(1)
N(4)	7993(2)	-2917(2)	6101(1)	21(1)
C(1)	7242(3)	-1213(2)	8932(2)	26(1)
C(2)	6947(4)	-1803(3)	9552(2)	33(1)
C(3)	8218(4)	-2089(3)	10094(2)	36(1)
C(4)	9740(4)	-1799(3)	9994(2)	31(1)
C(5)	9952(3)	-1203(2)	9359(1)	24(1)
C(6)	11545(3)	-816(2)	9204(1)	25(1)
C(7)	12789(3)	387(2)	8351(1)	21(1)
C(8)	14276(3)	742(2)	8818(2)	26(1)
C(9)	15500(3)	1317(3)	8529(2)	29(1)
C(10)	15287(3)	1512(3)	7775(2)	30(1)
C(11)	13814(3)	1170(3)	7306(2)	27(1)
C(12)	12557(3)	631(2)	7592(1)	21(1)
C(13)	6757(3)	426(2)	5757(2)	27(1)
C(14)	6868(3)	1083(3)	5127(2)	32(1)
C(15)	7556(3)	600(3)	4607(2)	33(1)
C(16)	8124(3)	-538(3)	4721(1)	29(1)
C(17)	7950(3)	-1156(2)	5353(1)	23(1)
C(18)	8492(3)	-2399(2)	5516(1)	24(1)
C(19)	8284(3)	-4133(2)	6313(1)	22(1)
C(20)	8640(3)	-5040(3)	5859(2)	26(1)
C(21)	8834(3)	-6216(3)	6115(2)	29(1)
C(22)	8679(3)	-6511(3)	6827(2)	31(1)
C(23)	8345(3)	-5615(2)	7286(2)	26(1)
C(24)	8144(3)	-4429(2)	7039(1)	22(1)
N(5)	3542(3)	-4400(2)	7008(2)	35(1)
C(51)	3005(4)	-5072(3)	6257(2)	46(1)
C(52)	4261(4)	-5671(4)	6016(2)	59(1)
C(53)	4060(4)	-5223(3)	7638(2)	40(1)
C(54)	2736(4)	-6110(3)	7812(2)	54(1)
C(55)	2300(4)	-3637(3)	7135(2)	39(1)
C(56)	2820(4)	-2786(3)	7812(2)	49(1)

N(6)	2653(8)	-4769(6)	9481(4)	58(2)
C(61)	4611(15)	-4409(11)	9333(7)	50(3)
C(62)	5661(14)	-5288(11)	9538(6)	94(3)
C(63)	3344(12)	-4058(9)	10071(6)	77(3)
C(64)	2367(12)	-4492(9)	10672(6)	79(3)
C(65)	902(13)	-4788(10)	9389(6)	85(3)
C(66)	-612(12)	-5171(11)	9794(6)	91(3)
C(67)	3830(20)	-4601(18)	9650(11)	53(4)

5.4.6 [**11**·($HNEt_3$)]

Table 1: Crystal data and structure refinement for V(N-2-mercaptophenyl-2'-pyridinecarboxamide)$_2$·($HNEt_3$)

Empirical formula	C30 H32 N5 O2 S2 V
Formula weight	609.67
Temperature	153(2) K
Wavelength	0.71073 Å
Crystal system, space group	Triclinic, P-1
Unit cell dimensions	a = 10.6472(9) Å alpha = 88.555(2)°.
	b = 10.9097(9) Å beta = 70.7530(10)°.
	c = 12.8210(11) Å gamma = 89.178(2)°.
Volume	1405.5(2) A^3
Z, Calculated density	2, 1.441 Mg/m^3
Absorption coefficient	0.540 mm^{-1}
F(000)	636
Crystal size	0.58 x 0.24 x 0.07 mm
Theta range for data collection	2.17 to 27.50 deg.
Limiting indices	-13<=h<=13, -7<=k<=13, -16<=l<=14
Reflections collected / unique	9289 / 6022 [R(int) = 0.0212]
Completeness to theta = 27.50	93.3 %
Absorption correction	Semi-empirical from equivalents
Max. and min. transmission	0.9632 and 0.7449
Refinement method	Full-matrix least-squares on F^2
Data / restraints / parameters	6022 / 0 / 368
Goodness-of-fit on F^2	0.932
Final R indices [I>2sigma(I)]	R1 = 0.0415, wR2 = 0.0858
R indices (all data)	R1 = 0.0586, wR2 = 0.0909
Largest diff. peak and hole	0.483 and -0.411 $e.A^{-3}$

Table 2: Atomic coordinates (x 10^4) and equivalent isotropic displacement parameters (A^2 x 10^3) for **11**·$HNEt_3$. U(eq) is defined as one third of the trace of the orthogonalized Uij tensor

	x	y	z	U(eq)
V(1)	11852(1)	12135(1)	2292(1)	17(1)
S(1)	10755(1)	13518(1)	3677(1)	23(1)
S(2)	13974(1)	13056(1)	1429(1)	19(1)
O(1)	13100(2)	9235(2)	3908(1)	24(1)
O(2)	9663(2)	12478(2)	159(1)	32(1)
N(1)	12241(2)	11022(2)	893(2)	18(1)
N(2)	10647(2)	12923(2)	1491(1)	15(1)
N(3)	10588(2)	10659(2)	3049(1)	17(1)
N(4)	12924(2)	11172(2)	3141(1)	16(1)
N(5)	13370(2)	15884(2)	2471(2)	21(1)
C(1)	9803(2)	14325(2)	2984(2)	19(1)
C(2)	9027(2)	15322(2)	3474(2)	22(1)
C(3)	8288(2)	15978(2)	2928(2)	28(1)
C(4)	8349(2)	15638(2)	1882(2)	27(1)
C(5)	9099(2)	14636(2)	1391(2)	22(1)
C(6)	9831(2)	13952(2)	1928(2)	18(1)
C(7)	10490(2)	12312(2)	632(2)	20(1)
C(8)	11476(2)	11280(2)	258(2)	19(1)
C(9)	11601(2)	10636(2)	-696(2)	23(1)
C(10)	12530(2)	9702(2)	-991(2)	29(1)
C(11)	13308(2)	9431(2)	-339(2)	27(1)
C(12)	13134(2)	10099(2)	587(2)	21(1)
C(13)	14743(2)	12562(2)	2399(2)	16(1)
C(14)	15944(2)	13065(2)	2398(2)	20(1)
C(15)	16505(2)	12715(2)	3190(2)	21(1)
C(16)	15887(2)	11839(2)	3990(2)	24(1)
C(17)	14722(2)	11290(2)	3980(2)	22(1)
C(18)	14138(2)	11636(2)	3187(2)	17(1)
C(19)	12511(2)	10041(2)	3551(2)	18(1)
C(20)	11125(2)	9791(2)	3552(2)	17(1)
C(21)	10418(2)	8776(2)	4080(2)	21(1)
C(22)	9115(2)	8643(2)	4109(2)	23(1)
C(23)	8567(2)	9525(2)	3597(2)	22(1)
C(24)	9324(2)	10516(2)	3077(2)	23(1)
C(25)	12509(3)	16194(3)	874(2)	36(1)
C(26)	12372(2)	16537(2)	2044(2)	28(1)
C(27)	15141(3)	17506(2)	1758(2)	35(1)
C(28)	14795(2)	16172(2)	1795(2)	23(1)
C(29)	13913(3)	15381(3)	4201(2)	37(1)
C(30)	13047(2)	16103(2)	3686(2)	27(1)

5.4.7 [**14**·$6H_2O$]

Table 1: Crystal data and structure refinement for $(H^+)_2C23]_2[(H^+)_2V_{10}O_{28}]\}\cdot 6H_2O$

Empirical formula	$C_{28}H_{78}N_4O_{44}V_{10}$
Formula weight	1684.34
Temperature	153(2) K
Wavelength	0.71073Å
Crystal system, space group	Orthorhombisch, Pbca
Unit cell dimensions	a = 11.502(2)Å alpha = 90 °.
	b = 19.688(3)Å beta = 90 °.
	c = 25.516(4)Å gamma = 90 °.
Volume	5778.1(17) A^3
Z, Calculated density	4, 1.936 Mg/m^3
Absorption coefficient	1.653 mm^{-1}
F(000)	3424
Crystal size	0.4 x 0.2 x 0.1 mm
Theta range for data collection	2.07 to 27.49 °
Limiting indices	-13<=h<=14, -25<=k<=24, -33<=l<=22
Reflections collected / unique	33297 / 6563 [R(int) = 0.0587]
Completeness to theta = 27.49	99.0 %
Refinement method	Full-matrix least-squares on F^2
Data / restraints / parameters	6563 / 31 / 432
Goodness-of-fit on F^2	1.008
Final R indices [I>2sigma(I)]	R1 = 0.0364, wR2 = 0.0825
R indices (all data)	R1 = 0.0498, wR2 = 0.0870
Largest diff. peak and hole	0.653 and -0.452 $e.A^{-3}$

Table 2: Atomic coordinates (x 10^4) and equivalent isotropic displacement parameters (A^2 x 10^3) for **14**·$6H_2O$.U(eq) is defined as one third of the trace of the orthogonalized Uij tensor

	x	y	z	U(eq)
V(1)	4218(1)	1084(1)	4452(1)	12(1)
V(2)	6237(1)	-10(1)	4682(1)	12(1)
V(3)	5671(1)	1190(1)	5424(1)	13(1)
V(4)	4869(1)	-45(1)	3661(1)	15(1)
V(5)	2523(1)	-99(1)	4246(1)	15(1)
O(1)	5271(2)	-116(1)	3063(1)	22(1)
O(2)	5117(2)	1047(1)	6147(1)	15(1)
O(3)	5564(2)	2002(1)	5390(1)	16(1)
O(4)	1185(2)	-151(1)	4084(1)	23(1)
O(5)	7567(1)	55(1)	4956(1)	15(1)
O(6)	4228(2)	1897(1)	4400(1)	17(1)
O(7)	3277(2)	-159(1)	3629(1)	17(1)
O(8)	7111(1)	1045(1)	5608(1)	16(1)
O(9)	4784(1)	845(1)	3773(1)	14(1)
O(10)	4001(1)	959(1)	5195(1)	13(1)
O(11)	4434(1)	-56(1)	4547(1)	12(1)
O(12)	5867(1)	961(1)	4701(1)	13(1)
O(13)	6406(1)	-47(1)	4024(1)	15(1)
O(14)	2765(1)	836(1)	4293(1)	15(1)
O(15)	6360(2)	1805(1)	3387(1)	26(1)
O(16)	461(2)	2214(1)	7310(1)	27(1)
O(17)	3447(2)	1957(1)	6449(1)	34(1)
O(30)	6541(2)	-3797(1)	3022(1)	26(1)
O(31)	6205(2)	-3244(1)	4030(1)	23(1)
O(33)	9288(2)	-1434(1)	3655(1)	24(1)
O(34)	7731(2)	-1098(1)	2846(1)	23(1)
O(36)	7918(2)	-3176(1)	2102(1)	23(1)
N(1)	8259(2)	-2484(1)	4396(1)	22(1)
N(2)	8220(2)	-1755(1)	1835(1)	20(1)
C(1)	5479(2)	-3870(1)	3306(1)	30(1)
C(2)	5738(3)	-3886(1)	3874(1)	33(1)
C(3)	6605(2)	-3267(1)	4555(1)	24(1)
C(4)	7163(2)	-2602(1)	4695(1)	22(1)
C(5)	8817(3)	-1827(1)	4545(1)	28(1)
C(6)	9742(2)	-1615(1)	4157(1)	29(1)
C(7)	8599(2)	-832(1)	3676(1)	25(1)
C(8)	8363(3)	-590(1)	3130(1)	26(1)
C(9)	7316(3)	-845(1)	2360(1)	27(1)
C(10)	7101(2)	-1433(1)	1996(1)	25(1)
C(11)	8089(3)	-2322(1)	1445(1)	24(1)
C(13)	7544(3)	-3857(1)	2206(1)	26(1)
C(14)	6389(3)	-3903(1)	2474(1)	28(1)
C(12)	7382(3)	-2909(1)	1645(1)	27(1)

5.4.8 [**15**·$9H_2O$]

Table 1: Crystal data and structure refinement for $\{(C211)_2[(H_3O)^+][(H^+)_2V_{10}O_{28}]\}\cdot 9H_2O$

Empirical formula	$C_{28}H_{80}N_4O_{45}V_{10}$
Formula weight	1682.20
Temperature	153(2) K
Wavelength	0.71073Å
Crystal system, space group	Monoclinic, C2/m
Unit cell dimensions	a = 12.7249(18)Å alpha = 90 °.
	b = 20.194(3)Å beta = 113.754(2) °.
	c = 12.2549(17)Å gamma = 90°.
Volume	2882.4(7) A^3
Z, Calculated density	2, 1.938 Mg/m^3
Absorption coefficient	1.658 mm^{-1}
F(000)	1692
Crystal size	0.6 x 0.3 x 0.15 mm
Theta range for data collection	1.82 to 27.53°
Limiting indices	-16<=h<=14, -26<=k<=14, -14<=l<=15
Reflections collected / unique	9368 / 3326 [R(int) = 0.0351]
Completeness to theta = 27.53	97.2 %
Refinement method	Full-matrix least-squares on F^2
Data / restraints / parameters	3326 / 0 / 221
Goodness-of-fit on F^2	1.047
Final R indices [I>2sigma(I)]	R1 = 0.0455, wR2 = 0.1240
R indices (all data)	R1 = 0.0547, wR2 = 0.1343
Largest diff. peak and hole	1.327 and -0.919 $e.A^{-3}$

Table 2 : Atomic coordinates (x 10^4) and equivalent isotropic displacement parameters (A^2 x 10^3) for **15**·H_2O. U(eq) is defined as one third of the trace of the orthogonalized Uij tensor

	x	y	z	U(eq)
V(1)	139(1)	0	3725(1)	12(1)
V(2)	2730(1)	0	5089(1)	21(1)
V(3)	1289(1)	1115(1)	5672(1)	14(1)
V(4)	2504(1)	0	7479(1)	17(1)
O(10)	1160(2)	0	5525(2)	13(1)
O(11)	78(2)	934(1)	4028(2)	14(1)
O(12)	1320(2)	0	3446(2)	17(1)
O(13)	3740(2)	0	4632(3)	26(1)
O(14)	2395(2)	910(1)	5050(2)	17(1)
O(15)	3472(2)	0	6707(2)	17(1)
O(16)	1322(2)	1911(1)	5638(2)	20(1)
O(17)	2218(2)	913(1)	7162(2)	16(1)
O(18)	3333(2)	0	8870(3)	22(1)
O(19)	1002(2)	0	7627(2)	15(1)
N(1)	38(2)	-1973(1)	1721(2)	21(1)
C(1)	1244(3)	-1733(2)	2396(3)	30(1)
C(2)	1724(3)	-1423(2)	1580(3)	28(1)
O(1)	1653(2)	-1908(1)	702(2)	21(1)
C(3)	1899(2)	-1645(2)	-260(3)	22(1)
C(4)	813(2)	-1414(2)	-1270(3)	23(1)
C(5)	293(3)	-2472(2)	-2452(3)	26(1)
C(7)	129(3)	-3146(2)	2267(3)	27(1)
O(2)	290(2)	-3219(1)	-1010(2)	22(1)
C(6)	201(2)	-3778(1)	667(3)	22(1)
O(33)	3838(2)	1705(1)	4532(2)	35(1)
O(32)	-2283(5)	0	9456(5)	74(1)
O(31)	5843(4)	188(3)	7467(5)	55(3)
O(30)	-70(10)	0	9611(7)	58(2)

5.4.9 [**16**·8H_2O]

Table 1: Crystal data and structure refinement for [C22(H^+)$_2$]$_2$NEt_4[$H_4PV_{14}O_{42}$]·8H_2O

Empirical formula	$C_{32}H_{96}N_5O_{58}PV_{14}$	
Formula weight	2223.27	
Temperature	183(2) K	
Wavelength	0.71073 Å	
Crystal system, space group	orthorhombic, Pban	
Unit cell dimensions	a = 14.1171(7) Å	alpha = 90°.
	b = 22.0317(11) Å	beta = 90°.
	c = 11.8500(6) Å	gamma = 90 °.
Volume	3685.6(3) $Å^3$	
Z, Calculated density	2, 2.003 g/cm^3	
Absorption coefficient	1.824 mm^{-1}	
F(000)	2248	
Crystal size	0.32 x 0.12 x 0.05 mm	
Theta range for data collection	1.71 to 27.00 deg	
Index ranges	-18<=h<=11, -28<=k<=27, -14<=l<=15	
Reflections collected / unique	20319 / 4013 [R(int) = 0.0298]	
Refinement method	Full-matrix least-squares on F^2	
Data / restraints / parameters	4010 / 3 / 273	
Goodness-of-fit on F^2	1.150	
Final R indices [I>2sigma(I)]	R1 = 0.0358, wR2 = 0.1078	
R indices (all data)	R1 = 0.0482, wR2 = 0.1187	
Largest diff. peak and hole	1.420 and -0.734 e. $Å^{-3}$	

Table 2: Atomic coordinates (x 10^4) and equivalent isotropic displacement parameters ($Å^2$ x 10^3) for **16**·8 H_2O.U(eq) is defined as one third of the trace of the orthogonalized Uij tensor

	x	y	z	U(eq)
V(1)	669(1)	3591(1)	9833(1)	17(1)
V(2)	685(1)	2492(1)	12001(1)	16(1)
V(3)	2496(1)	1445(1)	12153(1)	16(1)
V(4)	2500	760(1)	10000	18(1)
P(1)	2500	2500	10000	11(1)
O(1)	3325(1)	1130(1)	10967(2)	18(1)
O(2)	2609(1)	913(1)	13063(2)	23(1)
O(3)	3328(1)	1972(1)	12554(2)	18(1)
O(4)	-77(2)	4124(1)	10057(2)	27(1)
O(5)	3426(1)	963(1)	8890(1)	17(1)
O(6)	-89(1)	2582(1)	12975(2)	24(1)
O(7)	1394(1)	1825(1)	12799(2)	18(1)
O(8)	2500	32(1)	10000	30(1)
O(9)	385(1)	3026(1)	10990(2)	19(1)
O(10)	1873(1)	2901(1)	9234(1)	14(1)
O(11)	112(1)	3191(1)	8768(2)	19(1)
O(12)	6253(2)	908(1)	3980(2)	32(1)
O(13)	5786(2)	717(1)	6205(2)	32(1)
N(1)	4303(2)	132(1)	7434(2)	25(1)
C(1)	5332(2)	61(2)	7689(3)	33(1)
C(2)	5856(2)	631(2)	7398(3)	35(1)
C(3)	6214(3)	1276(2)	5853(3)	35(1)
C(4)	5937(3)	1396(2)	4655(3)	37(1)
C(5)	3714(2)	-398(2)	7779(3)	34(1)
C(6)	6023(3)	980(2)	2814(3)	39(1)
N(2)	2500	-2500	10000	23(1)
C(7)	1841(5)	-1952(3)	10008(6)	33(2)
C(8)	2500	-1340(3)	10000	71(2)
C(9)	3141(5)	-2497(3)	8977(7)	36(2)
C(10)	2500	-2500	7830(5)	65(2)
O(14)	1370(2)	324(1)	14856(2)	57(1)
O(15)	1496(2)	1641(1)	15084(2)	39(1)

5.4.10 [**17**·$8H_2O$]

Table 1: Crystal data and structure refinement for $[C221(H^+)_2]_2[H_5PV_{14}O_{42}]\cdot 8H_2O$

Empirical formula	$C_{32}H_{89}N_4O_{60}PV_{14}$
Formula weight	2234.20
Temperature	153(2) K
Wavelength	0.71073Å
Crystal system, space group	triclinic, P-1
Unit cell dimensions	a = 15.7078(5)Å alpha = 81.9280(10)°.
	b = 15.8453(5)Å beta = 75.1620(10) °.
	c = 16.1954(5)Å gamma = 69.8030(10) °.
Volume	3650.9(2)$Å^3$
Z, Calculated density	2, 2.032 Mg/m^3
Absorption coefficient	1.844 mm^{-1}
F(000)	2252
Crystal size	0.5 x 0.2 x 0.1 mm
Theta range for data collection	2.27 to 32.55 deg.
Limiting indices	-23<=h<=23, -23<=k<=23, -24<=l<=24
Reflections collected / unique	100541 / 25788 [R(int) = 0.0625]
Completeness to theta = 32.55	97.2 %
Refinement method	Full-matrix least-squares on F^2
Data / restraints / parameters	25788 / 30 / 1103
Goodness-of-fit on F^2	0.924
Final R indices [I>2sigma(I)]	R1 = 0.0447, wR2 = 0.0868
R indices (all data)	R1 = 0.0716, wR2 = 0.0931
Largest diff. peak and hole	1.101 and -0.914 $e.A^{-3}$

Table 2: Atomic coordinates (x 10^4) and equivalent isotropic displacement parameters (A^2 x 10^3) for **17**·$8H_2O$. U(eq) is defined as one third of the trace of the orthogonalized Uij tensor

	x	y	z	U(eq)
P(1)	6137(1)	8148(1)	2365(1)	9(1)
V(1)	7608(1)	7659(1)	271(1)	11(1)
V(2)	3848(1)	8202(1)	2812(1)	11(1)
V(3)	5142(1)	7661(1)	850(1)	10(1)
V(4)	6726(1)	5869(1)	1818(1)	11(1)
V(5)	8453(1)	6318(1)	1473(1)	12(1)
V(6)	7642(1)	6294(1)	3352(1)	12(1)
V(7)	4895(1)	8593(1)	4410(1)	11(1)
V(8)	5711(1)	10287(1)	2938(1)	11(1)
V(9)	8475(1)	8066(1)	1915(1)	12(1)
V(10)	7121(1)	8505(1)	3960(1)	13(1)
V(11)	7127(1)	9624(1)	915(1)	12(1)
V(12)	4696(1)	9833(1)	1343(1)	10(1)
V(13)	5499(1)	6416(1)	3702(1)	12(1)
V(14)	3899(1)	10004(1)	3309(1)	11(1)
O(51)	7476(1)	8804(1)	32(1)	12(1)
O(52)	7697(1)	8587(1)	4610(1)	19(1)
O(53)	5924(1)	8671(1)	4806(1)	13(1)
O(54)	8150(1)	7254(1)	-637(1)	16(1)
O(55)	6296(1)	7890(1)	246(1)	12(1)
O(56)	7248(1)	10496(1)	331(1)	17(1)
O(57)	8420(1)	6890(1)	2402(1)	12(1)
O(58)	3967(1)	7822(1)	1698(1)	12(1)
O(59)	2770(1)	8277(1)	3189(1)	16(1)
O(60)	7347(1)	7364(1)	3916(1)	13(1)
O(61)	8592(1)	7392(1)	860(1)	12(1)
O(62)	4710(1)	10318(1)	2396(1)	11(1)
O(63)	9562(1)	7914(1)	1808(1)	16(1)
O(64)	8483(1)	5622(1)	3762(1)	17(1)
O(65)	7514(1)	6523(1)	938(1)	11(1)
O(66)	4829(1)	7397(1)	86(1)	15(1)
O(67)	6503(1)	10161(1)	1995(1)	12(1)
O(68)	4013(1)	10736(1)	970(1)	14(1)
O(69)	4122(1)	8810(1)	5293(1)	14(1)
O(70)	5985(1)	5651(1)	2752(1)	12(1)
O(71)	5745(1)	6663(1)	1289(1)	12(1)
O(72)	4580(1)	9016(1)	642(1)	12(1)
O(73)	5394(1)	11331(1)	3106(1)	16(1)
O(74)	5935(1)	8720(1)	3141(1)	11(1)
O(75)	4965(1)	5829(1)	4379(1)	17(1)
O(76)	7030(1)	4968(1)	1321(1)	16(1)
O(77)	6942(1)	8317(1)	1677(1)	10(1)
O(78)	4469(1)	7190(1)	3196(1)	12(1)
O(79)	3611(1)	9539(1)	2302(1)	11(1)

O(80)	7798(1)	5667(1)	2320(1)	12(1)
O(81)	7956(1)	8544(1)	2889(1)	13(1)
O(82)	4009(1)	8840(1)	3678(1)	11(1)
O(83)	5248(1)	8432(1)	1999(1)	10(1)
O(84)	5780(1)	9851(1)	861(1)	11(1)
O(85)	6388(1)	7148(1)	2662(1)	11(1)
O(86)	5218(1)	7471(1)	4358(1)	13(1)
O(87)	2896(1)	10746(1)	3587(1)	16(1)
O(88)	9420(1)	5575(1)	1090(1)	18(1)
O(89)	6545(1)	9831(1)	3688(1)	13(1)
O(90)	6713(1)	5961(1)	3943(1)	13(1)
O(91)	8197(1)	9144(1)	1198(1)	13(1)
O(92)	4609(1)	10030(1)	3989(1)	13(1)
O(1)	7224(2)	6098(1)	8414(1)	50(1)
O(2)	6209(3)	5142(2)	8580(2)	34(1)
O(3)	6673(2)	5748(1)	6368(1)	28(1)
O(4)	8991(1)	5624(1)	6727(1)	25(1)
O(5)	8523(1)	4097(1)	7567(1)	25(1)
N(1)	7337(2)	7004(1)	6877(1)	16(1)
N(2)	6840(2)	4181(1)	7300(1)	18(1)
C(1)	7031(2)	7503(2)	7685(2)	25(1)
C(2)	6576(2)	6984(2)	8405(2)	25(1)
C(3)	7132(2)	5590(2)	9196(2)	29(1)
C(4)	6253(2)	5359(2)	9444(2)	34(1)
C(5)	5637(3)	4735(4)	8578(2)	75(2)
C(6)	5837(2)	4357(2)	7750(2)	23(1)
C(7)	6991(2)	4164(2)	6352(2)	26(1)
C(8)	6532(2)	5082(2)	5956(2)	27(1)
C(9)	6654(2)	6548(2)	5848(2)	23(1)
C(10)	6561(2)	7267(2)	6409(2)	26(1)
C(11)	8219(2)	7109(2)	6312(2)	26(1)
C(12)	9027(2)	6517(2)	6667(2)	29(1)
C(13)	9435(2)	5059(2)	7375(2)	23(1)
C(14)	9449(2)	4123(2)	7322(2)	25(1)
C(15)	7455(2)	3332(2)	7675(2)	21(1)
C(16)	8467(2)	3265(2)	7401(2)	23(1)
OB2	6166(4)	4660(3)	9086(3)	27(1)
O(41)	9413(2)	1014(1)	1727(1)	33(1)
O(42)	8630(2)	1098(2)	3399(1)	39(1)
O(43)	8691(1)	3362(1)	2229(1)	22(1)
O(44)	7584(2)	2282(2)	886(2)	58(1)
O(45)	6539(2)	2748(2)	2599(2)	50(1)
N(41)	9270(2)	2513(2)	633(1)	27(1)
N(42)	7461(2)	2868(2)	3751(2)	30(1)
C(41)	10167(2)	1733(2)	568(2)	35(1)
C(42)	9950(2)	871(2)	886(2)	35(1)
C(43)	9131(3)	279(2)	2144(2)	51(1)
C(44)	8424(3)	536(2)	2916(2)	53(1)
C(45)	8048(3)	1266(2)	4225(2)	46(1)
C(46)	7905(3)	2214(2)	4403(2)	48(1)
C(47)	7719(2)	3716(2)	3599(2)	34(1)

C(48)	8675(2)	3575(2)	3054(2)	27(1)
C(49)	9506(2)	3434(2)	1630(2)	28(1)
C(50)	9387(2)	3389(2)	751(2)	35(1)
C(51)	8824(3)	2595(2)	-102(2)	51(1)
C(52)	7762(3)	2902(3)	244(3)	68(2)
C(53)	6619(3)	2316(3)	1275(3)	22(1)
C(54)	6155(3)	3004(4)	1874(3)	78(2)
C(55)	6041(2)	3401(3)	3201(3)	63(1)
C(56)	6426(2)	3074(2)	3971(2)	49(1)
CB53	6634(8)	2982(7)	968(7)	8(2)
CC53	6396(9)	2311(9)	1703(8)	9(2)
OA1	2344(2)	8576(2)	1213(1)	32(1)
OA2	2082(1)	10393(1)	1687(1)	25(1)
OA3	10537(2)	1484(2)	2763(2)	57(1)
OA4	9261(2)	3020(2)	5011(2)	72(1)
OA5	1037(2)	10768(2)	4318(3)	89(1)
OA6	8867(4)	4737(5)	5317(4)	46(2)
OA7	10340(2)	1586(3)	5933(4)	142(2)
OA8	897(3)	9284(3)	3434(5)	202(3)
OA61	9357(6)	4765(8)	5128(6)	64(3)

5.4.11 [**18**·11H_2O]

Table 1: Crystal data and structure refinement for $[(H^+)_2C22]_{2.5}[PV_2W_{10}O_{40}]\cdot 11H_2O$

Empirical formula	$C_{30}H_{90}N_5O_{61}PV_2W_{10}$
Formula weight	3468.42
Temperature	153(2) K
Wavelength	0.71073Å
Crystal system, space group	triclinic, P-1
Unit cell dimensions	a = 12.7216(16) Å alpha = 97.643(2) °.
	b = 13.4272(16) Å beta = 90.482(2) °.
	c = 23.807(3) Å gamma = 112.410(2) °.
Volume	3718.4(8)$Å^3$
Z, Calculated density	2, 3.098 Mg/m^3
Absorption coefficient	15.775 mm^{-1}
F(000)	3188
Crystal size	0.36 x 0.17 x 0.10 mm
Theta range for data collection	1.99 to 26.50 deg.
Limiting indices	-9<=h<=15, -16<=k<=16, -29<=l<=29
Reflections collected / unique	22805 / 14796 [R(int) = 0.0589]
Completeness to theta = 26.50	96.2 %
Max. and min. transmission	0.3014 and 0.0700
Refinement method	Full-matrix least-squares on F^2
Data / restraints / parameters	14796 / 43 / 999
Goodness-of-fit on F^2	1.011
Final R indices [I>2sigma(I)]	R1 = 0.0558, wR2 = 0.1360
R indices (all data)	R1 = 0.0727, wR2 = 0.1437
Largest diff. peak and hole	5.176 and -3.785 $e.A^{-3}$

Table 2: Atomic coordinates (x 10^4) and equivalent isotropic displacement parameters (A^2 x 10^3) for **18**·$11H_2O$. U(eq) is defined as one third of the trace of the orthogonalized Uij tensor.

	x	y	z	U(eq)
W(1)	3343(1)	4909(1)	2528(1)	23(1)
W(2)	4946(1)	7139(1)	1956(1)	16(1)
W(3)	6375(1)	5756(1)	4104(1)	19(1)
W(4)	8101(1)	8192(1)	3470(1)	18(1)
W(5)	4748(1)	3300(1)	1700(1)	26(1)
W(6)	6347(1)	5510(1)	1125(1)	17(1)
W(7)	4752(1)	3442(1)	3258(1)	25(1)
W(8)	8092(1)	8081(1)	2047(1)	16(1)
W(9)	4954(1)	7233(1)	3385(1)	17(1)
W(10)	7571(1)	4304(1)	3342(1)	25(1)
W(11)	9314(1)	6695(1)	2703(1)	20(1)
W(12)	7555(1)	4137(1)	1807(1)	21(1)
V(1)	7571(1)	4304(1)	3342(1)	25(1)
V(2)	9314(1)	6695(1)	2703(1)	20(1)
V(3)	7555(1)	4137(1)	1807(1)	21(1)
P(1)	6333(2)	5736(2)	2613(1)	11(1)
O(1)	1913(8)	4225(7)	2470(4)	22(2)
O(2)	4484(8)	7833(7)	1549(4)	20(2)
O(3)	6407(8)	6077(7)	4827(4)	22(2)
O(4)	8685(8)	9315(7)	3981(4)	21(2)
O(5)	3776(8)	2105(8)	1365(4)	25(2)
O(6)	6366(8)	5691(7)	416(4)	21(2)
O(7)	3814(8)	2319(7)	3465(4)	24(2)
O(8)	8679(8)	9117(8)	1662(4)	24(2)
O(9)	4504(8)	8015(7)	3871(4)	20(2)
O(10)	8354(8)	3710(7)	3553(4)	26(2)
O(11)	10679(7)	6896(7)	2710(4)	23(2)
O(12)	8383(7)	3527(8)	1523(4)	26(2)
O(13)	5313(7)	6094(6)	2624(3)	12(2)
O(14)	7448(7)	6757(6)	2676(3)	13(2)
O(15)	6269(7)	5110(7)	3108(3)	15(2)
O(16)	6264(7)	5008(6)	2048(4)	13(2)
O(17)	3806(7)	4046(7)	1959(4)	16(2)
O(18)	9332(7)	7828(7)	3295(4)	18(2)
O(19)	5291(7)	6145(7)	1411(3)	18(2)
O(20)	4773(7)	3005(7)	2465(4)	20(2)
O(21)	8312(7)	8877(7)	2792(4)	16(2)
O(22)	3801(7)	4135(7)	3044(4)	19(2)
O(23)	8708(7)	5657(7)	3184(4)	18(2)
O(24)	7502(7)	7062(7)	3905(4)	17(2)
O(25)	3528(7)	5914(7)	2022(4)	15(2)
O(26)	7502(7)	6847(7)	1482(4)	19(2)
O(27)	6533(7)	7963(7)	2067(4)	16(2)
O(28)	5325(7)	6359(7)	3846(3)	18(2)
O(29)	6125(7)	3254(7)	3382(4)	19(2)

O(30)	4755(7)	7749(7)	2694(4)	18(2)
O(31)	3526(7)	6010(7)	3152(4)	18(2)
O(32)	8699(7)	5578(7)	2089(4)	21(2)
O(33)	5112(7)	4123(7)	1089(4)	18(2)
O(34)	7348(7)	4800(7)	1164(4)	15(2)
O(35)	5127(8)	4399(7)	3967(4)	19(2)
O(36)	6119(7)	3097(7)	1598(4)	21(2)
O(37)	9295(7)	7698(7)	2200(4)	17(2)
O(38)	7381(8)	5044(7)	4028(4)	22(2)
O(39)	7519(8)	3890(8)	2545(4)	22(2)
O(40)	6527(7)	8060(7)	3408(4)	20(2)
O(41)	4357(9)	1230(9)	4814(5)	35(3)
C(1)	3293(15)	1112(15)	5034(8)	45(5)
C(2)	2530(13)	1210(15)	4634(7)	41(4)
O(42)	2305(8)	331(9)	4149(4)	29(2)
C(3)	1552(12)	325(12)	3715(6)	27(3)
C(4)	1590(11)	-406(11)	3218(6)	25(3)
N(1)	2669(10)	55(10)	2907(5)	26(3)
C(5)	2745(14)	-621(13)	2399(7)	36(4)
C(6)	3737(17)	-22(15)	2088(7)	49(5)
O(43)	4700(11)	164(12)	2424(5)	59(4)
C(7)	5731(17)	680(20)	2178(8)	64(6)
C(8)	6700(20)	650(20)	2477(12)	88(10)
O(44)	6909(12)	1239(11)	3010(7)	60(4)
C(9)	7040(20)	690(20)	3458(13)	90(10)
C(10)	7176(16)	1400(20)	4022(12)	78(9)
N(2)	6182(10)	1731(9)	4076(6)	27(3)
C(11)	6251(16)	2349(16)	4629(8)	55(6)
C(12)	5085(12)	2337(11)	4773(6)	24(3)
C(13)	8939(12)	4594(15)	6324(7)	37(4)
N(3)	9008(14)	5375(13)	5925(6)	45(4)
C(14)	9280(13)	6478(12)	6214(7)	32(4)
C(15)	9274(13)	7213(14)	5758(7)	34(4)
O(45)	10064(10)	7168(9)	5367(5)	35(3)
C(16)	10070(15)	7784(15)	4907(8)	41(4)
C(17)	10840(30)	7699(19)	4501(9)	84(9)
O(46)	10613(14)	6620(12)	4260(7)	39(4)
O(461)	11380(20)	6990(20)	4510(11)	18(6)
C(18)	11534(16)	6551(18)	3951(8)	53(5)
C(19)	8973(12)	4611(12)	-1440(6)	27(3)
N(4)	9008(10)	5345(10)	-891(5)	26(3)
C(20)	9236(13)	6456(13)	-965(7)	32(4)
C(21)	9116(14)	7122(12)	-406(7)	34(4)
O(47)	9915(8)	7170(9)	2(4)	33(2)
C(22)	9745(13)	7663(12)	535(7)	31(3)
C(23)	10675(14)	7715(11)	950(7)	31(3)
O(48)	10531(9)	6645(8)	999(5)	39(3)
C(24)	11377(12)	6564(12)	1365(6)	28(3)
C(25)	7538(19)	1008(17)	733(10)	64(7)
N(5)	6780(10)	1205(9)	344(6)	28(3)
C(26)	7171(13)	2287(12)	261(7)	38(4)

C(27)	6332(16)	2476(14)	-114(7)	41(4)
O(49)	5315(11)	2293(11)	174(7)	65(5)
C(28)	4480(20)	2631(17)	-52(13)	101(12)
C(29)	3650(30)	1820(20)	-468(13)	38(7)
C(291)	3520(30)	2110(30)	-32(14)	26(7)
O(50)	3130(11)	752(10)	-276(7)	59(4)
C(30)	2980(20)	80(20)	-798(10)	77(8)
O(51)	8949(9)	4817(9)	296(4)	27(2)
O(52)	6763(9)	4884(10)	-664(4)	33(3)
O(53)	1953(9)	1598(9)	2430(6)	39(3)
O(54)	9873(10)	11154(9)	2862(6)	42(3)
O(55)	6748(10)	4822(10)	5620(5)	36(3)
O(56)	4145(9)	9867(8)	3742(5)	34(3)
O(57)	4321(12)	337(10)	709(6)	48(3)
O(58)	9088(14)	4858(13)	4759(7)	76(5)
O(59)	9446(15)	12728(12)	2404(7)	80(6)
O(60)	8948(12)	9696(14)	-248(6)	66(4)
O(61)	9010(20)	9720(20)	-1400(9)	71(8)
O(62)	9470(90)	9140(80)	-1250(40)	40(20)
O(63)	9080(120)	9060(100)	-1350(70)	60(40)

5.5 Toxicity of vanadium complexes and environmental protection

Vanadiumtrichloride

Arbeitsplatz: Raum 531, Institut für Anorganische und Angewandte Chemie
Gefahrstoffbezeichnung: Vanadiumtrichlorid, VCl_3
Gefahr für Mensch und Umwelt: Reizt die Augen, Atmungsorgane und die Haut, gesundheitsschädlich beim Verschlucken, reagiert heftig mit Wasser.
Allgemein zeigen Vanadiumverbindungen im menschlichen Körper folgende toxische Wirkungen:
- Akut: Kopfschmerz, Zittern, Sinken der Körpertemperatur, Verlangsamung der Atmung, schwächere Herzaktivität
- Beim Einatmen von Stäuben: Reizung der Atemwege, Blutungsneigung der Lungen
- Chronisch: Nierenschäden, Bronchitis, psychische Störungen
- Schutzmaßnahmen und Verhaltensregeln: Vorbeugender Augen- und Handschutz, Einatmen von Stäuben vermeiden. Bei Berührung mit den Augen gründlich mit Wasser ausspülen und Arzt konsultieren.
Verhalten im Gefahrfall: Verschüttete Substanz trocken aufnehmen, der Entsorgung zuführen. Eventuell entstehende Stäube nicht einatmen. Unter Wasserzutritt entstehen giftige und ätzende Dämpfe.
Erste Hilfe: Nach Hautkontakt: Gründlich mit Wasser abspülen. Nach Augenkontakt: Mit viel Wasser spülen, zum Augenarzt. Nach Verschlucken: Kein Erbrechen auslösen, sofort zum Arzt. Nach Einatmen: Frischluft, bei Unwohlsein zum Arzt.
Sachgerechte Entsorgung: Unter dem Abzug vorsichtig mit viel Wasser hydrolysieren und die Lösung den sauren metallsalzhaltigen Lösungen zuführen.

Dichloromethane

Arbeitsplatz: Raum 531, Institut für Anorganische und Angewandte Chemie
Gefahren für Mensch und Umwelt: Gesundheitsschädlich, irreversibler Schaden möglich
Schutzmaßnahmen und Verhaltensregeln: Dämpfe nicht einatmen, durch Schutzkleidung Kontakt mit Augen und Haut vermeiden.
Verhalten im Gefahrfall: Verschüttete Mengen mit Universalbinder aufnehmen und als Sondermüll beseitigen.

Erste Hilfe: Nach Inhalation: Frischluft. Nach Haut- und Augenkontakt: betroffene Hautpartien mit viel Wasser abspülen und mit Seife abwaschen, benetzte Kleidung entfernen. Nach Verschlucken: Mund ausspülen, kein Erbrechen auslösen.
Sachgerechte Entsorgung: Sammlung in einem entsprechend gekennzeichneten Behälter für halogenierte Lösungsmittel.

Waste management

Nach dem Abfallgesetz ist jeder Labor- oder Industriebetrieb dazu verpflichtet, Abfälle zu vermeiden bzw. zu minimieren und dennoch anfallende Abfälle nach Sammlung und Umwandlung in weniger gefährliche Stoffe einer fachgerechten Entsorgung zuzuführen. Dies kann durch verschiedene Maßnahmen erfolgen:
- Möglichst kleine Forschungsansätze (meist ca. 0,5 mmol, entsprechend 10 -20 ml Lösungsmittel)
- Wiedergewinnung von Lösungsmitteln. Dies ist jedoch nur sinnvoll, wenn es sich um für Reinigungszwecke verwendetes Ethanol oder Aceton handelt, das durch einfache Destillation wiederverwendungsfähig gemacht werden kann. Lösungsmittel aus Forschungsansätzen werden wegen des zu hohen Reinigungsaufwands nicht aufgearbeitet.
- Bereits zur Trocknung von Lösungsmitteln benutztes Molekularsieb kann durch dreitägige Trocknung bei 200° C im Vakuum regeneriert werden.
- Einsatz ungefährlicherer Edukte. Z. B. durch die Substitution von Benzol durch Toluol wird die spätere Entsorgung entlastet.

Nachstehend sind die wichtigsten Entsorgungsarten der in dieser Arbeit verwendeten Stoffe aufgeführt.
Flüssigkeiten:
Lösungsmittel für Forschungsansätze wurden abdestilliert und in bruchsicheren PE-Behältern für halogenierte bzw. nicht halogenierte Lösungsmittel entsorgt.
Wässrige, schwermetallhaltige Lösungen wurden angesäuert und in einem Behälter für saure Schwermetallabfälle gesammelt.
Verunreinigtes Heizbadöl und Öl aus Vakuumpumpen wurde als stark kontaminiertes Altöl der Entsorgung zugeführt.
Feststoffe:
Vanadium enthaltende Rückstände wurden vorsichtig, eventuell unter Kühlung, mit H_2SO_4/H_2O_2 oxidativ aufgeschlossen und nach Verkochen des überschüssigen Peroxids in

einem Behälter für saure, schwermetallsalzhaltige Lösungen gesammelt. Alkalimetallsalzreste wurden mit Toluol überschichtet und durch tropfenweise Zugabe von 2-Propanol oxidiert. Nach Zugabe von Wasser und 15 min Rühren wurde die organische Phase in den Behälter für halogenfreie Lösungsmittel entsorgt. Die wässrige Phase wurde nach Neutralisation verworfen.
Mit Chemikalien kontaminierte Papierfilter und Kieselgel wurden weitestgehend von Lösungsmittelresten befreit und in den Behälter für Filter- und Aufsaugmassen gegeben. Filterpapiere und andere Labormaterialien (Papiertücher, Schläuche, Bürsten etc.), die mit chemischen Rückständen behaftet waren, wurden in dem Behälter für mit Chemikalien verunreinigte Betriebsmittel gesammelt.
Stark mit Chemikalien verunreinigte Pipetten, Reagenzgläser und Glasbruch wurde in einem Behälter für kontaminiertes Glas entsorgt.
Gesäuberte Glasgefäße und -geräte wurden nach Entfernung jeglicher Etiketten zum normalen fürs Recycling bestimmten Glasmüll gegeben.

Stoffbilanz
Folgend wird ein Überblick über die für die ca. 100 Forschungsansätze und die ca. 10 Ligandendarstellungen benötigten Chemikalienmengen gegeben. Aufgelistet sind die Substanzen mit dem größten Anteil am Gesamtverbrauch.
- An Metallkomponenten wurden 5g V_2O_5, 10g VCl_3, 20g $VO(acac)_2$, 20g $VOCl_2(THF)_2$, 10g Natrium, sowie 30g Diethylaluminiumethoxid und 15 g Butyllithium eingesetzt.
- Insgesamt wurden 53 l Lösungsmittel verbraucht, davon 37 l für Ligandendarstellungen (8 l Ethanol, 8 l Diethylether, 6 l Petrolether, 3 l Chloroform, 4 l Ethylacetat, ferner Dichlormethan, Methanol, Dimethylformamid, Aceton, Pentan und Toluol). Für Forschungsansätze wurden im wesentlichen 6 l Tetrahydrofuran, 4 l Dichlormethan, 2 l Acetonitril, 2 l Dimethylsulfoxid und 2 l Pentan benötigt.
- An Zielverbindungen wurden daraus ca. 100 g Vanadiumkomplexe dargestellt.
- Zu Reinigungszwecken wurden 4 l Schwefelsäure und 6 l Wasserstoffperoxid sowie 10 l Extran und 3 l Aceton verwendet.

6 References:

1. (a) Chasteen, N. D.; Vanadium in Biologocal Systems; Kluwer Academic Publishers: Dordrecht, The Netherlands, **1990**. (b) Butler, A.; Carrano, C. *J. Coord. Chem. Rev.* **1991**, 109, 61. (c) Rehder, D. *Angew. Chem., Int. Ed. Engl.* **1991**, 30, 148
2. (a) Arber, J. M.; De Boer, E.; Garner, C. D.; Hasnain, S. S. and Wever, R. *Biochemistry* **1989**, 28, 7968. (b) Clague, M. J.; Keder, N. L. and Butler A. *Inorg. Chem.* **1993**, 32, 754 (c) Carrano, J.; Mohan, M.; Holmes, S. M.; De la Rosa, R.; Bulter, A.; Charnock, J. M. and Garner, C. D. *Inorg. Chem.* **1994**, 33, 646. (d) Butler, A.; Walker, J. V. *Chem. Rev.* **1993**, 93. 1937.
3. Robson, R. L.; Eady, R. R.; Richardson, T. H.; Miller, R. W.; Hawkins, M.; Postgate, J. R. *Nature* (London) **1986**, 322, 388.
4. Hirao, T.; Mori, M.; Ohshiro, Y. *J. Org, Chem*. **1990**, 55, 358. (b) Hirao, T.; Fujii, T.; Tanaka, T.; Ohshiro, Y. *J. Chem. Soc. Perkin Trans*. **1994**, 1, 3.
5. (a) Lindquist, R. N.; Lynn, J. L.; Lienhard, G. E. *J. Am. Chem. Soc*. **1973**, 95, 8762. (b) Crans, D. C.; Simone, C.M.; Blanchard, *J. Am. Chem. Soc*. **1992**, 114, 4926.
6. (a) Cremo, C. R.; Long, G. T.; Grammer, J. C., *Biochem*. **1990**, 29, 7982. (b) Muhlrad, A.; Peyser, M. Y.; Ringel, I. *Biochem*. **1991**, 30, 958. (c) Cremo, C. R.; Loo, J. A.; Edmonds, C. G.; Hatlelid, K. M. *Biochem*. **1992**, 32, 491.
7. Rehder, D. *Coord. Chem. Rev*. **1999**, 182, 297.
8. Rehder, D.; Bashirpoor, M.; Jantzen, S.; Schmidt, H; Farahbakhsh, M.; Nekola, H. *Vanadium Compounds* Eds. Alan, S. T.; Crans, D. C. *American chemistry society*, Washington, DC. P60
9. Percival, M. D.; Doherty, K.; Gresser, M. J. *Biochemistry* **1990**, 29, 2764.
10. Gresser, M. J.; Tracey, A. S.; Stankiewicz, P. J. *Adv. Prot. Phosphatase* **1987**, 4, 35.
11. Hoffmann *Ber*. **1880**, 13, 1236.
12. Green *Perkin, J. Chem. Soc*. **1903**, 83, 1204.
13. Shaver, A.; Ng, J. B.; Hall, D. A.; Lum, B. S.; Posner, B. I., *Inorg. Chem*. **1993**, 32, 3109.
14. Dutton, J. C.; Fallon, G. D.; Murray, K. S. *Inorg. Chem.* **1988** 27, 34.
15. Farahbakhsh, M.; Nekola, H.; Schmidt, H.; Rehder, D. *Chem. Ber./Recueil* **1997**, 130, 1129.
16. Wang, D.; Ebel, M.; Schulzke, C; Grüning, C.; Hazari, S. K. S.; Rehder, D., *Eur. J. Inorg. Chem.* **2001**, 935.

17. Crans, D. C.; Chen, H.; Anderson, O.P.; Miller, M.M. *J. Am. Chem. Soc*. **1993**, 11, 6769.
18. Schmidt, H.; Bashirpoor, M.; Rehder, D. *J. Chem. Soc. Dalton Trans*. **1996**, 3865.
19. Bashirpoor, M.; Schmidt, H.; Schulzke, C.; Rehder, D. *Ber. Recueil* **1997**, 130, 1127.
20. Kessissoglou, D. P.; Butler, W. M.; Pecoraro, V. L. *Inorg. Chem*. **1987**, 26, 495.
21. Manzur, C.; Bustos, C.; Schrebler, R.; Carrillo, D.; Knobler, C. B.; Gouzerh, P.; Jeannin, Y. *Polyhedron*, **1989**, 8, 2321.
22. Warner, L. G.; Ottersen, T.; Seff, T. *Inorg. Chem*. **1974**, 13, 2529.
23. Betrand, J. A.; Breece, J. L. *Inorg. Chim. Acta* **1974**, 8, 267.
24. Atkinson, M. A.; Maclare, N. K. *Sci. Am*. **1990**, 263, 62.
25. (a) Shechter, Y. *Diabetes* **1990**, 39, 1. (b) Shechter, Y.; Meyerovitch, J.; Farfel, Z.; Sach, J.; Bruck, R.; Insulin mimetic effects of vanadium. In vanadium in biological systems, physiology and biochemistry; Chasteen, N. D., Ed.; Kluwer academic publishers: Dordrecht, **1990**, pp 129.
26. Lyonnet, B. M.; Martz-Martin, E. *La Presse Medicale* **1899**, 7, 191.
27. Heyliger, C. E.; Tahiliani, A. G.; McNeill, J.H. S*cience* **1985**, 227, 1474.
28. Filat, C.; Rodriguez-Gil, J. E.; Guinovart, J.J. *Biochem. J.* **1992**, 282, 659.
29. Shisheva, A.; Gefel, D.; Shechter, Y. *Diabetes* **1992**, 41, 982.
30. Nechay, B. R.; Nanninga, L. B.; Nechay, P. S. E.; Post, R. L. Grantham, J. J.; Macara, I. G.; Kubena, L. F.; Phillips, T. D.; Nielsen, F. H.; *Fed. Proc*. **1986**, 45, 123.
31. Nadel, J. A.; *J. Clin. Invest*. **1996**, 97, 2689.
32. (a)Tolman, E. L.; Barris, E.; Burns, M.; Pansisni, A.; Partridge, R. *Life Sci*. **1979**, 25, 1159. (b) Shechter, Y.; Karlish, S.D.T. *Nature* (London) **1980**, 284, 556.
33. Gil, J.; Miralpeix, M.; Carreras, J.; Bartrons, R. *J. Biol. Chem*. **1988**, 263,1868.
34. Blondel, O. ; Simon, J. ; Chevalier, B.; Porta, B. *Am. J. Physisol*. **1990**, 258, E459.
35. Brichard, S. M.; Assimacopulos-Jeannet, F.; Jeanrenaud. B. *Endocrinology* **1992**, 131, 311.
36. Bendayan, M.; Gingras, D. *Diabetologia* **1989**, 32, 561.
37. Remanadham, S.; Cros, G. H.; Mongold, J. J.; Serrano, J. J.; McNeill, J. H.; *Can. J. Physiol. Pharmacol*. **1990**, 68, 486.
38. Remanadham, S.; Mongold, J. J.; Brownsy, R. W.; Cros, G. H.; McNeill, J. H. *Am. J. Physiol*. **1989**, 257, 904.
39. Remanadham, S.; Brownsy, R. W.; Cros, G. H.; Mongold, J. J.; McNeill, J. H.; *Metabolism* **1989**, 38, 1022.

40. Pederson, R. A.; Remanadham, S.; Buchan, A. M.; McNeill, J. H. *Diabetes* **1989**, 38, 1390.
41. Setyawati, I.A.; Thomopson, K. H.; Yuen, V. G.; Sun, Y.; Battell, M.; Lyster, D. M.; Vo, C.; Ruzh, T. J.; Zeisler, S.; McNeill, J. H.; Orvig C. *J. Am. Physiol. Soc*. **1989**, 569.
42. McNeill, J. H.; Yuen, V. G.; Hoveyda, H. R.; Orvig, C. *J. Med. Chem*. **1992**, 35, 1489.
43. Caravan, P.; Gelmini, L.; Glover, N.; Herring, F. G.; Li, H.; McNeill, J. H. Rettig, S. J.; Setyawati, I. A.; Shuter, E.; Sun, Y.; Tracey, A. S.; Yuen, V. G.; Orvig, C. *J. Am. Chem. Soc*. **1995**, 117, 12759.
44. Yuen, V. G.; Orvig, C.; McNeill, J. H. *Can. J. Physiol. Pharmacol*. **1995**, 73, 311.
45. Fujimoto, S.; Tamura, H.; Sakurai, H. *31th Intern. Conf. Coord. Chem.; Vancouver, Canada*, **1996**, Abs. P.21.
46. Sakurai, H; Fujii, K.; Watanabe, H.; Tamura, H.; *Biochem. Biophys. Res. Commun.* **1995**, 214, 1095.
47. Melchior, M.; Thompson, K. H.; Jong, J. M.; Rettig, S. J.; Shuter, E.; Yuen, V. G.; Zhou, Y.; McNeill, J. H. and Orvig, C. *Inorg. Chem*. **1999**, 38, 2288.
48. Wieghardt, K. *Inorg. Chem*. **1978**, 17, 57.
49. Nuber, B.; Weiss, J.; Wieghardt, K. *Z. Nturforsch*. **1978**, 33B, 265.
50. Kawabe, K.; Tadokoro, M.; Kojima, Y.; Fujisawa, Y.; Sakurai, H.; *Chem. Lett*: **1998**, 9.
51. Fondacaro, J. V.; Greco, D. S.; Crans, D. C. *Proceedings of the 17th Annual Veterinary Medical Forum* **1999**, abstr. 75, p710.
52. Plottnick, A. N.; Greco, D. S.; Crans, D. C.; Elfrey, S. *Proc. Annu. Vet. Med. Forum* **1995**, 13, 5.
53. Greco, D. S.; *Diabetes* **1997**, 46 (Suppl.), 1274.
54. Crans, D. C.; Keramidas, A. D.; Drouza, C. *Phosphorus, Sulfur SiliconRrelat. Elem*. **1996**, 109-110, 245.
55. Crans, D. C. *J. Inorg. Biochem*. **2000**, 80, 123.
56. Souchay, P. *Polycations* Gauthier-Villars: *Pairs*. **1963**.
57. Pope. M. T. Heteropoly and isopoly oxometalates; Springer-Verlag: New York, **1983**.
58. Pope. M. T.; Müller, A. *Angew. Chem., Int. Ed. Engl.* **1991**, 36, 34.
59. Matveev, K. I. *Kinet. Katal*. **1977**, 18, 862.
60. Ono, Y. *Perspectives in caalysis*; Thomas, J. M.; Zamaraev, K.I.; (Eds.); Blackwell: London, **1992**; p 431.
61. Kozhevnikov, I. V.; Matveev, K. I. *Appl. Catal*. **1983**, 5, 135; *Russ. Chem. Rev*. **1982**,51,1057.

62. Kozhevnikov, I. V. *Russ. Chem. Rev*. **1987**,56,811.
63. Kozhevnikov, I. V. *Stud. Surf. Sci. Catal*. **1994**, 90, 21; *Russ. Chem. Rev*. **1993**,62,473.
64. Kozhevnikov, I. V. *Catal. Rev. Sci. Eng.* **1995**, 37, 311.
65. Moffat, J. B. *Rev. Chem. Intermed.* **1987**, 8, 1; *Chem. Eng. Commun*. **1989**, 83, 9.
66. Misono, M. *In new frontiers in catalysis* ; Guczi, L., (Eds.); Elsevier: Amsterdam, **1993**; p 69.
67. Misono, M.; Nojiri, N. *Appl. Catal*. **1990**, 64, 1.
68. Izumi, Y.; Urabe, K.; Onaka, M. Zeolite, *Clay and Heteropoly acids in organic reactions*; Kodansha/VCH : Tokyo, **1992**; p99.
69. Okuhara, T.; Mizuno, N.; Misono, M. *Adv. Catal*. **1996**, 41, 113.
70. Hil, C. L.; Prosser-McCartha, C. M. *Coord. Chem. Rev*. **1995**, 143, 407.
71. Corma, A. *Chem. Rev*. **1995**, 95, 559.
72. Polyoxometalates : from Platonic Solids to Anti-Retroviral Activity; Pope, M. T., Müller, A., (Eds.); *Kluwer Academic Publishers*: Dordrecht, **1994**.
73. Okuhara, T.; Mizuno, N.; Misono, M. *Adv. Catal*. **1996**, 41, 113.
74. (a) Misono, M.; Nojiri, N. *Appl. Catal*. **1990**, 64, 1. (b) Nojiri, N.; Misono, M. *Appl. Catal*. **1993**, 93, 103.
75. Noritaka M.; Misono, M. *Chem. Rev*. **1998**, 98, 199.
76. Cherman, J. C.; Sinoussi, F. C.; Jasmin, C. *Biochem. Biophys. Res. Commun*. **1975**, 65, 1229.
77. Tsing, H.; Atanasiu, P.; Chermann, J. C.; *J. Gen. Virol*. **1978**, 40, 665.
78. Bussereau, F.; Chermann, J.; De Clercq, E.; Hannoun, C. *Ann. Virol*. **1983**, 134E, 127.
79. Bussereau, F.; Ermine, A. *Ann. Virol*. (Inst. Pasteur) **1983**, 134E, 487.
80. Souyri-Caporale, M; Tovey, G.; Ono, K.; Jasmin, C.; Chermann, J. C.; *J. Gen. Virol*. **1984**, 65, 831.
81. (a) Crans, D. C.; Schelble, S. M.; *Biochemistry* **1990**, 29, 6698. (b) Crans, D. C.; Simone, C. M.; *Biochemistry* **1991**, 30, 6734. (c) Crans, D. C.; Sudhakar, K.; Zamboborelli, T. J. *Biochemistry* **1992**, 31, 6812. (d) Crans, D. C.; Simone, C. M.; Saha, A.K.; Glew, R.H. *Biochem. Biophys. Res. Commun*. **1989**, 165, 246.
82. (a) Crans, D. C.; Willing, E. M.; Butler, S. R. *J. Am. Chem. Soc*. **1990**, 112, 427. (b) Crans, D. C. in Polyoxometalates: From Platonic solids to anti-restroviral activity; Müller, A.; Pope, M. T.; (Eds.); *Kluwer Academic Publishers*: Dordrecht, The Netherlands **1993**, 399.

83. (a) Cremo, C.R.; Grammer, J. C.; Yount, R. G.; *Meth. Enzymol*. **1991**, 196, 442. (b) Ringel, I.; Peyser, Y. M.; Muhlrad, A. *Biochemistry,* **1990**, 29, 9091.
84. (a) Boyd, D. W.: Kustin, K. ; Niwa, M. *Biochim. Biophys. Acta* **1985**, 827, 472. (b) Demaster, E. G.; Mitchell, R. A.; *Biochemistry*, **1973**, 12, 3616. (c) Soman, G.; Chang, Y. C.; Graves, D. J.; *Biochem*. **1983**, 22, 4994.
85. (a) Pai, E. F.; Sachsenheimer, W.; Schirmer, R. H.; Schulz, G. E. *J. Mol. Biol*. **1977**, 114, 37. (b) Csermely, P.; Martonosi, A.; Levy, G. C.; Ejchart, A. J. *Biochem. J*. **1985**, 230, 807.
86. Elvingson, K.; Fritzsche, M.; Rehder, D.; Pettersson, L. *Acta Chem. Scand*. **1994**, 48, 878.
87. Choleva, M.; Legge, G. J. F.; Weigold, H.; Holan, G.; Birch, C. J. *Life Sci.* **1994**, 54, 1607.
88. Arrieta, V *Polyhedron*, **1992**, 23, 3045.
89. Brown, I. D. in: M. O'Keefe, M. Navrotzky (Eds), Structure and Bonding in Crystals, vol. II *Academic Press*, New York, **1981**, ch. 14.
90. Kempf, J. Y.; Rohmer, M. M.; Poblet, J. M.; Bo, C.; Benard, M. *J. Am. Chem. Soc*. **1992**, 114, 1136.
91. Crans, D. C.; Mahroof-Tahir, M.; Anderson, O. P.; Miller, M. M., *Inorg. Chem*. **1994**, 33, 5586.
92. Farahbakhsh, M.; Schmidt, H.; Rehder, D. *Chem. Ber./Recueil* **1997**, 130, 1123.
93. Farahbakhsh, M.; Kögerler, P.; Schmidt, H.; Rehder, *Inorg. Chem. Commun* **1998**, 1, 114.
94. Hosnain, M. E.; Alam, M. N.; Ali, M. A.; Nazimuddin, M.; Smith, F. E.; Hynes, R. C. *Polyhedron* **1996**, 15, 973.
95. (a)West, D. X.; Yang, Y.; Klein, T. L.; Goldberg, K.I.; Liberta, A. E.; Valdes-Martinez, J.; Toscano, R. A., *Polyhedron* **1995**, 14, 1681. (b) Lu, Z.; White, C.; Rheingold, A. L.; Crabtree, R. H., *Inorg. Chem*. **1993**, 32, 3991. (c) Souza, P.; Matesanz, A. I.; Fernandez, V., *J. Chem. Soc. Dalton Trans*. **1996**, 3011. (d) Valdes-Martinez, J.; Toscano, R. A.; Zentella-Dehesa, A.; Salberg. M. M.; Brain, G. A.; West, D. X., *Polyhedron* **1996**, 15, 427.
96. Gerbeleu, N. V.; Burshtein, I. F.; Kiosse, G. A.; Filippova, I. G.; Bologa, O. A.; Lozan, V. I.; Malinovskii, T. I., *Dokl. Akad. Nauk SSSR* **1985**, 284, 155.
97. (a) Schmidt, H.; Rehder, D. *Inorg. Chim. Acta* **1998**, 267, 229. (b) Vergopoulos, V.; Jantzen, S.; Julien, N.; Rose, E.; Rehder, D. *Z. Naturforsch. B* **1994**, 49, 1127.

98. Tasiopoulos, A. J.; Troganis, A. N.; Evangelou, A.; Raptopoulou, C. R.; Terzis, A.; Deligiannakis, Y.; Kabanos, T. A., *Chem. Eur. J*. **1999**, 5, 910.
99. Root, C. A.; Hoeschele, J. D.; Cornman, C. R.; Kampf, J. W.; Pecoraro,V. L. *Inorg*. *Chem*. **1993**, *32*, 3855.
100. Hillerns, F.; Olbrich, F.; Behrens, U.; Rehder, D. *Angew*. *Chem*., *Int*. *Ed*. *Engl*. **1992**, *31*, 447.
101. (a) Syamal, A.; Kale, K. S. *Inorg*. *Chem*. **1979**, *18*, 992. (b) Carrano,C. J.; Nunn, C. M.; Quan, R.; Bonadies, J. A.; Pecoraro, V. L. *Inorg*. *Chem*. **1990**, *29*, 944. (c) Cotton, F. A.; Lewis, G. E.; Mott, G. N. *Inorg*. *Chem*. **1983**, *22*, 378.
102. Priebsch, W.; Rehder, D. *Inorg*. *Chem*. **1990**, *29*, 3013.
103. Crans, D. C.; Felty, R. A.; Miller, M. M. *J*. *Am*. *Chem*. *Soc*. **1991**,*113*, 265.
104. Lindl T, Bauer J **1987** *Zell- und Gewebekultur*. Fischer, Stuttgart.
105. Goda, T.; Sakurai, H.; Yashimura, T. *Nippon Kagaku Kaishi* **1988**, 654.
106. Heinzel, U.; Henke, A.; Mattes, R. *J. Chem. Soc. dalton Trans*. **1997**, 501.
107. Keramidas, A. D.; Papaioannou, A. B.; Vlahos, A.; Kabanos, T. A.; Bonas, G.; Makriyannis, A.; Rapropoulou, C. P.; Terzis, A. *Inorg. Chem*. **1996**, 35, 357.
108. Stankiewiez, P. J.; Tracey, A. S.; Crans, D. C. Vanadium and its role in life vol. 31 of metal ions in biological systems (Eds.) *Marcel Dekker. New York* **1995**, ch 9.
109. Howarth, O. W. *Progr. Nucl. Magn. Reson. Spectrosc* **1991**, 22, 453.
110. Day, V. W.; Klemperer, W. G.; Maltbie, D, J.; *J. Am. Chem. Soc*. **1987**, 109, 2991.
111. Roman, P.; Aranzabe, A.; Luque, A.; Gutierrez-Zorilla, J.M.; Martinez-Ripoll, M. *J. Chem. Soc. Dalton Trans*. **1995**, 2225.
112. Wery, A. S. J.; Gutierrez-Zorilla, J. M.; Luque, A.; Roman, P. *Polyhedron* **1996**, 24, 4555.
113. (a) Arrieta, J. M., *Polyhedron* **1992**, 23, 3045. (b). Wang, X.; Liu, H. X.; Xu, X. X.; You, X. Z. *Polyhedron* **1993**, 12, 77.
114. Debaerdemaker, T.; Arrieta, J. M.; Amigo, J. M., *Acta Cryst. B* **1982**, 38, 2465.
115. Caparelli, N. V.; Arnaiz, A.; Lorente, L.; Santiago, C.; Germain, G., *Acta Cryst.* **1988**, 44, 1004.
116. Angus-Dunne, S. J.; Batchelor, R. J.; Tracey, A. S.; Einstein, F. W. B. *J. Am. Chem. Soc*. **1995**, 117, 5292.
117. Capparelli, M. V.; Goodgame, D. M.; Hayman, P. B.; Shapski, A. C. *J. Chem. Soc., Chem. Commun* **1986**, 776.
118. Klemperer, W. G.; Shun, W. *J. Am. Chem. Soc.* **1977**, 99, 3544.

119. Rehder, D. in: "*Vanadium in biological Systems*", ed. N. D. Chasteen, (Eds.) Kluwer, Dordrecht, **1990**, 173.
120. Selling, A.; Andersson, I.; Pettersson, L.; Schramm, C. M.; Downey, S. L.; Grate, J. H., *Inorg. Chem*. **1994**, 33, 3141.
121. Kato, R.; Kobayashi, A.; Sasaki, Y.*, Inorg. Chem*. **1982**, 21, 240.
122. Pimentel, G. C., McClellan, A. L., (Eds).; *The Hydrogen Bond* W. H. Freeman: San Franciso, CA, **1960**; pp 225.
123. Domaille, P. J.; Watunya, G. *Inorg. Chem*. **1986**, 25, 1239.
124. Domaille, P. J.; Harlow, R. L, *J. Am. Chem. Soc*., **1986**, 108, 2108.
125. Farahbakhsh, M. *Dissertation*, Hamburg **1999**.
126. Fendesak, G.; *Analyse*, unveröffentlichtes Programm, Universität Hamburg **1988**.
127. Kopf, J.; Abeln, D.; *Y290*, *Programm zur Steuerung des Hilger & Watts Y290*, Universität Hamburg **1992**.
128. Kopf, J.; Ruebcke, H.-C.; *WATSHEL*, unveröffentlichtes Programm, Universität Hamburg **1997**.
129. Sheldrick, G. M.; *SHELXTL PLUS-Release 4.21/V*, Siemens Crystallographic Research Systems, Siemens Analytical X-Ray Instr. Inc. **1990**.
130. Sheldrick, G. M.; *SHELXS-86*, Program for Crystal Structure Solution, Universität Göttingen **1986**.
131. Sheldrick, G. M.; *SHELXL-93*, Program for Crystal Structure Determination,Universität Göttingen **1993**.
132. Spek, A. L.; *PLUTON*, Program for the Display and Analysis of Crystal and Molecular Structures, University of Utrecht **1990**.
133. Sheldrick, G. M.; *XPW (Interactive Molecular Graphics), SHELXTL PLUS-Release 4.21/V*, Siemens Crystallographic Research Systems, Siemens Analytical X-Ray Instr. Inc. **1990**.
134. Spek, A. L.; *PLATON 95*, Program for the Automated Analysis of Molecular Geometry, University of Utrecht **1995**.
135. Tietz, H.; Schmelick, K.; Kreisel, G.; *Z. Chem*. **1985**, 25, 290.
136. L. E. Manzer in J. P. Fackler (Eds.): *Inorganic syntheses* Vol. XXI, Wiley, New York, **1982**, S. 138.
137. Marini, P. J.; Murray, K. S.; West, B. O., *J. Chem. Soc. Dalton Trans* **1983**, 143.
138. Tyler, L. A.; Noveron, J. C.; Olmstead, M. M.; Mascharak, P. K.*, Inorg. Chem*. **2000**, 39, 357.

139. Vlahos, A. T.; Tollis, E. I.; Raptopoulou, C.P.; Tsohos, A.; Sigalas, M. P.; Terzis, A.; Kabanos, T. A*, Inorg. Chem*. **2000,** 39, 2977.
140. Ping-Kay Hon; R. L. Belford; C. E. Pfluger, *J. Chem.l Phys.* **1965**, 43, 1323.
141. Purohit, S.; Koley, A. P.; Prasad, L. S.; Manoharan, P. T. *Inorg. Chem*. **1989**, 28, 3735.
142. Asgedom, G.; Sreedhara, A.; Kivikoski, J.; Valkonen, J.; Kolehmainen, E.; Rao, C.P. *Inorg. Chem.* **1996**, 35, 5674.

Publications:

1. “Vanadium (IV, V) complexes containing SNO (dithiocarbonylhydrazone; thiosemicarbazone) donor sets” Wang, D.; Ebel, M.; Schulzke, C.; Grüning, C.; Hazari, S. K. S.; Rehder, D. *Eur. J. Inorg. Chem*. **2001**, 935

2. “In vitro study of the insulin-mimetic behaviour of vanadium(IV, V) coordination compounds” Dieter Rehder, João Costa Pessoa, Carlos F. G. C. Geraldes, M. Margarida C. A. Castro, Themistoklis Kabanos, Tamás Kiss, Beate Meier, Giovanni Micera, Lage Pettersson, Maria Rangel, Athanasios Salifoglou, Iztok Turel, Dongren Wang *J Biol Inorg Chem* **2002** 7 384

3. “Thiofunctional vanadium complexes” Nekola, H.; Wang, D.; Grüning, C.; Gätjens, J.; Behrens, A.; Rehder, D. *Inorg. Chem*. **2002**, 41(9), 2379

4. “Molecular assembly of novel heterometal cluster: $[(O=MoS_3Cu_2)_2(\mu\text{-}Sn_2S_6)]^{4-}$ and $[(S=MoS_3Cu_2)_3(\mu_3\text{-}S)_2]^{4-}$” Zhang, W. J.; Wu, J. X.; Ebel, M.; Wang, D.; Rehder, D. *Inorg. Chem. Comm.* in print.

Curriculum vitae

Name:	Dongren Wang
Sex:	male
Date and place of birth:	30.11. 1966 in Liaoning province (P. R. China)
Family status:	married, one daughter
Nationality:	Chinese (P.R.)

Education

09.1973 ~ 07.1980	Primary School in Quanzhou city, Fujian province
09.1980 ~ 07.1986	Haicheng middle school in Liaoning province
09.1986 ~ 07.1990	Study in the Northeast Normal University (Department of Chemistry) in Changchun, Jilin PR China Bachelor of Science
09.1990 ~ 07.1993	Study in the NNU under the supervision of Prof. Rongshun Wang in Changchun, Jilin China. Master Degree (Synthesis and theorical study on the conducting properties of polyparaphenyl and substituted-polyparaphenyl)
07.1993 ~ 02.1998	Assistent of the Center for Analysis and Testing at the Northeast Normal University.
03.1998 ~ 01.1999	Study of the German language at the Tongji-University in Shanghai, China
05.1999 ~ 09. 2002	Ph.D. research in the group of Prof. Dr. Dieter Rehder at the Hamburg University
05. 1999 ~ 04. 2000	Supported by a fellowship of the P.R. China
05. 2000 ~ 04. 2001	a DFG-financed position (1/2 BAT IIa)
05. 2001 ~ 09. 2002	a fellowship within the Graduate School “Functional Materials”)